CONSTITUTIVE THEORY OF COHESIVE SOIL AND ITS APPLICATION TO STRESS WAVE PROPAGATION

BY

FUSAO OKA

CONSTITUTIVE THEORY OF COHESIVE SOIL AND ITS APPLICATION TO STRESS WAVE PROPAGATION

March 1978

BY

FUSAO OKA

CONTENTS

SUMMARY

In this thesis, both experimental and theoretical investigations on the problem of the dynamic behavior of cohesive soil are mainly conducted. In the experimental investigation, the stress wave propagation test through cohesive soil is performed using a special triaxial cell connected with a shock tube. On the other hand, the constitutive theory of two phase mixture composed of an inelastic solid and a fluid is proposed on the basis of the rational continuum mechanics from a view point of the thermodynamics and the internal variable theory. Relevant to this investigations, the Terzaghi's effective stress concept is manifested from its physical view point and, it is comprehensively clarified that the effective stress concept can be usefully employed in analyzing the dynamic behavior of cohesive soil. In the theoretical treatment, the saturated, normally consolidated clay is considered to be a mixture composed of an elastic fluid, and as elastic-viscoplastic or as viscoelastic-viscoplastic body. The one-dimensional bar wave propagation in consideration of the consitutive theory proposed is solved out by the characteristic method. The analytical results obtained are fairly consistent with the test results. In addition to the wave propagation problem, the proposed constitutive equation of cohesive soil can reasonably interprete the results obtained by various types of laboratory test, and the influences of the parameter used in the equation on the field quantity, such as strain and stress, is investigated in detail for a practical usage. As an exercise practically oriented, the elastic-viscoplastic stress-strain relation is approximately employed to analyze the dynamic response of layered soil system.

ACKNOWLEDGEMENTS

The author wishes to express his deep appreciation to Professor K.Akai of Kyoto University for his supervision, guidance, encouragement throughout the course of this study. Professor H.Goto and Assistant Professor H.Kameda are also gratefully acknowledged for their hearty support on completing this dissertation. He is also indebted sincere thanks to Professor K. Toki and Assistant Professor T. Adachi of the Disaster Prevension Research Institute of Kyoto University, for their daily suggestions and constructive criticism. The author heartily thanks Dr. Hori, Research Associate of Kyoto University, for his support, encouragement, suggestions and his devoted help of the translation into English. Acknowledgements are also made to Assistant Professor H. Ohta, Assistant Professor Y. Ohnishi, Assistant Professor T. Sato, Research Associate H. Sekiguchi and Research Associate T. Tamura of Kyoto University for their sincere discussions and constructive criticism.

The author gratefully wishes to acknowledge his parents for their support and understanding throughout the course of the study.

NOTATIONS

A	stress amplitude(in Chapter 2)
A	parameter(in Chapter 5)
$\bar{A}$	material constant
$\hat{A}$	material constant
A_0	velocity amplitude
A_{ij}	material tensor function
B	parameter
$\hat{B}$	material constant
C	soil compressibility(in Chapter 4)
C	wave velocity (in Chapter 6)
C_r	wave velocity (in Chapter 2)
C_p	phase velocity
C_0	velocity of wave front(in Chapter 2)
C_0	material parameter(in Chapter 5)
C_1	material parameter
$\bar{C}_1$	material parameter
C_2	material parameter
C_s	compressibility of soil particle
D	matrix
E	viscoelastic constant
E'	Young's Modulus
E_{KL}	strain tensor in Lagrangian form
E_{KL}^{ve}	viscoelastic strain tensor in Lagrangian form
E_{KL}^{vp}	viscoplastic strain tensor in Lagrangian form
$\dot{E}_{ij}^{\alpha}$	strain rate tensor of constituent α
F	material function
$\hat{F}$	arbitrary function
F_{ij}^{α}	deformation tensor of constituent α
G	shear modulus
$\hat{G}$	arbitrary function
$G(T_{IJ}^{s})$	material function
G_{KL}	coefficient(2nd order tensor)
H	entropy of body
J_2	second invariant of deviatoric stress tensor

$\sqrt{2J_2}$	value of $\sqrt{2J_2}$ on static stress path
K_0	coefficient of earth pressure at rest
M^*	value of $\sqrt{2J_2}/\sigma'_m$ at critical state
M_{IJKL}	parameter(4th order tensor)
N_{ijkl}	parameter(4th order tensor)
O_{ijkl}	parameter(4th order tensor)
P	parameter
P_c	confining pressure
P_i	preconsolidation pressure
P_0	maximum amplitude of input stress wave
P_{KL}	internal state variable(2nd order tensor)
Q	parameter(in Chapter 5)
Q	body heating(in Chapter 3)
R_j	position
S	arbitrary surface
S_{ij}	Kirchhoff stress tensor
dS	line element in Lagrangian form
T_{KL}	second kirchhoff stress tensor
T^{α}_{ij}	partial second Kirchhoff stress tensor
V	arbitrary volume
$V_{2(0)}$	surface velocity
W	Matrix
X_K	coordinate of particle in Lagrangian form
X^{α}_i	reference position of particle of constituent α
X	parameter(in Chapter 5)
X	coordinate of particle in Lagrangian form in X_1 direction
Y	parameter
Z	matrix
$a^{(1)}$	material constant
$a^{(2)}$	material constant
a_c	contact area between soil particles
$b^{(1)}$	material constant
$b^{(2)}$	mateial constant
b_i	component of external body force vector
b^{α}_i	component of external body force vector of constituent α

d	parameter
d^i	parameters
d_{ij}	deformation velocity tensor
e	void ratio
e_{ij}	deviatoric strain tensor
e_{ijkl}	permutation symbol
f	plastic potential(in Chapter 5)
f	material function(in Chapter 6)
f_s	static loading function(in Chapter 3)
f_s	yield function(in Chapter 5)
f_d	dynamic loading function
f'_i	component of thermodynamic force vector
g	gravitational acceleration
g_I	temperature gradient
h_i^α	component of heat flux vector of constituent α
k	permeability coeeficient
$\bar{k}$	viscoelastic parameter(=E/E')
$\hat{k}$	wave number
m	material constant
m_f	intrinsic compressibility of a fluid
n	porosity
q	heat flux vector(in Chapter 3)
q	deviator stress(in Chapter 5)
q_i^α	partial heat flux vector of constituent α
q_r	deviator stress at time t when total strain is maintained unchanged
r	heat supply
ds	line element in current form
s_{ij}	deviatoric stress tensor
$s_{ij(0)}$	initial deviatoric stress tensor
s^α	partial heat supply
t	time
t_{ij}	Cauchy's stress tensor
t^a_{ij}	partial stress tensor
t_0	material constant

t^{e}_{ij}	effective stress tensor
u	pore water pressure
u_{a_i}	diffusion velocity vector of constituent a
$\bar{u}$	displacement in x direction
Δu	pore water pressure due to effect of dilatancy
v_i	component of velocity vector
$\bar{v}_i$	relative velocity(in Chapter 4)
v	particle velocity in x direction
x	coordinate of particle in current form in x_1 direction
x_k	coordinate of particle in current form
x^{α}_i	position of paticular particle of constituent α
z	intrinsic time scale
α	material constant
$\bar{\alpha}$	parameter
$\tilde{\alpha}$	parameters
$\bar{\bar{\alpha}}$	material constant
α'	material constant
$\hat{\alpha}$	attenuation constant
β	relaxation velocity
$\hat{\beta}$	material constant
β_1	material function
β_2	material function
γ_1	material constant
γ_2	material constant
δ	internal dissipation
$\bar{\delta}$	slope of line in Fig.5.7
δ_{ij}	Kronecker's delta
ε	internal energy density(in Chapter 3)
ε	strain (in Chapter 6)
ε^{α}	partial energy density
$\dot{\varepsilon}^{p}$	plastic component of strain rate
ε_{ij}	strain tnsor
ε^{ve}_{ij}	viscoelastic strain tensor
ε^{vp}_{ij}	viscoplastic strain tensor

ζ	internal parameter
η	entropy density
η^{α}	partial entropy density
η_{KLMN}	material constant(4th order tensor)
θ	absolute temperature
θ_j	phase angle
κ	internal scalar variable(in Chapter 3 and 4)
κ	slope of e-σ'_m line of swelling test(in Chapter 5 and 6)
λ	slope of e-σ'_m line of consolidation test
$\bar{\lambda}$	Lame's constant
$1/\mu$	viscosity coefficient
$\bar{\mu}$	Lame's constant
ν	Poisson's ratio
ξ	internal parameter
ξ'_j	component of internal variable
ρ	density
ρ_0	initial density
$\bar{\rho}^s$	mass density of solid continuum
$\bar{\rho}^f$	mass density of fluid continuum
ρ^s	specific density of soil particle
ρ^f	specific density of water
π_i	component of interaction force vector
Σ	stress
Σ'	Fourier transformation of stress
σ	total stress
σ'	effective stress
$\bar{\sigma}$	entropy production
σ_i	principle stress
σ_{ij}	stress tensor
$\sigma_{ij(0)}$	initial stress tensor
σ'_m	mean effective stress tensor
$\sigma'_{m(0)}$	initial mean effective stress tensor
$\sigma'_{m(s)}$	mean effective stress on static stress path
$\sigma'_{m\nu}$	hardening parameter
$\sigma^{e'}_{ij}$	effective stress tensor
τ	relaxation time

τ_d	maximum shear stress
$\tau^{(1)}$	material constant
$\tau^{(2)}$	material constant
ϕ	complementary energy function
ϕ^α	partial complementary energy function
ϕ'	effective stress angle of shearing resistance
ψ	free energy function
ψ^α	partial free energy function
$\bar{\psi}$	intrinsic friction angle
ω	angular frequency
Ω	flow potential

Chapter 1 Introduction

1.1 General Remarks

Civil structures are quite sensitive to a motion of ground which is arised from earthquakes, traffics and construction machines. Occationally, it gives the harmfull effects on civil structures. As Japan is sited in the major seismic zone around the Pacific Ocean, strong earthquakes have imposed severe damages on the structures in Japan. Since the many big cities in Japan are located on the poor ground(for example, alluvial deposit), it is necessary to graps the ground motion quantitatively and qualitatively during earthuake, which takes account of the ground condition and the other surrounding conditions. For the last two decades, the earthquake-resistant engineering has been developed very well. One of the earthquake-resistant design procedures is well known as "dynamic analysis." In order to improve this method, it is imperative to clarify the eqthquake response of ground. At the present stage, the following subjects are important to predict the ground motion during dynamic loading as accurate as possible.

(1) Mechanical properties of materials which constitute the ground

(2) Form of loading

(3) Geological configuration of foundation

(4) Analytical procedure

Recently, large structures have to be built even on a soft ground because of social and economical reasons. For example, some oil storage tanks are constructed on the reclaimed ground beside the sea or on an alluvial soil deposit. On the other hand, the construction of nuclear power plants needs a careful earthquake-resistant design for its safety. In these cases, it is very important to investigate the dynamic characteristics of earth materials accurately. The problem concerning with dynamic characteristics of earth materials has been dealt in the field of the soil dynamics. The recent developememt of soil dynamics owes to the progress of digital computer

technique and equipment for measurement of dynamic test on soil in the field and/or the laboratory. Firstly, it is essential to obtain the stress-strain relationships of soil, which give mathematical expressions of the various dynamic characteristics of soil. However, a constitutive relation sufficient to express the soil behaviors has not yet been obtained. One of the reasons is that soil is a complex material, i.e. the mixture of soil particles, water and air. The other is that soil is characterized by inelastisity, nonlinearity and time dependency.

The theory of constitutive equation based on the rational continuum mechanics has been developed in the last two decades by many researchers. Rational mechanics is useful to deduce a constitutive equation of material.[1),2)] This developement owes successfully to a Coleman & Noll's[3)] mathematical theory of thermodynamics and a Noll's[4)] principle of objectivity, which restricts a constitutive relation. The Coleman & Noll's thermodynamics is also available to the theory of mixture. The research on the constitutive equation for an inelastic material, however, starts and is not completed yet. There exist many approaches to express the inelastic properties of material. One is the internal variable theory in which the state of general continuum is determined not only by an observable quantity, but also by internally hidden variables which govern the internal structure of materials. In this study, internal state variables are employed to describe the behavior of inelastic materials. A soil can be considered to be a continuum having an internal structure. The saturated soil can be also taken as a mixture of particles and one water. In the present, the saturated soil is regarded as a tow-phase mixture of inelastic material and fluid, using the mixture theory on the basis of the Coleman & Noll's thermodynamics.

Meanwhile, there exists an effective stress concept in soil mechanics which has played an essential role for the developement of soil mechanics, but physical meaning of this concept has been ambiguous. In this study,

a Terzaghi's effective stress concept is clarified from the view of the theory of mixture.

It is needless to say that the accumulation of experimental data is necessary for the analysis of soil dynamics. The one-dimentional stress wave propagation test was performed using the special triaxial cell connct-ed with the air shock tube in order to investigate a dynamic property of cohesive soil. The shock tube was used as a loading apparatus. From the obtained test results, the damping characteristics and elastic modulus of soil were studied.

In Chapter 7, applying the stress-strain relation proposed in this study to the boundary value problem,the dynamic response of layered cohesive soil is analysed. Distributions of not only the strain and the stress, but also of the pore water pressure induced by the earthquake motion are calcu-lated. In designing the earthquake-resistant structures under the ground, the distributions of strain, stress, velocity and pore water pressure during an earthquake must be preexamined. It is important to estimate the magnitude of pore water pressure developed in the ground.

1.2 Scope of This Study

In this thesis, a constitutive theory of cohesive soil is presented and stress wave propagation characteristics of soil are analylically and experimentally investigated as an application of the proposed theory to the boundary value problem. The constitutive theory for inelastic material is proposed from a view point of mathematical continuum mechanics.As an experimental study, the stress wave propagtion test is performed using a special triaxial cell connected to a shock tube under different confining pressure. The proposed theory is also applied to an investigation of the dynamic response of layered cohesive soil.

Chapter 2 deals with the experimental study of stress wave propagation characteristics of saturated cohesive soil. Using a shock tube as a loading

apparatus, a one-dimentional stress wave propagation test for cohesive soil carried out. The type of wave employed in the experiment is reffered to a "bar wave". The change of the form of stress wave with travelling, the wave velocity and pore water pressure are examined. Moreover, a dependence of attenuation and phase velocity on frequency is discussed by using the technique of Fourier transformation.

In Chapter 3, a thermodynamic theory for inelastic materials is developed based on the non-equilibrium thermodynamics including the internal variables. A viscoplastic potential is newly defined which is related to the energy functions. The rate dependency of the potential effects significantly the deduced stress-strain relation. In this chapter, both rate independent and rate dependent cases are compared.

Chapter 4 deals a mixture theory of fluid and solid. The fluid phase represents a free water in a pore of soil, and the solid phase is assumed to be an addition of soil skeleton and an internal water absorbing into the soil particles and/or existing in a micro pore in a particle. In this chapter, the mechanical meaning of principle of Terzaghi's effective stress is clarified from the view of two phase mixture. The concept of effective stress mainly depends on the axioms of mixture which concerned with the definition of total stress. The fundamental equations of consolidation can also be deduced based on the theory of mixture.

In Chapter 5, constitutive equations for a normally consolidated clay are developed by theories proposed in Chapters 3 and 4. Constitutive equations for both an elastic-viscoplastic material and a viscoelastic-viscoplastic material are deduced. The proposed theory is examined from the various test results; stress wave propagtion test, undrained stress relaxation test, undrained creep test and strain rate controlled triaxial compression test.

The purpose of Chapter 6 is to obtain a numeriacl solution during the one-dimentional stress wave propagtion through a cohesive soil by the charac-

teristics method. The numerical results are compared with the experimental results and the dependency of the results on the parameter is discussed. Moreover, the effect of momentum interaction between fluid phase and solid phase is discussed, and an approximate equation of motion is then given.

Chapter 7 is concerned with the dynamic response of horizontally layered cohesive soil. It is assumed that the soil deposit is consolidated under a K_0-condition and shear wave propagates from base rock to the surface of the ground. The proposed constitutive relation for cohesive soil in Chapter 5 is modified for the anisotropic consolidation. The characteristics method is used to obtain a numerical solution.

Finally, in Chapter 8, the summary of this thesis is mentioned and the significance of this study and the future recommendation is given.

References for Chapter 1

1) Truesdell, C. and R.A.Toupin : The Classical Field Theories, Handbuch der Physik(edited by Flügge,S.), Vol.III/1,Berlin, Springer-Verlag,. 1960.

2) Truesdell, C. and W.Noll: The Non-Linear Field Theories in Mechanics, Handbuch der Physik(edited by Flügge, S.), Vol.III/3, Berlin, Springer-Verlag, 1965.

3) Coleman, B.D. and W. Noll: The Thermodynamics of Elastic Materials with Heat Conduction and Viscosity, Arch. Rational Mech.Anal.,Vol.13, 1963, pp.167-178.

4) Noll,W.: A Mathematical Theory of the Mechanical Behavior of Contiuous Media, Arch. Rational Mech. Anal. Vol.2, 1958, pp.197-226.

Chapteter 2 Experimental Study of Stress Wave Propagation through Cohesive Soil

2.1 General Remarks

The stress propagating through a material such as soil is generally accompanied with energy dissipation, and propagates with finite velocity. By observing these phenomena, we can investigate the damping and elastic characteristics of soil by the experiment including the field and laboratory tests. The following methods are often used in the laboratory test.

(1) Stress wave propagation test with relatively high amplitude(for the wide range of strain)

(2) Pulse method(for small strain)

(3) Resonant column method(for small strain)

(4) Forced vibration test(for relatively large strain)

The ultra-sonic pulse method is appropriate to investigate the dynamic properties of soil within the range of small amplitude of strain. When the material is relatively soft such as soft clay, however, this method is not recommended because the wave energy dissipates rapidly during the propagation of the ultra-sonic pulse in the material. The resonant column method is the one to obtain the dynamic properties of soil by producing a particular vibrational system in the soil specimen. To arrange the experimental results obtained by this method and understand strictly the physical phenomena of the specimen, a certain stress-strain relation has to be assumed and the whole system of dynamic response has also to be formulated taking into account that stress-strain relation. This method is also restricted to the test within the range of small amplitude of strain. While, the amplitude of strain can easily be controlled by using the forced vibration test. The stress-strain relation is directly observed. The stress wave propagation test is aimed to investigate the dynamic behavior of soil under a high strain rate by making a stress wave

propagate in a soil of which boundary condition is made simple. Since a large amplitude of strain can be induced to the soil specimen, this method is applicable to study both linear and non-linear behavior of soil. A stress wave propagation test of soil has been conducted by many investigators; Whitman[1]; Salvadori et al.,[2] Heierli[3]; Stoll & Ebeido[4]; Seaman,[5] Vey & Strauss,[6] Hampton & Wetzel[7] and Akai & Hori et al.[8] Heierli performed the wave propagation test on a fairly uniform moist sand and a gravel with sand under the condition such that the lateral deformation was confined. The applied pressure at the end of the soil column was 3 kg/cm^2 to 25 kg/cm^2. The induced strain level was 5 % to 20 % corresponding to the pressure. Inelastic stress wave was observed and the stress-strain relation was locking type. The same type of stress-strain curve was observed by Stoll & Ebeido in the test on Ottawa sand.

Seaman conducted the one-dimensional stress wave propagation test on sand and clay. The wave propagation characteristics of two materials are very similar. The soil specimen was placed in 5 meter long tube and lateral deformation was confined. The pulsative stress was then applied to the end of the specimen. It was noticed that there existed the time dependent and time independent energy dissipation during the stress wave propagation. He also performed the one-dimensional dynamic compression test in order to obtain the soil properties; dynamic modulus and dissipation characteristics. The comparison between the results of stress wave propagation test and the results predicted from the dynamic compression test presented a good agreement.

Vey & Strauss used an air shock tube as a loading apparatus in order to carry out the stress wave propagation test on Kaolin clay. Lateral confining pressure was ranging from 0.35 to 1.05 kg/cm^2, and axial loading ranging from 0.35 to 2.45 kg/cm^2. In the test, plastic wave propagation was predominant.

Shock tube was also used in the wave propagation test on EPK clay and Ottawa sand by Hampton & Wetzel. The specimen was confined in a hollow aluminum cylinder and subjected to external shock pressure ranging from 3.5 to 21.0 kg/cm^2. The stress-strain curve was S-shaped for sand, but not remarkably for clay . Plastic strain occurred in both cases.

Akai et al.[8),9)] developed the new tools for a stress wave propagation test. At first, they employed the technique in which the stress wave was generated by hitting the end of specimen by means of a small steel ball. Later on, the shock tube was employed as a loading apparatus in order to control the external pressure more accurately. The shock tube was connected with a hollow steel cylinder or a special triaxial cell for a soil specimen to be tested. The hollow steel cylinder was used to confine the lateral deformation of soil specimen. While, the triaxial cell was designed such that the specimen was set with allowing the lateral deformation and the confining pressure was applied. The drainage system was also installed in the cell similar as the conventional triaxial cell. They were concerned mainly with the peak stress attenuation, the elastic property considered from the velocity of the wave front and the change of wave form with travelling. The condensor-type soil strain meter was devised to monitor the dynamic strain below 10^{-3} during the stress wave propagation. In this study, the same experimental technique as theirs was followed and the test was performed on a cohesive soil.

There can be considered three types of one-dimensional wave propagation in a soil column, which are divided by a sort of theoretical treatment for the wave. The first one is the rod wave which is theoretically treated as that no confining pressure is applied and a lateral displacement is not taken into account. Both equations of motion and stress-strain relation are one-dimensional in the form. This case is therefore essentially one-dimentional. On the other hand, in the following two cases,

only the equation of motion is treated as one-dimensional. The second one is the longitudinal wave in which lateral displacement is regarded to be zero, but lateral confining pressure is allowed to exist. The last one is called the bar wave in which lateral displacement is taken into account and also lateral confining pressure exists. The experiment of wave propagation in the soil specimen carried out in this study should correspond to the bar wave from a point of theoretical treatment.

The assumption that the wave is one-dimensional is satisfied only when the length of specimen is long enough compared with the wave length and the ratio of wave length to the radius of the cylindrical specimen is sufficiently small.

The elastic and damping characteristics of soil have been also examined by many researchers using the other testing technique. The resonant column method is frequently used to investigate the dependency of the elastic characteristics of soil on the physical quantities such as temperature, confining pressure etc.[10),11)] For instance, Hardin & Black[12)] have presented an expression in which the shear modulus of soil was related to the void ratio and the confining pressure. The effects of shear strain amplitude, time of loading, stress history and temperature on shear modulus have been also examined by many researchers.[13)]

2.2 Testing Apparatus

2.2.1 Shock Tube

Fig.2.1 shows the general view of shock tube and a diagram of the apparatus is illustrated in Fig.2.2. The shock tube consists of high pressure chamber, middle pressure chamber and low pressure chamber. The length of the low pressure chamber is 2 m long which is long enough to produce a uniform shock wave. These chambers are made of hollow cylindrical steel of which inside diameter is 7.76 cm and 1.2 cm in thickness. Each chamber is separated

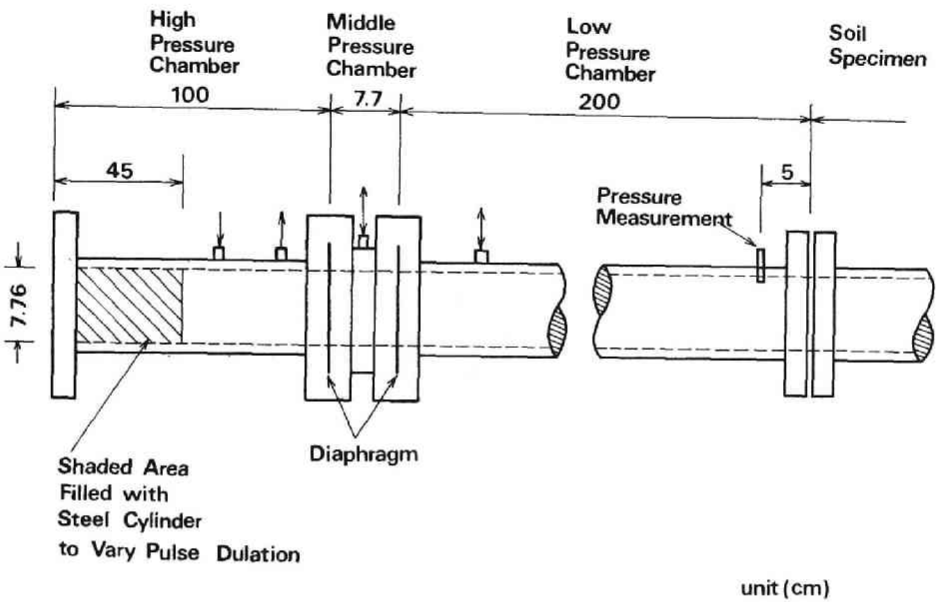

Fig.2.1 General view of shock tube.

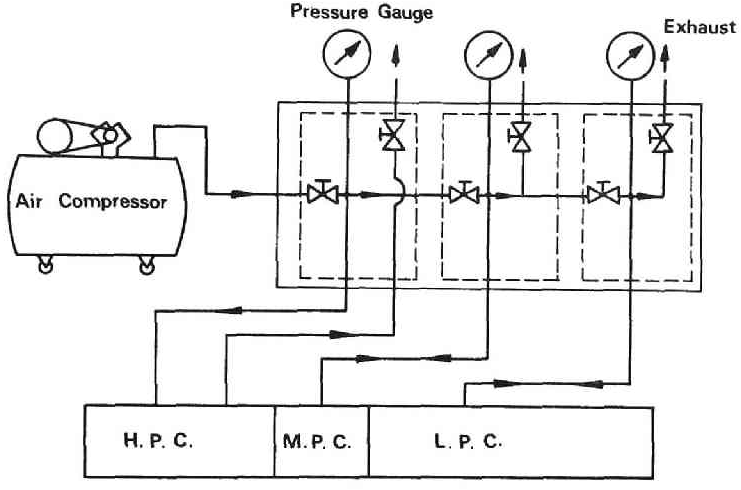

Fig.2.2 Schematic diagram of gass controlling system.

by a thin aluminum diaphram 0.1 to 0.3 mm in thickness with 17.5 cm in diameter. The low pressure chamber is kept in atmospheric, while appropriate pressure is supplied into the high and middle pressure chambers individually. When a difference of pressure between the high and middle pressure chambers becomes to be large enough to blow the thin aluminum diaphram, an air shock wave is generated and propagates in the low pressure chamber. In the experiment, the compressed air is supplied only in the high pressure chamber, and the pressure in the chamber is regulated such that the shock pressure of about 1.0 kg/cm^2 can be obtained and acts on the end of the cylindrical specimen.A semi-conductor type pressure gage is instrumented at the distance of 5 cm from the end of the shock tube as a triggering gauge.

2.2.2 Triaxial Cell

Photo.2.1 shows a view of the special triaxial cell. The diagram of triaxial cell is illustrated in Fig.2.3 . The triaxial cell consists of three lucite tubes, two aluminum rings and plates, steel pipes and steel angle with roller bearings. The outer diameter of the lucite tube is 32.4 cm, 28.4 cm in inner diameter and 50 cm in length. The rings are sandwiched between lucite tubes. The triaxial cell is horizontally and rigidly supported by two steel supports. Air shock pressure is transmitted to the cap of the specimen by a piston with a blass plate locating at the end of the shock tube. A soil sample is placed on a set of the rotational roller bearing which is sitting on the axial roller bearings to exclude frictional force around the specimen (see Fig.2.4). A soil sample is reconsolidated prior to the wave propagation test. The drainage system is schematically shown in Fig.2.5. This drainage system consists of filtering paper rolled around the specimen, porous stone and drainage pipe. The confining pressure, bellofram cylinder pressure and back pressure are controlled by air pressure regulator. Two bellofram cylinders are installed

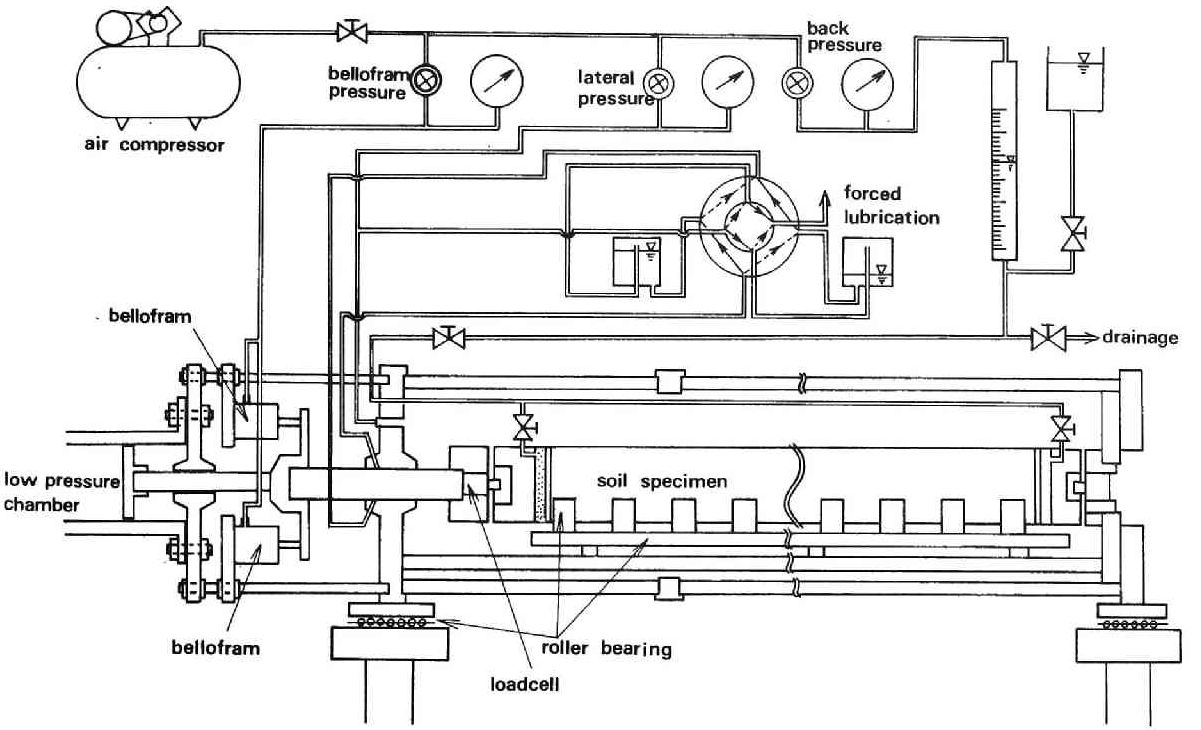

Fig.2.3 Schematic diagram of the triaxial compression chamber, the pressure system and water supply and drainage system.

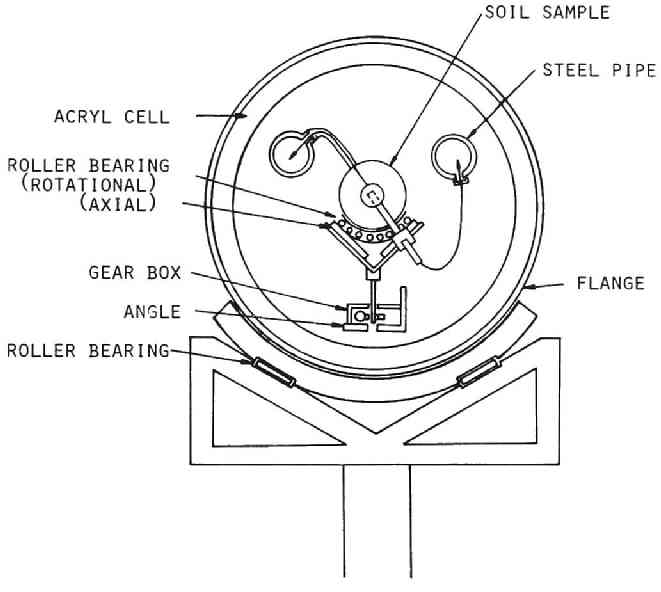

Fig.2.4 Section of the triaxial compression chamber.

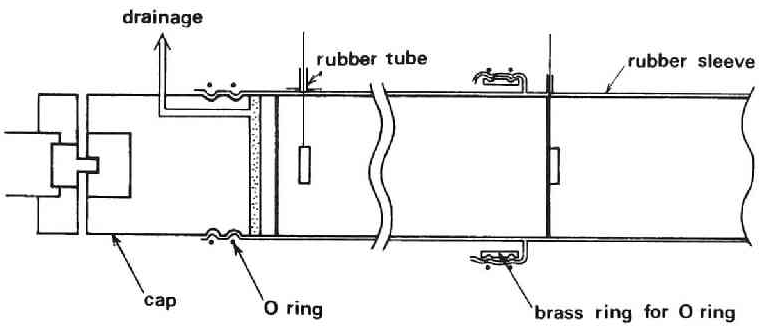

Fig.2.5 Drainage system.

to apply a force to the piston, equivalent to that acting on the cross section of the piston when the cell is under a certain pressure. In other words, the head of piston is touching to the cap of the specimen and feasibly balanced to maintain the position.

2.2.3 Equipment for Measurement

(1) Soil Stress Gauge

A semi-conductor type pressure gauge(B.E.E 10; capacity of 10 kg/cm^2) is used to measure the dynamic stress, which is a disc plate of 25 mm ϕ and 5 mm thick. To observe accurately the dynamic response of soil, it is necessary to employ a well-developed stress gauge of which natural frequency and sensitivity are relatively high compared with constituent frequency of the wave propagating through the soil. The calibration curve of this gauge is perfectly linear in the range from 0 to 2.4 kg/cm^2 as shown in Fig.2.6. The soil stress gauges are buried at two or three different positions in the specimen.

(2) Pore Pressure Transducer

Pore water pressure is measured by a semi-conductor type pressure transducer(TOYODA, 5H) with a needle-like tube partially filled with the porous stone (see Fig.2.7). Pore water pressure is measured at middle section of the specimen(see Photo.2.2).The calibration curve for the transducer is also shown in Fig.2.8.

(3) Accelerometer((BAL), SHINKO, $\pm$ 1g)

Since the accelerometer is very sensitive to a disturbance, it is used to measure wave velocity more accurately.

(4) Measuring System

The measuring system used in the experiment is shown in Fig.2.9. This system consists of soil stress gauge, pore pressure transducer, accelerometer, amplifier (KYOWA,TOYODA) and Syncroscopes(IWASAKI). The propagation stress

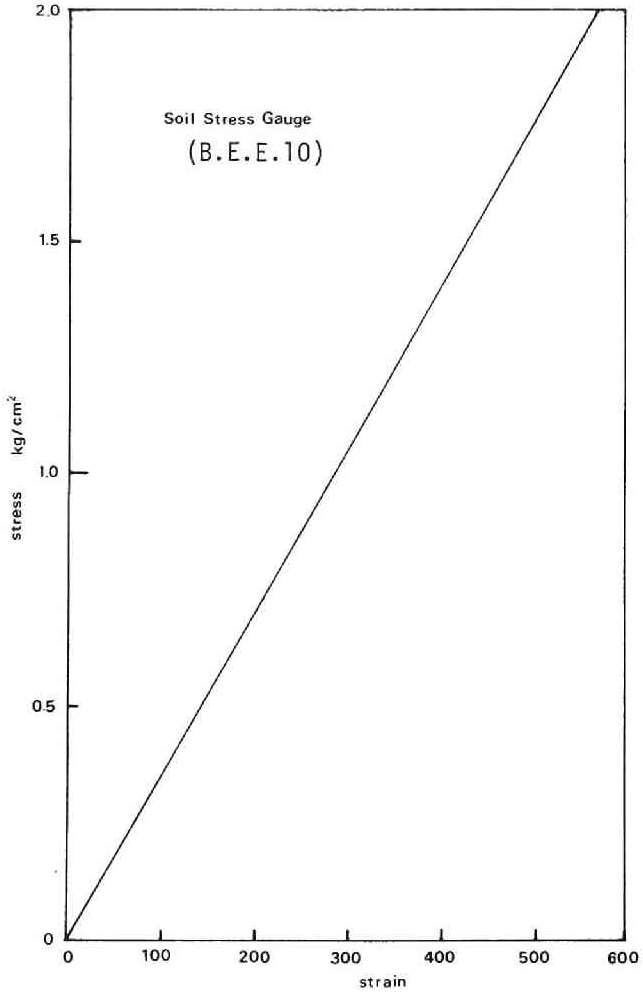

Fig.2.6 Calibration curve of soil stress gauge.

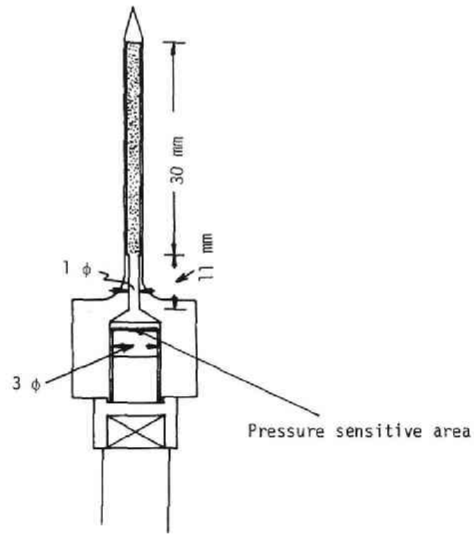

Fig.2.7 Equipment of pore water pressure.

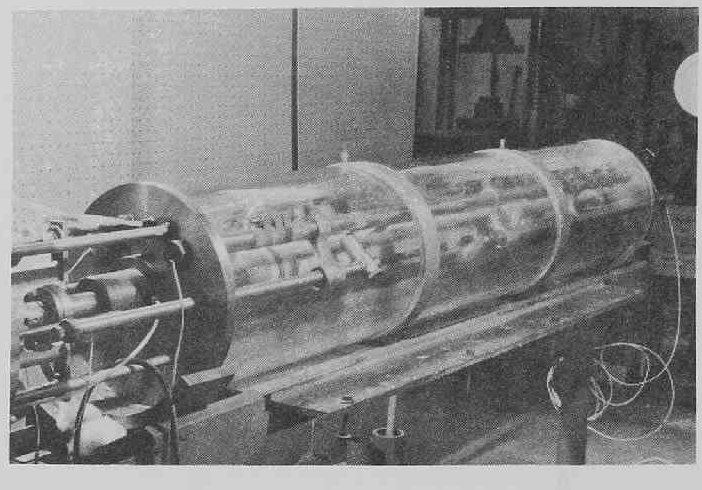

Photo.2.1 Special triaxial cell

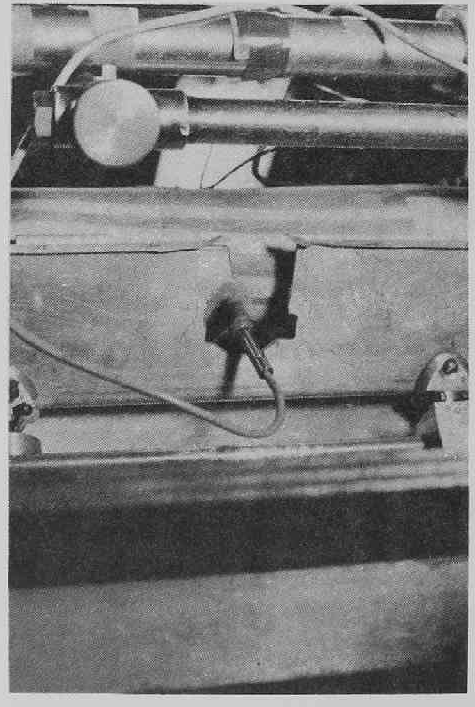

Photo.2.2 Measurement of pore water pressure.

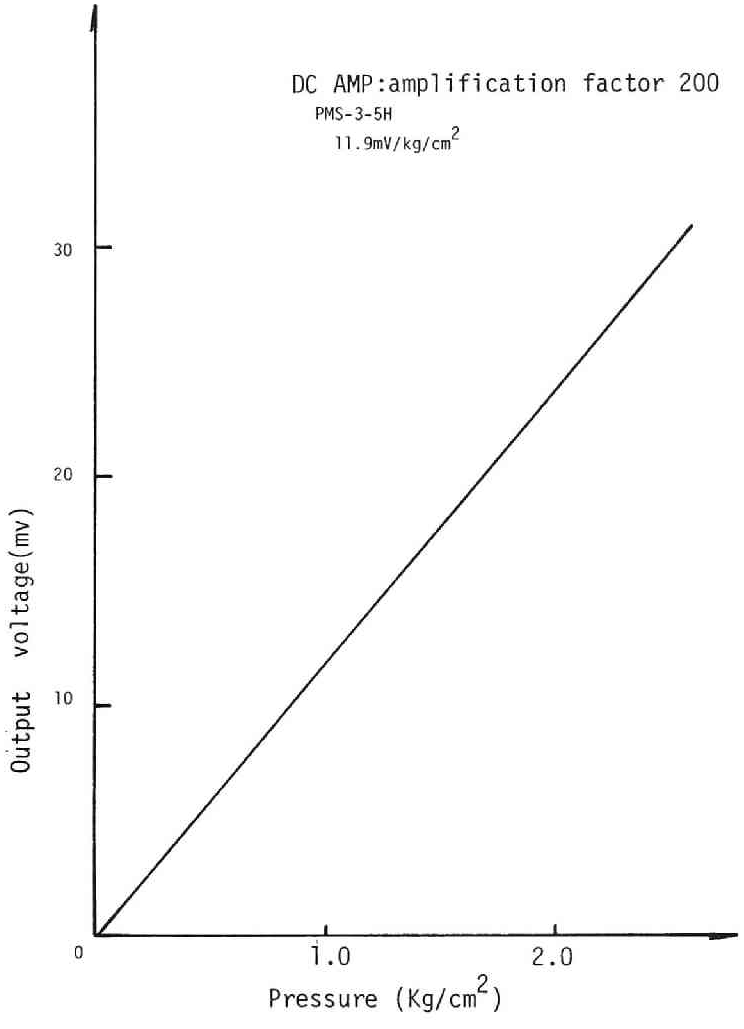

Fig.2.8 Calibration curve of pore pressure transducer.

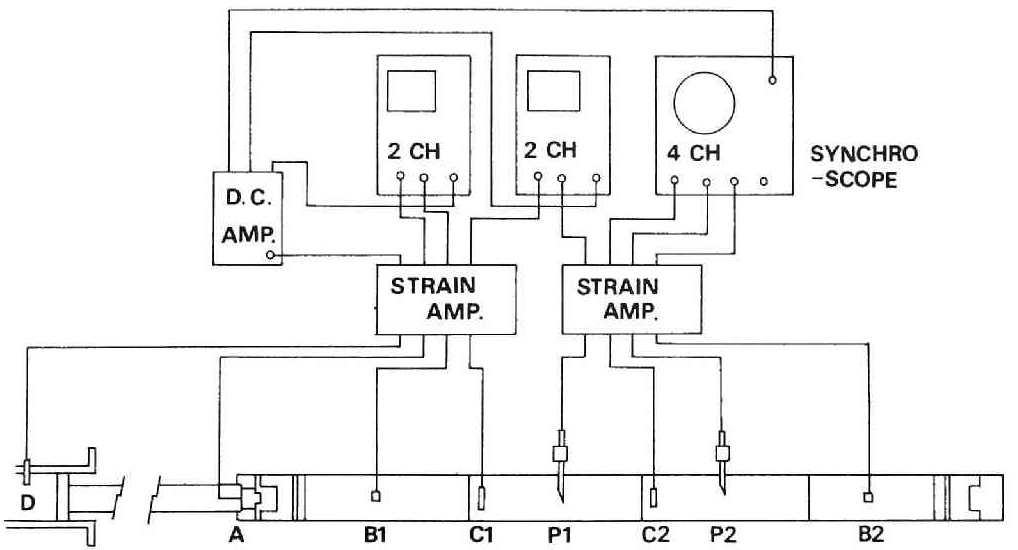

A Load cell
B 1,2 Acceleration meter
C 1,2 Soil stress gauge
D Pressure transducer for triggering
P 1,2 Pore water pressure equipment

Fig.2.9 Measuring system.

was directly recorded from synchroscopes by the help of Polaroid camera.

(5) Clayey Specimen and Test Procedure

The soil specimen is prepared from Fukakusa dry clay which is sieved by a 400 μ net, kneaded with water, and consolidated at a surcharge of 2.0 kg/cm^2 in a consolidation cylinder box of 60 cm in diameter and 1 m in height for about 40 days. After the consolidation, the specimen is taken out by a thin-walled blass sampler of which inner diameter is 75 mm and the each of the tube is sealed with Paraffin. Pre-consolidation pressure is from 0.6 to 0.85 kg/cm^2. The physical properties of the soil specimen are shown in Table 2.1 and the mechanical properties are shown in Figs.2.10 and 2.11.

A soil specimen for the wave propagation test with a length of about 130 cm and a diameter of 7.5 cm is assembled from four pieces of soil column. Each segment is about 32 cm long. The length of specimen is long enough to observe a one-dimensional wave phenomenon. After setting the soil stress gauges or the accelerometer in the specimen, these segments are put together. Each segment of the soil specimen is rolled by a sheet of filtering paper and covered with two rubber sleeves. Each sleeve is connected by using a O-ring and blass ring or it is sticked together with an adhesive.

2.3 Experimental Results and Discussions

2.3.1 Velocity of Wave Front

It can be observed that the stress wave propagates through soil with finite velocity. This physical meaning is that there is a limit in ability of energy propagation. That is to say, the wave velocity is related to a elastic property of soil. The velocity with which the stress wave propagates is calculated from the difference of the arrival time measured at two different positions by the accelerometers or soil stress gauges.

Fig.2.12 shows the relationship between the wave velocity C_r(m/sec) and the confining pressure P_c(kg/cm^2) on the logarithmic paper. It is expressed

Specific gravity	2.67
L L	50.5-60.0 %
P L	25.5-31.9 %
P I	21.6-34.5
Uniformity coef-ficient	2.85
Water content	36.7-42.5 %
Bulk density	1.72-1.83 g/cm^3

Table 2.1 Physical properties of the silty loam used.

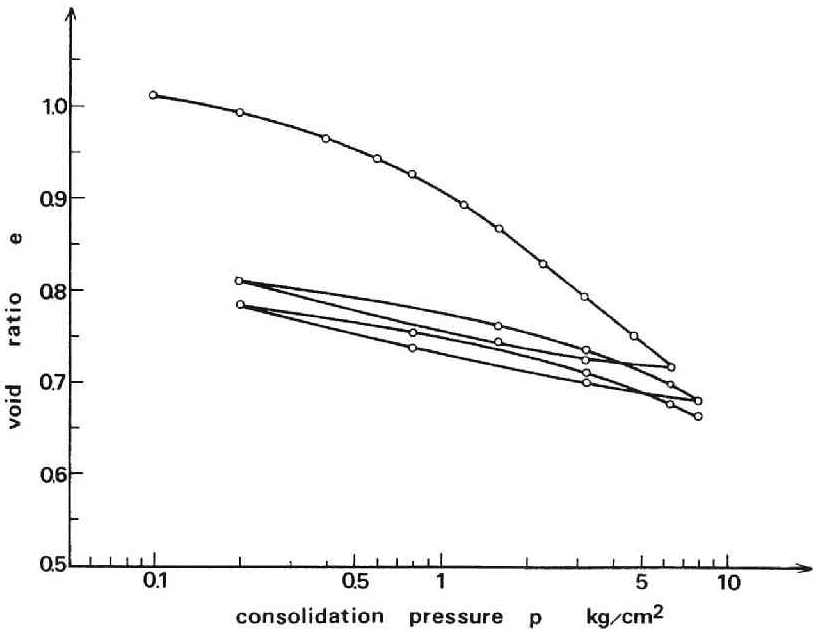

Fig.2.10 Typical e-log p curve.

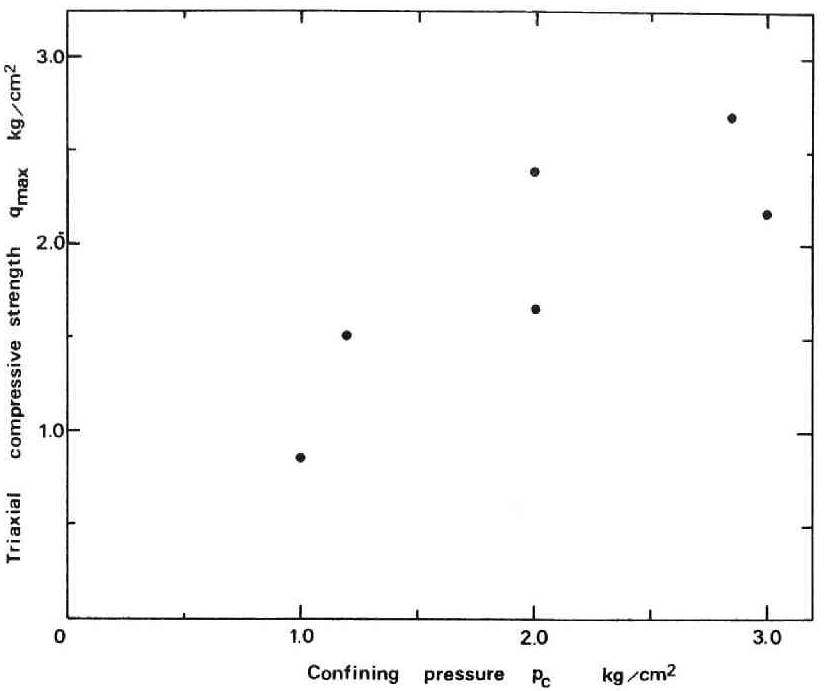

Fig.2.11 Relationship between P_c and q_{max}.

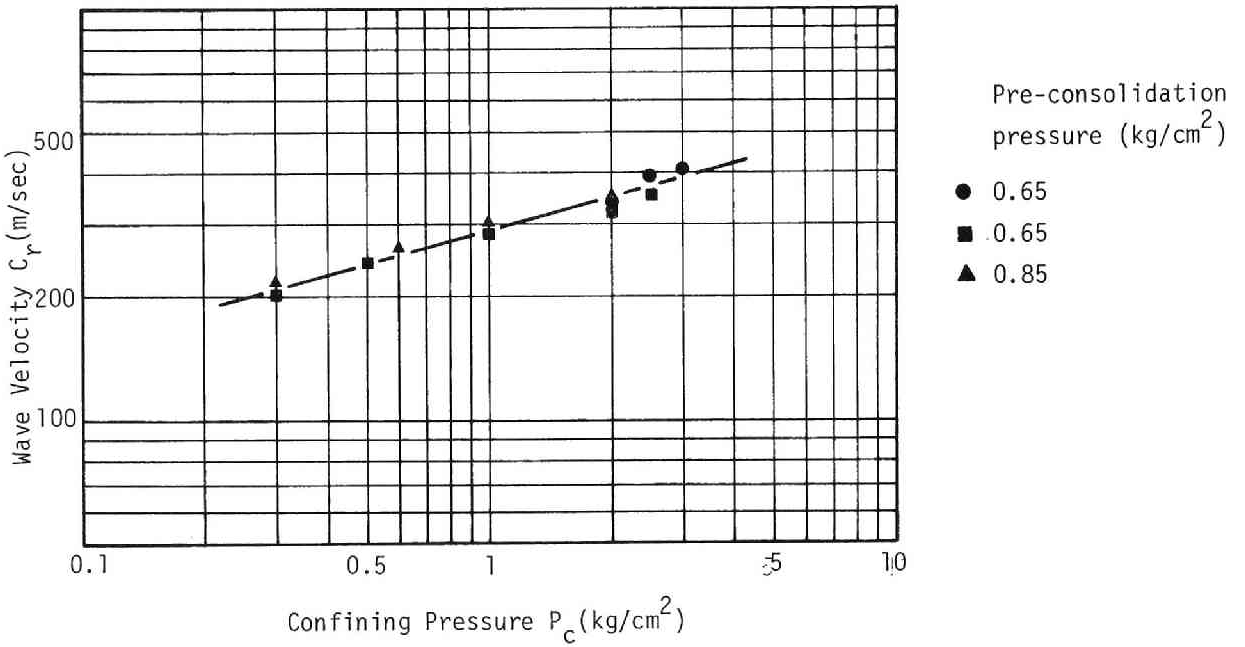

Fig.2.12 Relationship between C_r and P_c.

by

$$C_r = 290\ P_c^{0.25} \text{(under the normally consolidated state)} \quad (2.1)$$

According to the studies reported by many researchers, it is seen that the wave velocity through soil depends both on void ratio and on confining pressure. It is impossible, however, to change individually only the void ratio of soil specimen with maintaining a mean effective stress, because the void ratio of a normally consolidated clay is a single-valued function of mean effective stress. Two types of tests have been carried out to reveal a ralationship between the wave velocity and the confining pressure which determines uniquely the void ratio of the present clay used. The first one is preferred to Test A, as shown in which the test is performed in Fig.2.13, under the condition of normal consolidation. The second one is the test, corresponding to Test B and Test C in Fig.2.13, where the clay specimen is firstly consolidated under a certain pressure and the confining pressure is then released with some degree without allowing pore water flow in the specimen, that is, the void ratio is remained unchange. It may be seen from the results obtained by Test A,B and C that for the specimen which is normally consolidated, the wave velocity increases with the consolidation pressure with a relation expressed by Eq.(2.1).While, for the specimen subjected to a process of confining pressure described above Test B and C, the velocity does not strongly change with the confining pressure, but seems to depend on a pre-consolidation pressure. Consequently, the wave velocity with which a wave propagates through a clayey soil is a function of only term of the void ratio.

According to the theory of elasticity, the wave velocity of one-dimensional bar wave with no volume change is expressed by

$$C_r = \sqrt{E'/\rho} \quad (2.2)$$

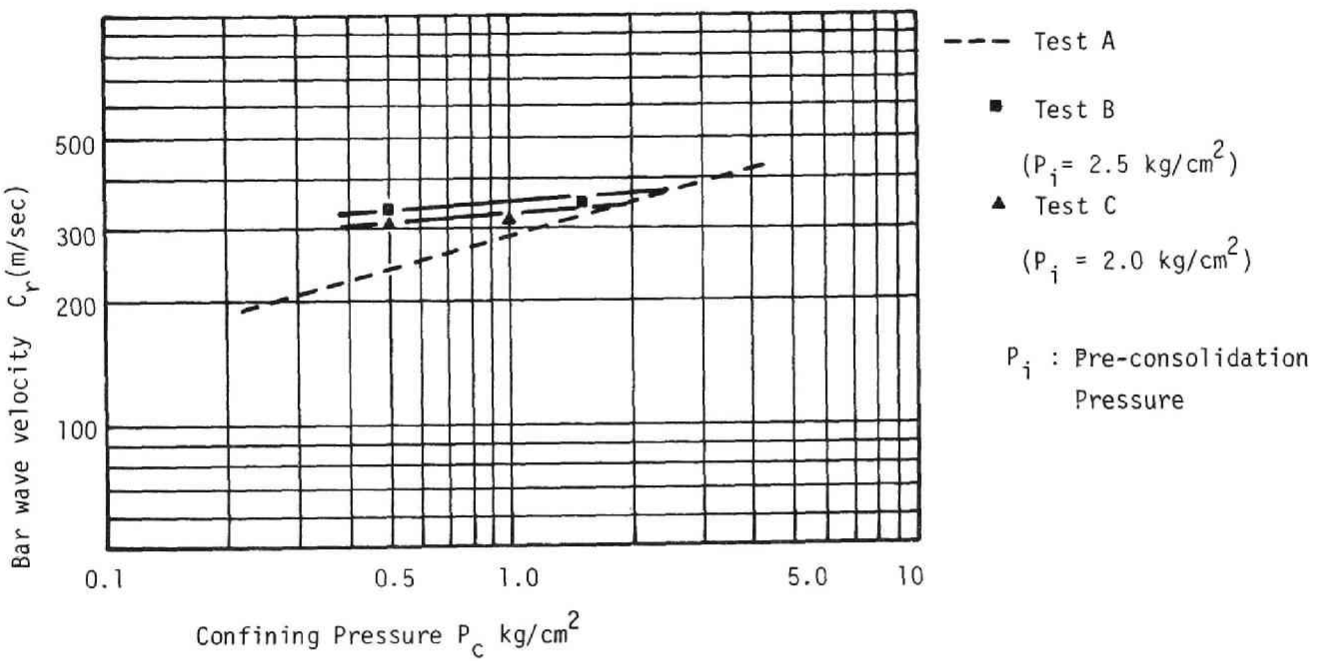

Fig.2.13 Relationship between C_r and P_c.

where E' is a Young's modulus and ρ is the density. Therefore, elastic modulus of soil specimen can be obtained from the velocity of wave front. The derivation of Eq.(2.2) is discussed in Chapter 6.

2.3.2 Attenuation of Peak Stress

Resulting from a dissipation property of soil, stress wave attenuates in the amplitude with travel distance, as well as changes in the form of the wave. These two apparant observations of the wave, are concerned separately to simplify a physical explanation of the phenomena. Figs.2.14 and 2.15 represent the test results of the attenuation of peak stress with the distance, in which a remarkable attenuation of peak stress can be seen. The stress attenuates almost 30 to 50 % by the distance 0.32 m from the top of the specimen,thereafter the rate of attenuation slows down. Vey & Strauss[6] reported the similar results that the stress wave attenuates about 90 % of the total in the first 22.5 cm of the specimen. Fig.2.16 is obtained by rearrangement of the results of stress wave propagation test conducted by Akai, Hori and Shimogami[12]. From Figs.2.14, 2.15 and 2.16, it may be noted that the rate of attenuation behind the position of the soil stress gauge, which locates about 30 cm from the top of the specimen, is greater as the ratio P_0/P_c increases , where P_0 is the amplitude of the input wave and P_c is the confining pressure. While, in case when the test is carried out under the lower confining pressure than the preconsolidation pressure P_i, as described in the previous section,the ratio is taken as P_0/P_i, instead of P_c. The experimental fact that the greater attenuation takes place as the ratio P_0/P_c increases, indicates that characteristics of dissipation of soil are non-linear with respect to stress ratio and/or stress magnitude.

2.3.3 Rise Time and Change of Wave Form

To evaluate a change of wave form, a rise time of stress wave is

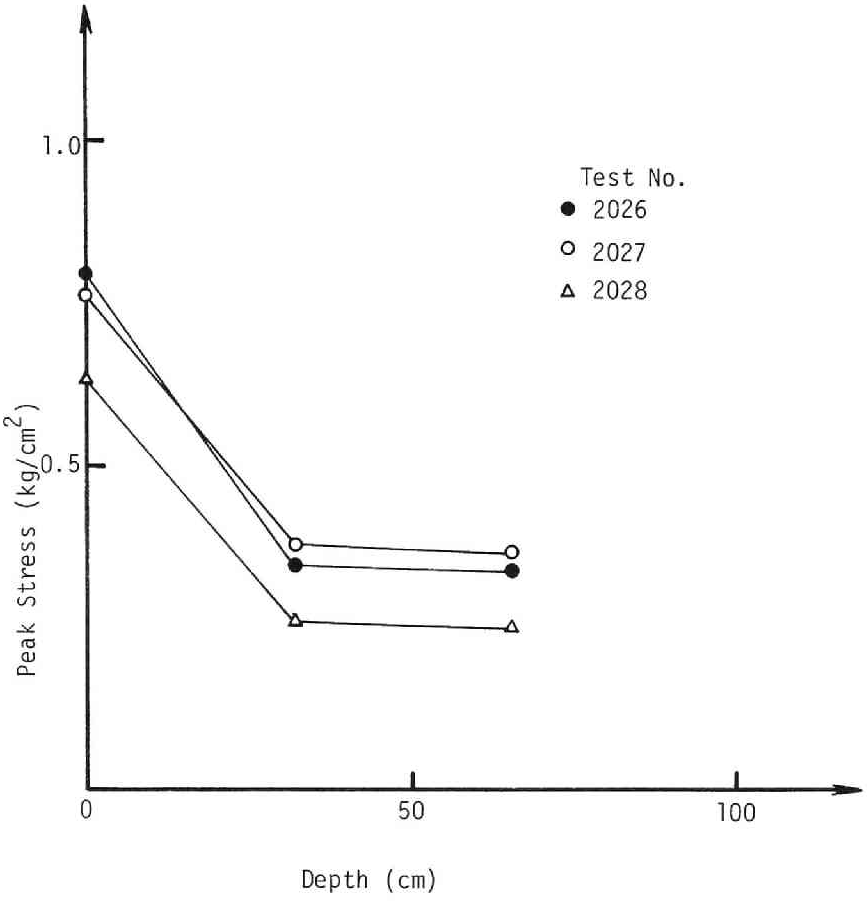

Fig.2.14 Attenuation of peak stress with travelling distance in the propagation test.

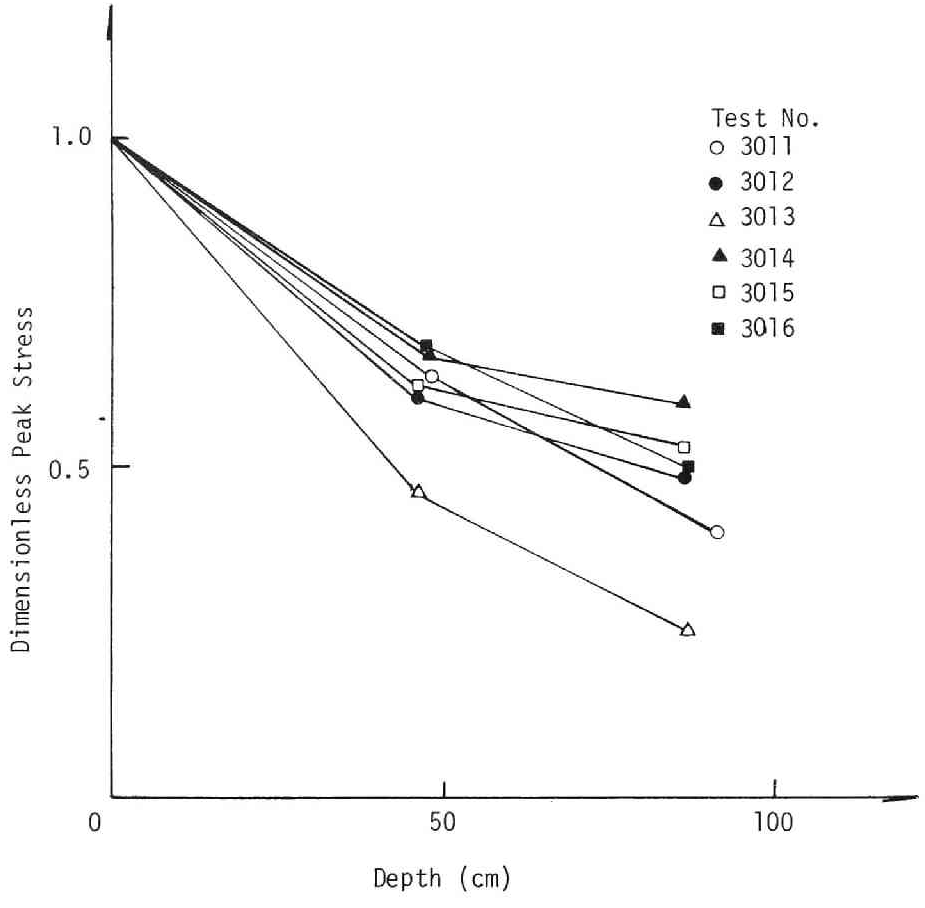

Fig.2.15 Attenuation of peak stress with travelling distance in the propagation test.

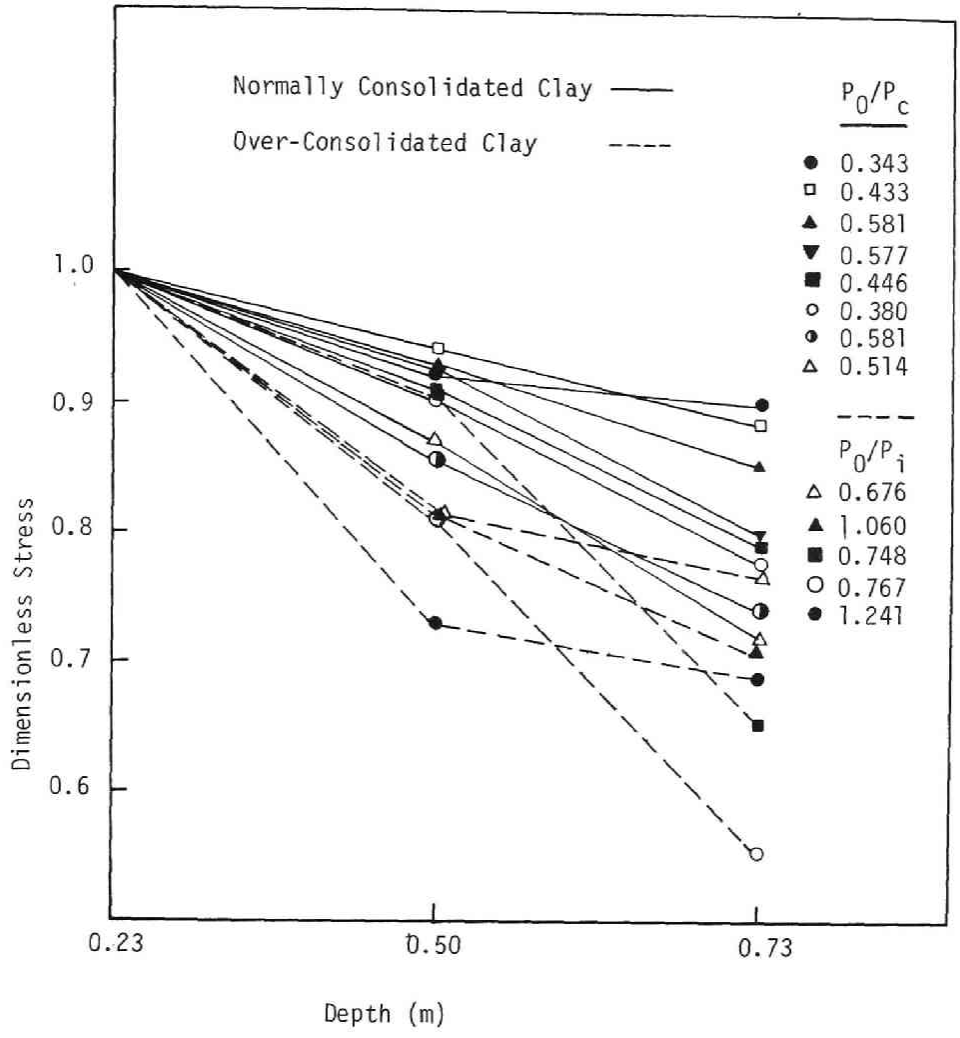

Fig.2.16 Attenuation of peak stress with travelling distance in the wave propagation test.

measured as a difference between the arrival time of wave front and the peak of the wave. From Fig. 2.17, it is shown that the rise time increases with distance and finally approaches constant. The wave form collapses with travelling. It is also seen that the rate of change of the rise time with travelling increases as the stress ratio P_0/P_c increases. From the above discussion in section (2.3.2), the attenuation of a peak stress is considered to be closely related to the change of wave form.

2.3.4 Pore Water Pressure

Pore water pressure is developed under the undrained condition during the stress wave propagation. It is necessary to measure pore water pressure to investigate its behavior in term of effective stress. Up to date, however, the data of pore water pressure during the stress wave propagation have been hardly obtained because of the difficulties in measuring system. In this experiment, pore water pressure is attempted to measure by using a pressure transducer with a needle-like tube filling with porous stone as shown in Fig.2.7.

Fig.2.18 shows the obtained form of pore water pressure of which peak pressure decreases slightly and the rise time increases with travelling time as similar as in the form of the stress. Table 2.2 summarizes the measured value of the peak stress and the peak pore water pressure. It may be noted from this table that a peak value of stress attenuates rapidly more than that of pore water pressure. Rate of increase in the rise time of pore water pressure is greater than that of the stress.The time rate of pore water pressure will be discussed in detail in Chapter 5.

2.3.5 Fourier Transformation of Stress and Pore Water Pressure Waves

The pressure form in the experiment was pulsative and contained the wide range of frequency components. In this section, a pulsative stress wave

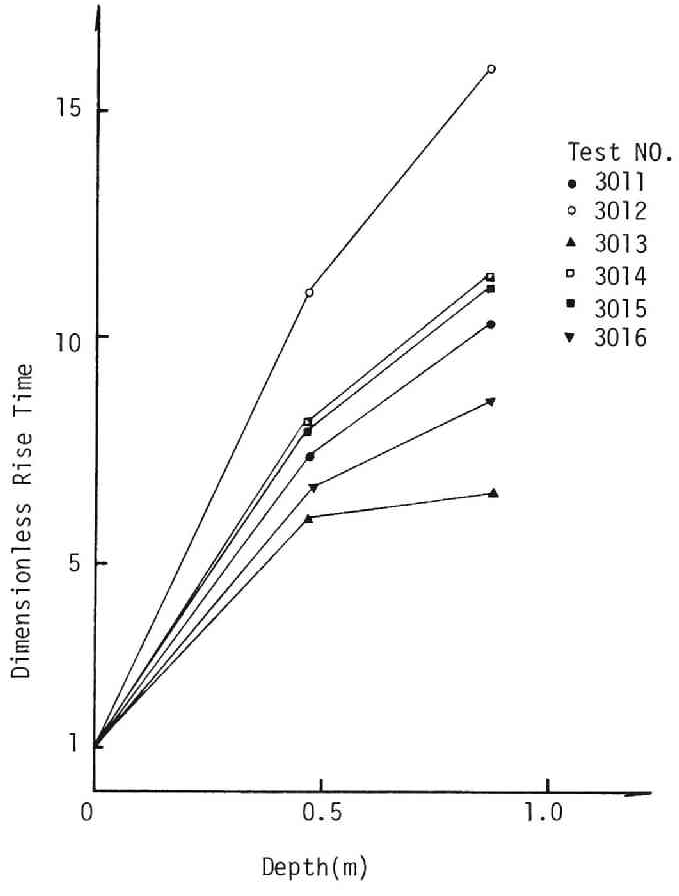

Fig.2.17 Relationship between rise time and depth.

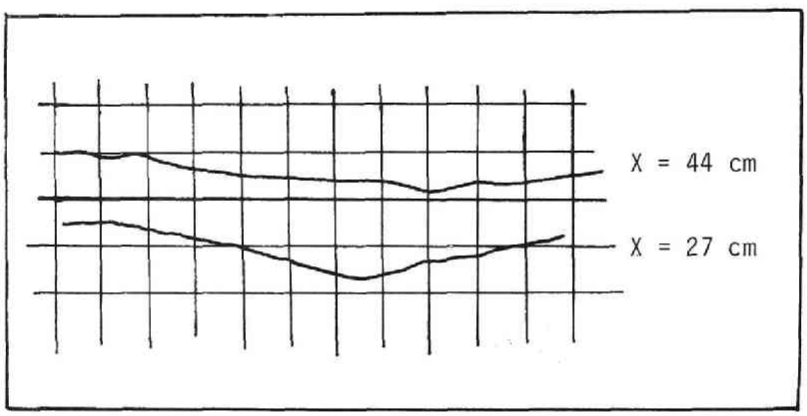

Horizontal Scale (2 msec)
Vertical Scale(0.02kg/cm^2/cm)

Fig.2.18 Typical record of pore water pressure.

TEST NO.	PICKUP	DEPTH m	RISE TIME msec	PEAK STRESS kg/cm^2	P_o/P_c
1	S	86.2	7.6	0.164	0.273
	S	113.0	8.8	0.139	0.232
	P	27.0	12.0	0.051	—
	P	44.0	16.0	0.024	—
2	S	86.2	6.6	0.175	0.292
	S	113.0	7.5	0.142	0.237
	P	27.0	11.2	0.051	—
	P	44.0	14.0	0.016	—
3	S	37.5	7.2	0.242	0.219
	S	68.0	6.5	0.232	0.210
	P	43.5	8.0	0.010	—
	P	58.0	8.8	0.008	—

S :STRESS GAUGE P: PORE PRESSURE GAUGE

p_0: Input peak stress

P_c: Confining pressure

Table 2.2 Measured value of peak stress and peak pore water pressure.

is analyzed into each component of harmonic wave and the character of dispersion is discussed by a point of view of the phase velocity and attenuation coefficient. The method is similar as that used by Collins & Lee [14]. It is assumed that stress wave is smooth and can be replaced by the combination of harmonic wave.

$$\Sigma = A \exp\{i[\omega t+(k+i\hat{\alpha})x]\} \tag{2.3}$$

where Σ is the stress, A:the amplitude, ω ;angular frequency, $\hat{k}$: the wave number and $\hat{\alpha}$ the attenuation coefficient. Σ is transformed by Fourier transformation to Σ',

$$\Sigma' = \frac{1}{T}\int_{-T/2}^{T/2} \Sigma \exp(i\omega t)dt \tag{2.4}$$

$$= A \exp(-\hat{\alpha}x + i\frac{\omega x}{C_p})$$

where $\hat{\alpha}$ and C_p are determined from the position and the phase angle at two different positions.

$$\hat{\alpha} = -\frac{1}{R_2-R_1}\ln\{\Sigma_2'(i\omega)/\Sigma_1'(i\omega)\} \tag{2.5}$$

$$C_p = \omega\frac{R_2-R_1}{\theta_2-\theta_1} \tag{2.6}$$

where C_p is phase velocity, θ_j the phase angle(j =1,2),R_j the position of observation(j=1,2). This analysis is conducted in the range of low stress level of the stress wave where the attenuation is apparantly none.

Fig.2.19 shows the spectrum of stress wave. The predominant frequency range of the stress wave is from 0 to 200 cps.

(1) Phase Velocity

Fig.2.20 shows the relationship between non-dimensional phase velocity

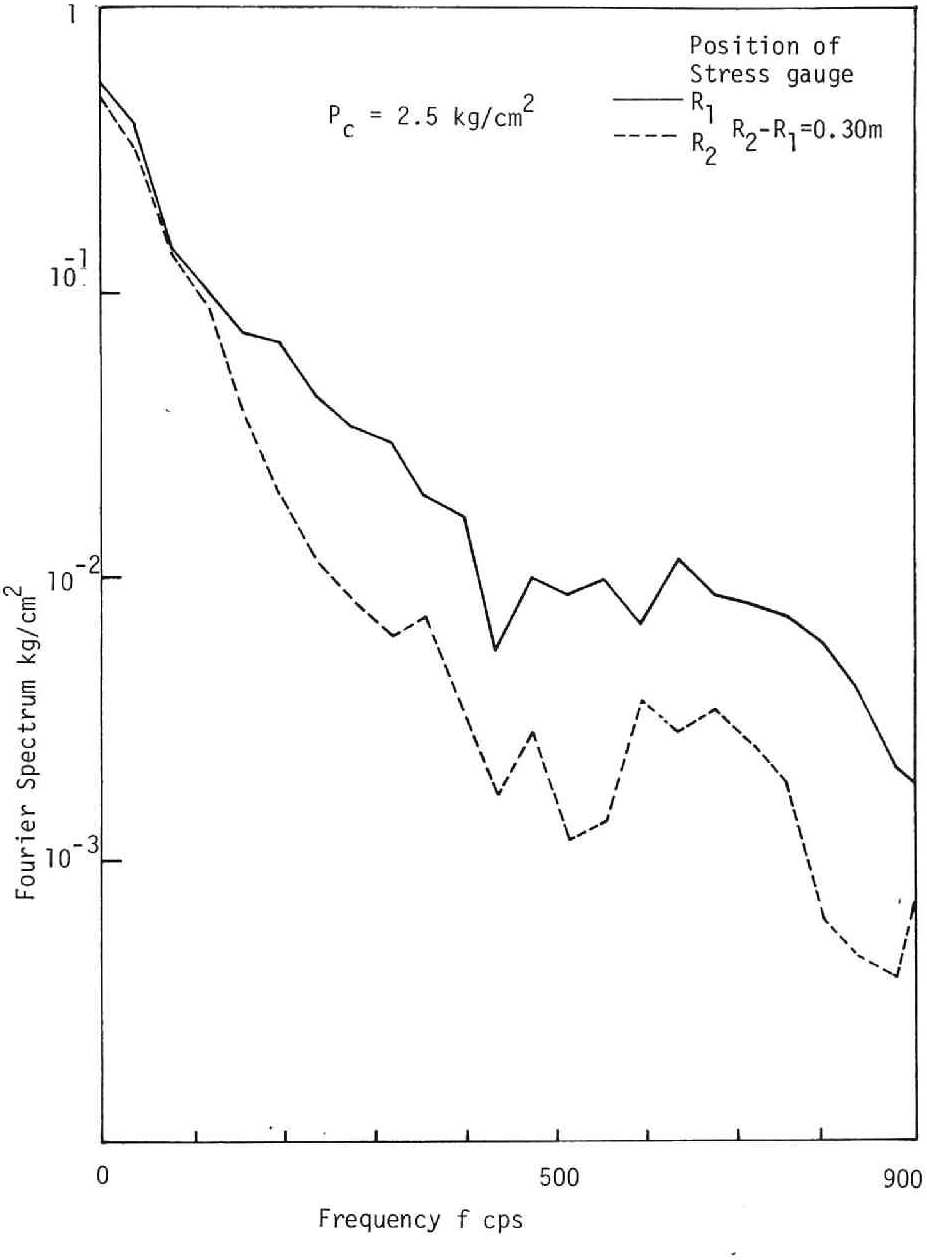

Fig.2.19 Typical Fourier spectrum of stress wave

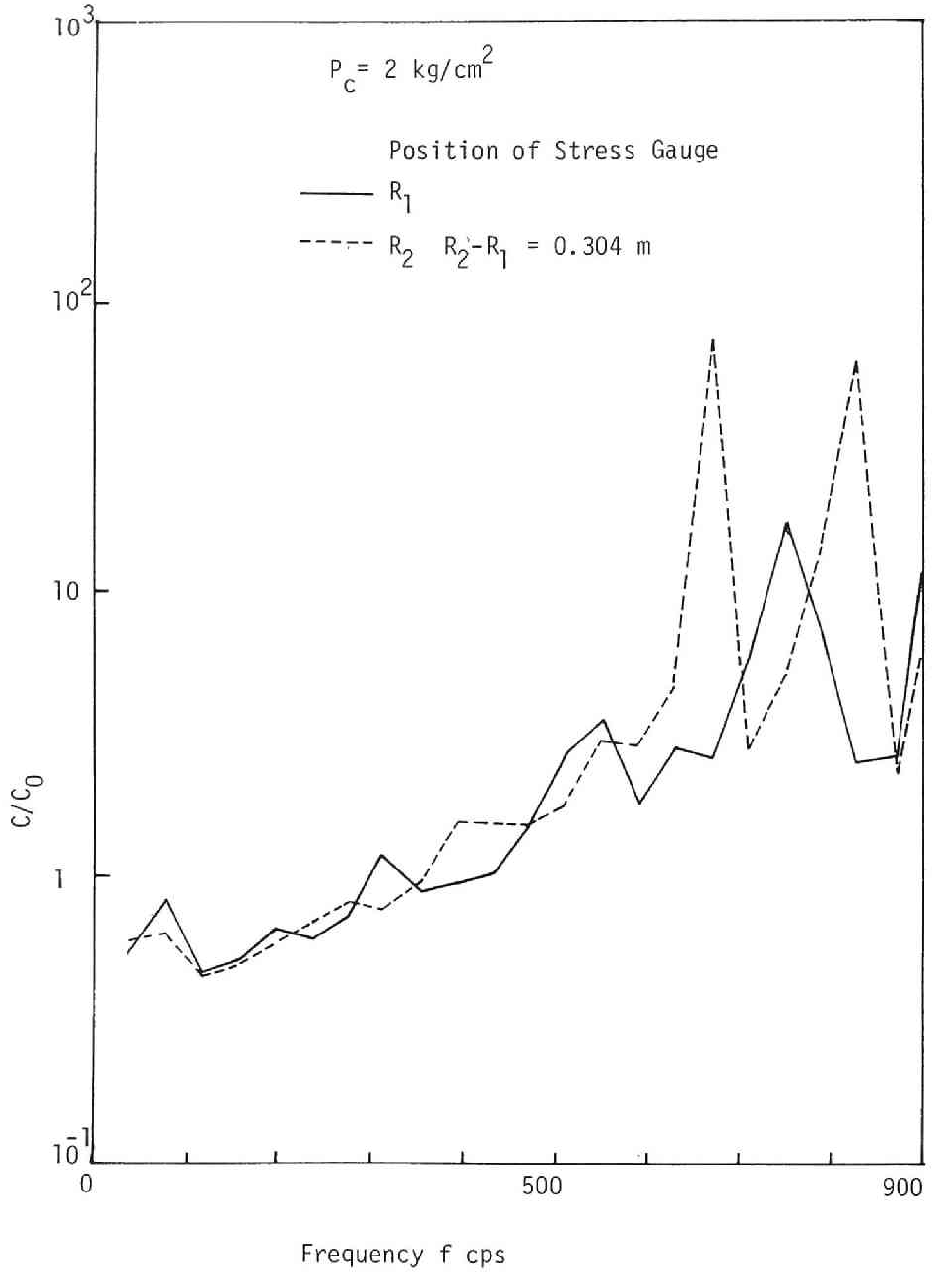

Fig.2.20 Relationship between phase velocity and frequency.

and frequency, where C_0 is a velocity of wave front. The phase velocity has a tendency to increase in the frequency and exceed C_0 at approximately 350 cps. Fig.2.21 also shows the relationship between phase velocity and frequency with dependence of the confining pressure P_c. From this figure, it can be seen that the relationship is not strongly affected by the confining pressure. Under an assumption of the linear viscoelastic body which has an instantaneous elasticity, phase velocity asymptotically approaches the velocity of wave front as the frequency increases. Contrarily, for the linear Voigt type viscoelastic body, phase velocity is always greater than the wave velocity at zero frequency and increases in frequency. Table 2.3 shows the comparison between the average velocity and the local velocity. The local velocity is taken as the velocity measured in the interval between the end of the specimen and the soil stress gauge embeded in the sample. Fig.2.22 shows a relationship between the local velocity and the peak stress at a distance. In this figure, a group of points connected by a straight line are obtained at the same time in the test. It is seen from detail inspection of the results that local velocity gradually decreases as wave propagates. This would be resulting from the gradual change of wave form with travelling. Similarly, accordingly to the wave characteristics of the linear Voigt model, the wave changes considerably and depending on a rate of loading, the apparant wave velocity on the front accordingly changes with travelling distance. From the above discussion and experimental results, it is likely that elastic properties of cohesive soil are described by a linear Voigt model.

(2) Attenuation Coefficient

A degree of attenuation of stress during the wave propagation can be feasibly expressed by the use of attenuation coefficient $\hat{\alpha}$. Figs.2.23,2.24 and 2.25 show the relation between $\hat{\alpha}$ and frequency in relation to the con-

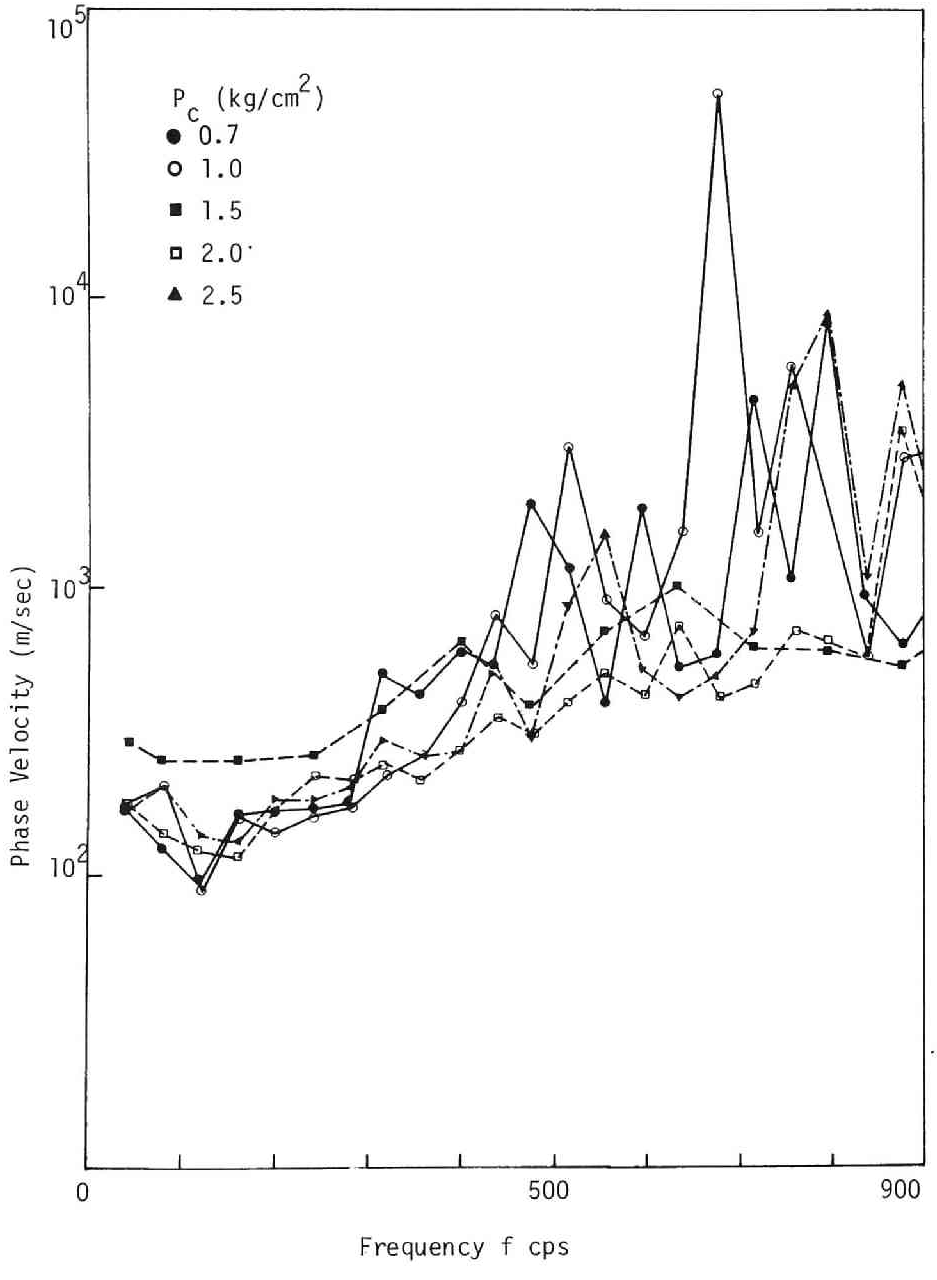

Fig.2.21 Relationship between phase velocity and frequency.

Test No.	P_c Kg/cm^2	Average wave velocity	Local 1 Velocity	Local 2 Velocity
		m/sec	Loadcell → Gage 1	Gage 1 → Gage 2
2022	0.5	242	——	246
2023	1.0	248	——	320
3011	0.3	217	248	141
3012	0.6	264	469	291
3013	1.0	295	390	337
3014	2.0	349	413	422
3015	1.0	319	434	400
3021	0.8	319	376	253

Table 2.3 Comparison of average wave velocity and local velocity.

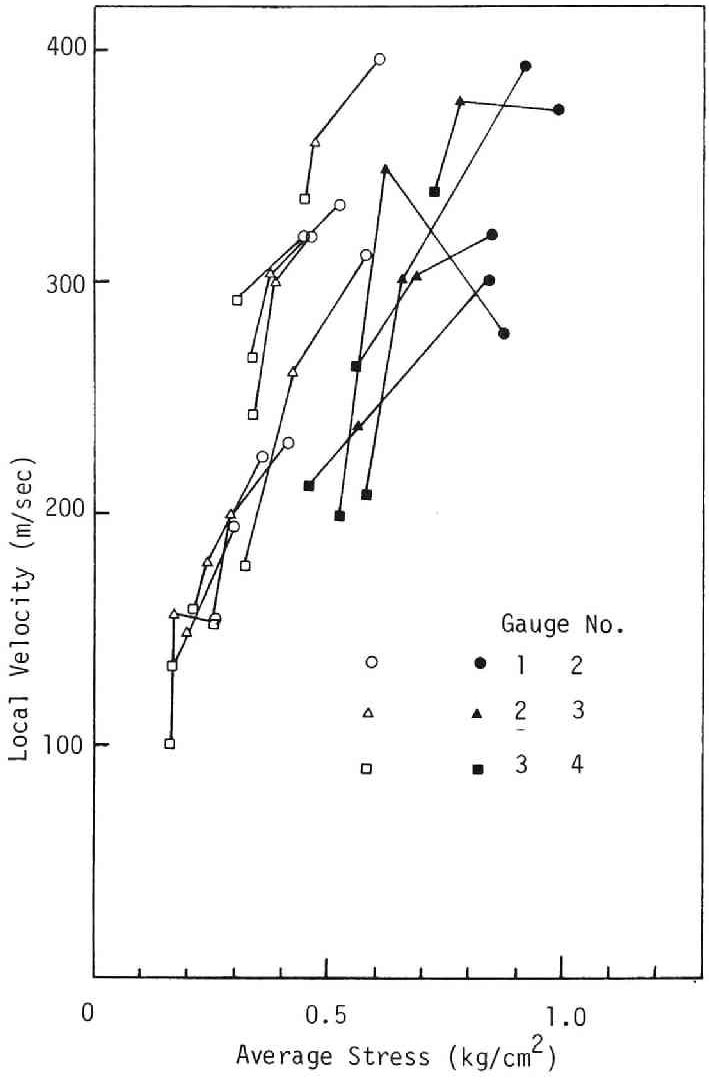

Fig.2.22 Relationship between local velocity and peak stress.

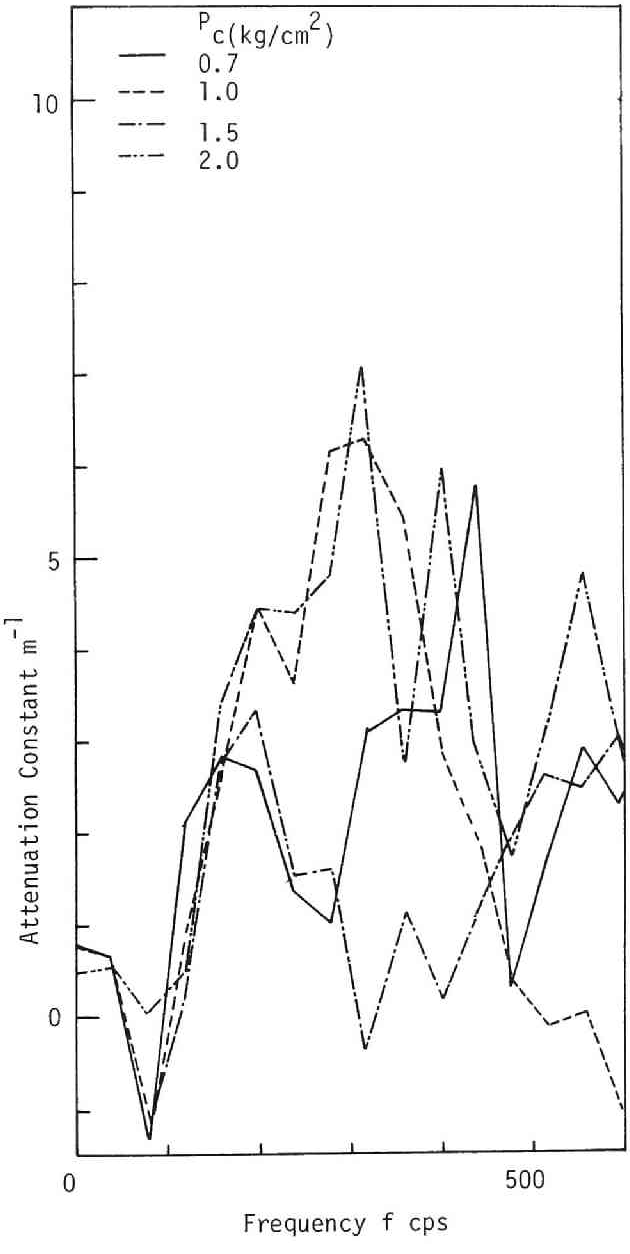

Fig.2.23 Relationship between attenuation coefficient and frequency.

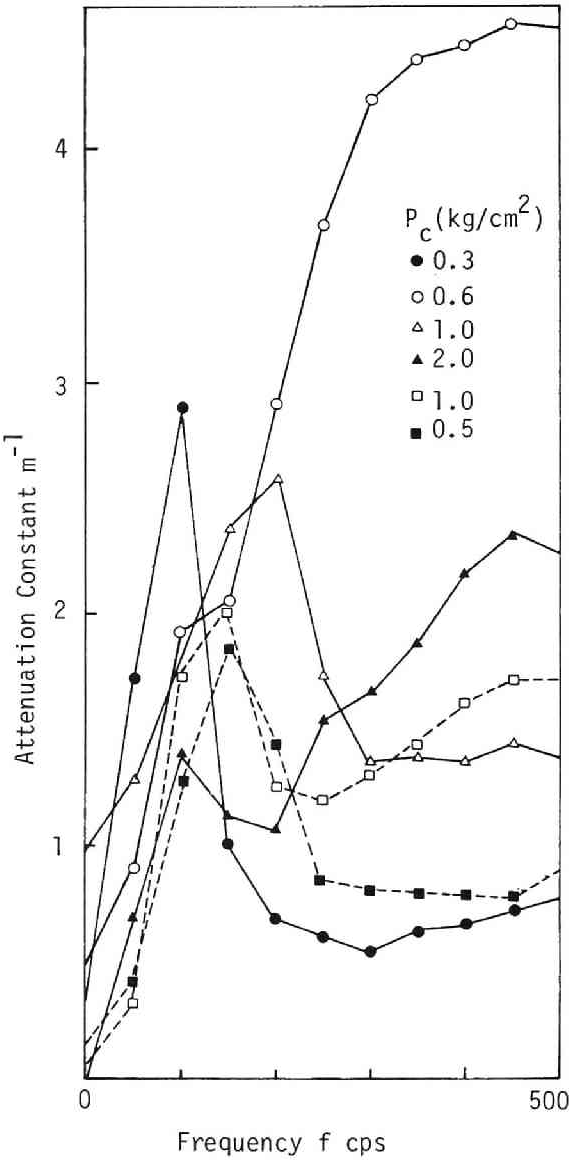

Fig.2.24 Relationship between attenuation coefficient and frequency.

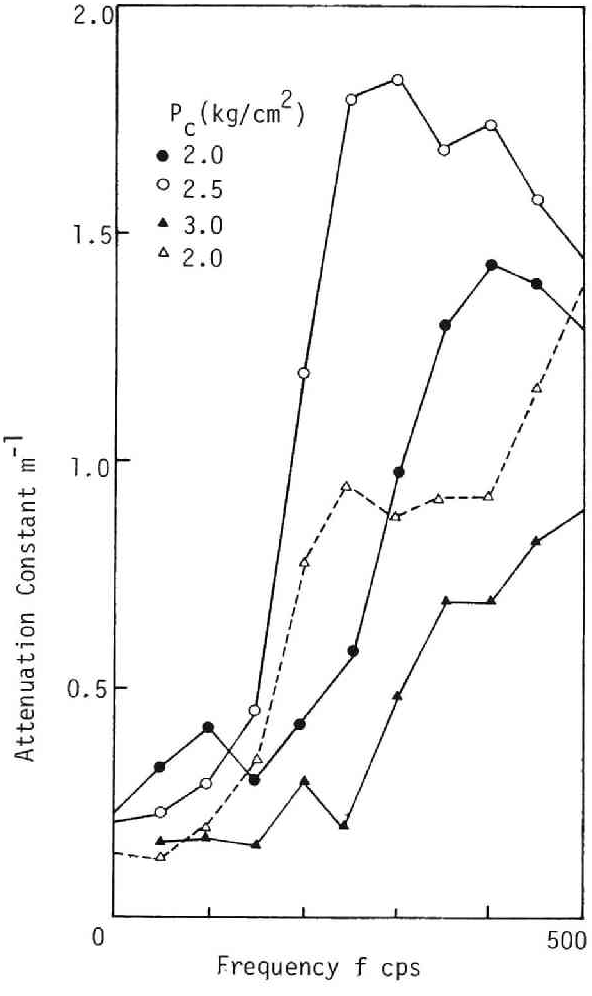

Fig.2.25 Relationship between attenuation coefficient and frequency.

fining pressure. From these figures, it can be seen that the attenuation coefficient increases generally with the frequency. $\hat{\alpha}$ begins to increase starting from almost 0 cps in Fig.2.24, on the other hand, starting from almost about 100 cps for the results shown in Fig.2.25, which have been obtained from the test performed under relatively high confining pressure. The tendency is that $\hat{\alpha}$ does not increase monotonously, but maximum value occurs between 150 cps to 400 cps, depending on confining pressure. It is also noticed that absolute value of $\hat{\alpha}$ gets smaller with increase of the confining pressure. Considering from the experimental results and these Fourier spectrum of the phase velocity and the attenuation coefficient, one of the main conclusions is drawn that C/C_0 is less than 1.0 and $\hat{\alpha}$ increases appreciably in a range of frequency between 0 to 100 cps. These natures are similar as these of the linear spring-Voigt model.[15] Consequently, the wave characteristcis of this soil sample under a low stress level and a limited frequency range might be able to be explained by using this model.

(3) Fourier Transformation of Pore Water Pressure Wave

Fig.2.26 shows the Fourier spectrum of pore water pressure wave. It is analyzed in a frequency range mainly between 0 to 160 cps. From Figs. 2.26 and 2.19, it can be seen that two spectra have a similar tendency. The relationship between phase velocity and frequency of pore water pressure is shown in Fig.2.27. As described for the stress wave, phase velocity exceeds the velocity of wave front as frequency increases. Fig.2.28 shows the relation between the attenuation coefficient and the frequency. The attenuation coefficient is oscillating in a wide range of frequency, but the mean value is almost constant. This is not similar to that of stress wave. This reason is considered as follows. The pore water pressure depends not only on the mean stress, but also the dilatancy character of soil. In other

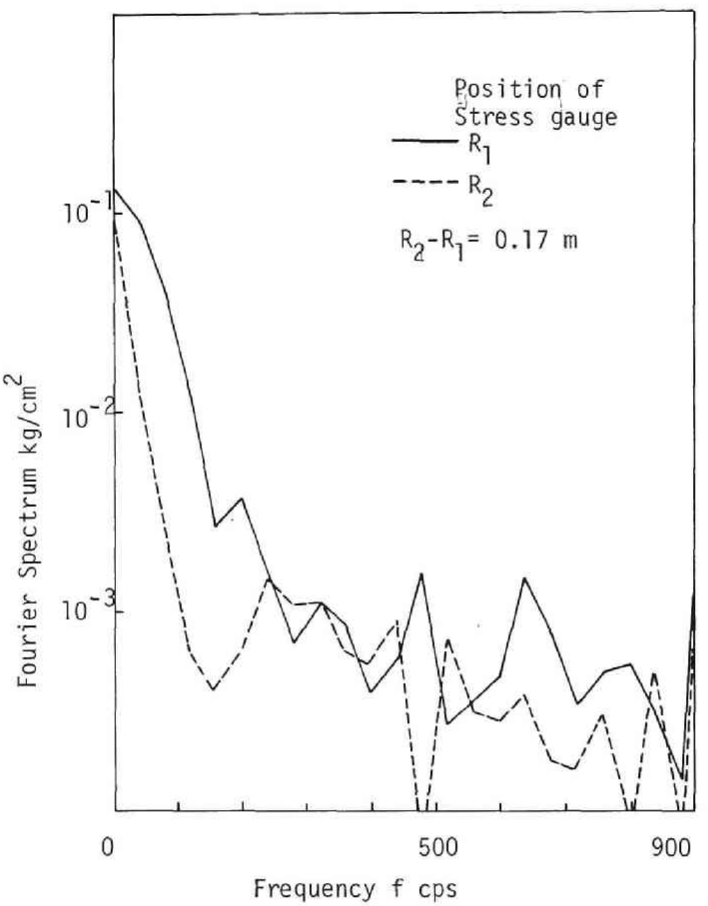

Fig.2.26 Fourier spectrum of pore water pressure.

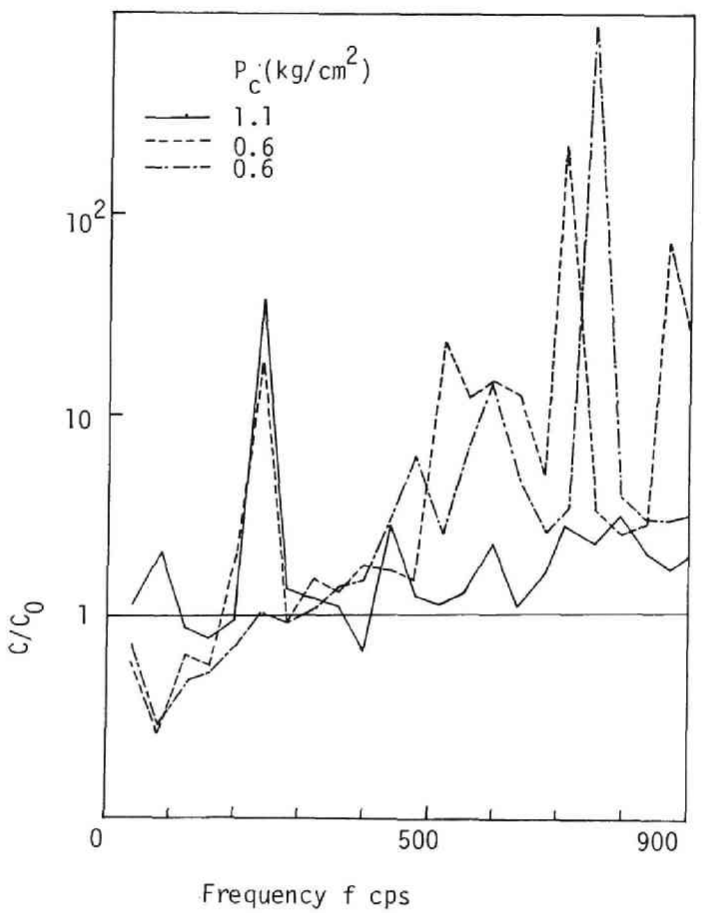

Fig.2.27 Relationship between non-dimensional phase velocity and frequency.

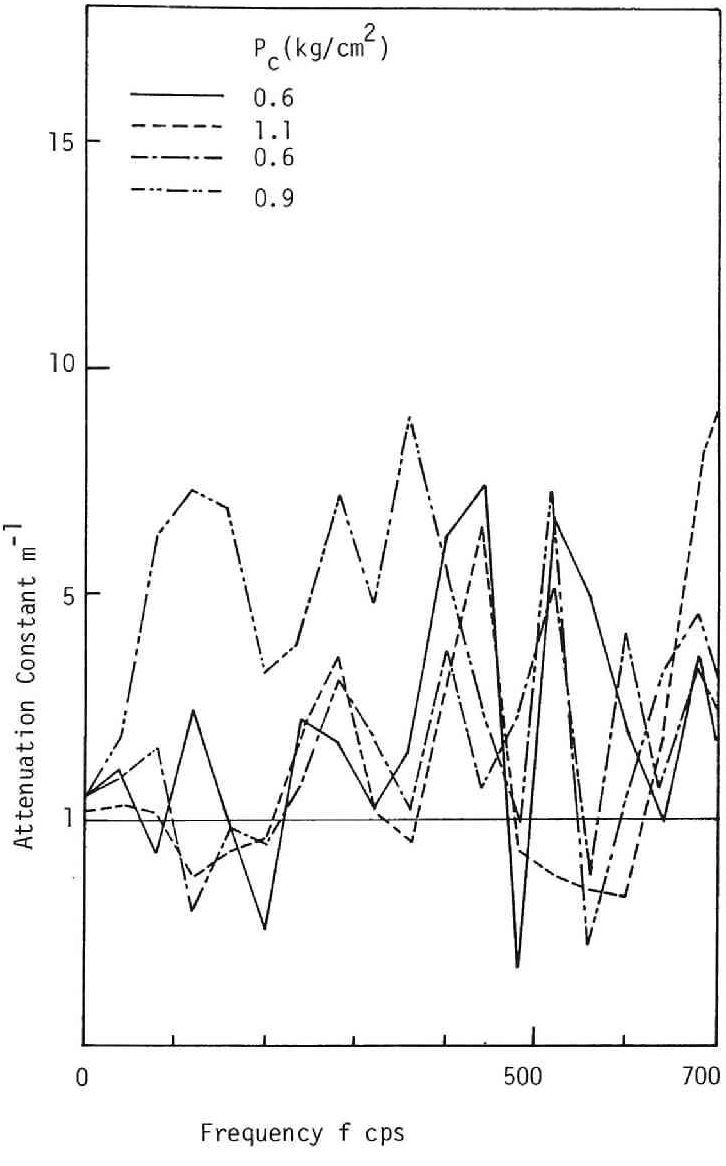

Fig.2.28 Relationship beween attenuation coefficient and frequency.

word, the generation of pore water pressure is due to the variation of total stress and the effective stress.

2.4 Conclusions

In this chapter, stress wave propagation characteristics of consolidated silty clay have been studied by means of the special triaxial cell connected with the shock tube. The bar wave was observed at the experiment. The velocity of wave front, the attenuation of stress, the change of wave form and pore water pressure were discussed in detail. Moreover, Fourier transform technique was used in order to obtain the attenuation coefficient and phase velocity at the low stress level. The wave velocity reflects the elastic properties of cohesive soil and the mechanism of energy dissipation can be considered from the attenuation of stress. Throughout of this chapter, the following main conclusions are obtained.

(1) The peak stress attenuates almost 30-50 % within 0.32 m from the top of the specimen, thereafter gradually attenuates.

(2) The attenuation of the stress during propagation depends on the ratio P_0/P_c; P_0 is the input peak stress and P_c is the confining pressure. In other words, the dissipation property of cohesive soil is dependent upon the stress level.

(3) The relationship between bar wave velocity(c_r;m/sec) and confining pressure(P_c;kg/cm^2) under the normally consolidated states is given by $c_r = 290 P_c^{0.25}$.

(4) From the test results carried out under the condition that the void ratio is constant and the cell pressure is less than the consolidation pressure, it is concluded that the wave velocity mainly depend on the pre-consolidation pressure.

(5) The rise time which represents the change of wave form increases with distance and thereafter becomes constant. Besides, the rate of change

of the rise time increases as the stress ratio P_0/P_c increases.

(6) The pore water pressure could be measured by the pressure transducer with a needle-like tube filling with porous stone. The maximum value of the pore water pressure decreases and rise time increases with travelling.

(7) The pulsative waves of stress and pore water pressure observed in the experiment contain the wide range of frequency component, predominantly 0 to 200 cps in stress wave and 0 to 160 cps in pore water pressure wave at low stress level.

(8) The phase velocity of stress and pore water pressure waves is greater than the velocity of wave front at low frequency and increases with the frequency. The trend is similar to that of linear Voigt model.

(9) The attenuation coefficient $\hat{\alpha}$ of stress wave becomes large as the frequency increases and a maximum value occurs in a frequency range between 150 to 400 cps. Increasing in a confining pressure, $\hat{\alpha}$ decreases and the frequency increases at which $\hat{\alpha}$ reaches the maximum.

(10) From the conclusions (8) and (9), in the range of the frequency less than 100 cps, the viscoelastic property of cohesive soil can be described by a linear spring-Voigt model.

(11) The relationship of the attenuation coefficient $\hat{\alpha}$ of pore water pressure to the frequency is not similar to that of stress wave. This is due to that the development of pore water pressure depends not only on the total stress, but also on the dilatancy effect.

References for Chapter 2

1) Whitman, R. V. : Testing Soils with Transient Loads, Conf. Soils Engineering Purpose, Mexico City, ASTM, Spec. Tech. Publ., No.232, 1957, pp.242-267.

2) Salvadori, M.G., R. Shalak and P. Weidlinger: Waves and Shocks in Locking and Dissipative Media, Proc. ASCE, Vol.86, No.EM2, 1960, pp.77-105.

3) Heierli, W.: Inelastic Wave Propagation in Soil Columns, Proc.ASCE, Vol.88 , No.SM6, 1962, pp.33-63.

4) Stoll, R.D. and I.A. Ebeido : Shock Waves in Granular Soil, Proc. ASCE, No.SM4, pp.107-125.

5) Seaman, L.: One-dimensional Stress Wave Propagation in Soils, Stanford Research Inst., AD-632106, DASA 1757, 1966, pp.19-40.

6) Vey, E. and L.V. Strauss: Stress-Strain Relationships in Clay Due to Propagating Stress Waves, Proc. Int. Symp. on Wave Propagation and Dynamic Properties of Earth Materials, 1967, pp.575-586.

7) Hampton, D. and R.A. Wetzel : Stress Wave Propagation in Confined Soils, Proc. Int. Symp. on Wave Propagation and Dynamic Properties of Earth Materials, 1967, pp.433-442.

8) Akai, K., M. Hori and T. Shimogami: Study on Stress Wave Propagation through Saturated Cohesive Soils by Means of Triaxial Shock Tube, Proc. JSCE. No.228, August 1974, pp.99-108.

9) Akai, K., M. Hori, N. Ando and T. Shimogami : Shock Tube Study on Stress Wave Propagation in Confined Soils, Proc. JSCE, No.200, April, 1972, pp.127-141.

10) Anderson, D.G. and F.E. Richart, Jr. : Stress-History Effects on

Shear Modulus of Soils, Soils and Foundations, Vol.13, No.1, March, 1973, pp.77-95.

11) Anderson, D.G. and F.E. Richart, Jr. : Temperature Effect on Shear Wave Velocity in Clays,Journal of the Geotechnical Engineering Division, ASCE, Vol.100, No.GT12, Dec.,1974, pp.1316-1320.

12) Hardin, B.D. and W.L.Black : Vibration Modulus of Normally Consolidated Clay, Proc. ASCE, Vol.94, No.SM2, 1968, pp.353-369.

13) Afifi, S.S. and F.E. Richart : Stress-History Effects on Shear Modulus of Soils, Soils and Foundations, Vol.13, No.1, pp.77-95.

14) Collins, F. and C.C. Lee : Seismic Wave Attenuation Characteristics from Pulse Experiments, Geophysics, Vol.21, No.1, Jan., 1956, pp.16-40.

15) Akai,K. and M. Hori: Considerations of Wave Characteristics in Soil Assumed as a Viscoelastic Material, Proc. JSCE, No.221, Jan., 1974, pp.81-91.

Chapter 3 Thermodynamic Theory of Inelastic Materials

3.1 General Remarks

Generally, the deformation of material is accompanied with the energy dissipation. The macroscopic energy dissipation is due to the internal elementary process on a micro scale. There have been developed two methods to treat analytically the energy dissipation, i.e."macroscopic" and "microscopic". The microscopic motion of internal structure cannot be observed with a present technique. So, in this chapter, the energy dissipation is treated from the macroscopic viewpoint.

There exist several phenomenological approaches which account for the energy dissipation of continuum. The most simplest one is to introduce a viscous stress which depends upon the rate of strain. The second one is to assume that the entire history of strain influences the stress on a manner so as to be compatible with a principle of fading memory.[1] This method demands the entire history of material in order to predict a future thermomechanical response. But this seems to be impossible in practice. The last one is to postulate internal state variables which influence the dissipation effects. This idea includes the theory of plasticity, viscoplasticuty and viscoelasticity. The state of the unit system of continuum is determined, not only by the quantity which is observed on the surface of the unit system, but also by the quantity which governs the internal structure of the material. The quantity which is not able to be observed on the surface of unit system of the material, is referred as internal state variable. For example, a displacement of interior point in a mass relative to their equilibrium position is considered to be internal variable.

These phenomenological theories must be based on the thermodynamical

laws. Many investigators have been studying the thermodynamics of continuous media; Onsager, Coleman & Noll [2], Meixner [3], Truesdell [4], Müller [5], Valanis [6], Day [7], Nemat-Nasser [8] and Coleman & Owen [9] et al.. Onsager, Biot [10], Ziegler [11], Coleman & Noll, Valanis and Nemat-Nasser introduce the internal state variables to formulate the non-equilibrium thermodynamics. Coleman and Gurtin [12] developed the internal state variable theory based on the thermodynamics of continuous media developed by Coleman & Noll [2]. They assumed the existence of entropy, internal state variables and the evolutionary equation governing the internal state variables axiomatically. Valanis and Nemat-Nasser used the generalized or modified Caratheodory's principle as the second law of thermodynamics. Furthermore, with assumption of the first law of thermodynamics and the existence of temperature, they tries to establish the non-equilibrium thermodynamics involving the internal state variables. They consequently showed that the existence of entropy could be reduced from the postulate of internal variables and the entropy played a role of a potential at a constant value of internal variables. The constitutive theory of continuous medium introducing a continuous distribution of internal state variables has been developed by Perzyna [13], Kratochivil [14], Kröner [15], Mróz [16], Valanis, Lubliner [17], Rice [18], Mandel [19] et al.. In this chapter, the author will derive the constitutive theory of inelastic materials based on a Coleman & Noll's non-equilibrium thermodynamics.

3.2 Preliminaries

Introducing a rectangular Cartesian coordinate fixed in a space, the coordinate of any particle is expressed by X_K in Lagrangian form and x_k in current coordinate. A motion of the body is described by

$$x_k = x_k(X_K, t) \qquad (k,K = 1,2,3) \tag{3.1}$$

where x_k represents a single function of position X_K and time t. The line element of the substance is denoted by the following equations;

$$dS^2 = dX_K dX_K \tag{3.2}$$

$$ds^2 = dx_k dx_k = x_{k,K} x_{k,L} dX_K dX_L \tag{3.3}$$

The strain tensor E_{KL} in Lagrangian form is defined by Eq.(3.4), using Kronecker's delta δ_{KL};

$$\begin{aligned} ds^2 - dS^2 &= (x_{k,K} x_{k,L} - \delta_{KL}) dX_K dX_L \\ &= 2E_{KL} dX_K dX_L \end{aligned} \tag{3.4}$$

Cauchy's stress tensor t_{kl} is expressed by a second Kirchhoff stress tensor T_{KL} as follows:

$$t_{kl} = \frac{\rho}{\rho_0} x_{k,K} x_{l,L} T_{KL} \tag{3.5}$$

where ρ is the current density and ρ_0 is the initial density.

The deformation velocity tensor is defined by

$$d_{ij} = \dot{E}_{KL} X_{K,i} X_{L,j} \tag{3.6}$$

where a dot denotes the time derivative of the variable.

3.3 Thermodynamics Based on the Clausius-Duhem Inequality

The energy balance equation for non-polar case in the local form is expressed as follows;

$$\rho\dot{\varepsilon} - t_{kl} d_{kl} = \rho r + \mathrm{div} q \tag{3.7}$$

where ε denotes the internal energy density, q the heat flux vector and r the heat supply per unit time and unit mass.

Fundamental thermodynamical assumptions have been stated by many ways. As mentioned before, Valanis and Nemat-Nasser used the Caratheodory's principle. And introducing the entropy by the fundamental thermodynamical inequality and the principle of fading memory. Day's inequality is less restrictive than the Clausius-Duhem inequality. On the other hand, Coleman & Owen axiomatically reduced the entropy function as the upper potential of the quantity $[\int_0^t (r - \frac{\mathrm{div}(q)}{\rho})/\theta dt + \int_0^t q_i \frac{1}{\rho\theta^2}\theta_{,i}\, dt]$ called an action (where θ is a temperature and $\theta_{,i}$ shows $\partial\theta/\partial x_i$) and stated the second law of thermodynamics by the property of the action. In this thesis, the author is based on the Clausius-Duhem inequality for the formulation of a constitutive equation.

In the homogeneous process,the Clausius-Plank's inequality is given by

$$\dot{H} \geq \frac{Q}{\theta} \tag{3.8}$$

where H is the entropy of the body, Q the heating and θ the absolute temperature.

In the non-homogeneous process, the Clausius-Duhem inequality may now be written by

$$\dot{H} \geq \int_S \frac{q}{\theta} ds + \int_V \frac{\rho r}{\theta} dv \tag{3.9}$$

In the local form, the above equation can be rewritten,

$$\theta\rho\dot{\eta} - \rho r - \theta \mathrm{div}\left(\frac{q}{\theta}\right) \geq 0 \tag{3.10}$$

where η is the entropy density. In a view of Eq.(3.7), this becomes

$$\rho\dot{\eta} - \frac{1}{\theta}(\rho\dot{\varepsilon} - t_{kl} d_{kl}) + \frac{1}{\theta^2} q_k \theta_{,k} \geq 0 \tag{3.11}$$

The internal dissipation δ is defined as subtraction of local heating from the product of the rate of the entropy and the temperature.

$$\delta \equiv \theta\dot{\eta} - \frac{1}{\rho}(\mathrm{div}(h) + \rho s) \tag{3.12}$$

Accounting for the Clausius-Plank inequality in the homogeneous process, the Plank's inequality is given by

$$\delta \geq 0 \tag{3.13}$$

The free energy density ψ is now introduced which is defined as

$$\psi = \varepsilon - \theta\eta \tag{3.14}$$

Complementary energy density function ϕ is also introduced by

$$\phi = \frac{1}{\rho_0} E_{KL} T_{KL} - \psi \tag{3.15}$$

Then

$$\dot{\phi} = \frac{1}{\rho_0} (\dot{E}_{KL} T_{KL} + E_{KL} \dot{T}_{KL}) - \dot{\psi} \tag{3.16}$$

Differentiating Eq.(3.14) and substituting this into Eq.(3.16), the following equation is derived from Eq.(3.11),

$$-\eta\dot{\theta} + \dot{\phi} - \frac{1}{\rho_0} E_{KL} \dot{T}_{KL} + \frac{1}{\rho_0 \theta} q_k \theta_{,k} \geq 0 \tag{3.17}$$

$$\delta + \frac{1}{\rho_0 \theta} q_k \theta_{,k} \geq 0 \tag{3.18}$$

On the other hand, Fourier's inequality is expressed by

$$q_k \theta_{,k} \geq 0 \tag{3.19}$$

Therefore, Eqs.(3.18) and (3.13) cannot be reduced from Eq.(3.10) independently. Coleman & Noll's thermodynamics is based on the idea that Eq.(3.17) is the identical inequality, and the body force and r can be determined to satisfy the equation of motion and Eq.(3.7) if T_{KL}, ε, q_K and the motion of the body are given. Müller [20] criticized this point and pointed out that determing r and b may be impossible. And also, in Müller's thermodynamics, the assumption used in Eq.(3.8) that entropy flux and heat flux over temperature are equal is omitted. Instead, he introduced the independent entropy flux subject to the constitutive assumption.

3.4 Constitutive Assumption

It is assumed that the behavior of material at the point X_K is characterazed by six response functions;

$$\begin{aligned}
\phi &= \hat{\phi}(\, T_{KL},\, P_{KL},\, \kappa,\, \theta,\, g_k \,) \\
\eta &= \hat{\eta}(\, T_{KL},\, P_{KL},\, \kappa,\, \theta,\, g_k \,) \\
E_{KL} &= \hat{E}_{KL}(T_{KL},\, P_{KL},\, \kappa,\, \theta,\, g_k \,) \\
q_k &= \hat{q}_k(\, T_{KL},\, P_{KL},\, \kappa,\, \theta,\, g_k \,) \\
\dot{P}_{KL} &= \hat{\dot{P}}_{KL}(T_{KL},\, P_{KL},\, \kappa,\, \theta,\, g_k \,) \\
\dot{\kappa} &= \hat{\dot{\kappa}}(\, T_{KL},\, P_{KL},\, \kappa,\, \theta,\, g_k \,)
\end{aligned} \tag{3.20}$$

where g_k is the temperature gradient, P_{KL} and κ are internal state variables. Generally, the internal state variables are the components of n-th order tensor. Here, in order to simplify the reduction of the theory, only scalar and second order tensor are used as the internal variables.

The rate equation of ϕ is given by

$$\dot{\phi} = \frac{\partial \phi}{\partial T_{KL}} \dot{T}_{KL} + \frac{\partial \phi}{\partial P_{KL}} \dot{P}_{KL} + \frac{\partial \phi}{\partial \kappa} \dot{\kappa} + \frac{\partial \phi}{\partial \theta} \dot{\theta} + \frac{\partial \phi}{\partial g_k} \dot{g}_k \tag{3.21}$$

Substituting Eq.(3.21) into Eq.(3.17), we get

$$\left(\frac{\partial \phi}{\partial T_{KL}} - \frac{1}{\rho_0} E_{KL}\right) \dot{T}_{KL} + \frac{\partial \phi}{\partial P_{KL}} \dot{P}_{KL} + \frac{\partial \phi}{\partial \kappa} \dot{\kappa} + \left(\frac{\partial \phi}{\partial \theta} - \eta\right) \dot{\theta} + \frac{\partial \phi}{\partial g_k} \dot{g}_k > 0 \tag{3.22}$$

Following a Coleman's method, we get the relations as follows:

$$\frac{1}{\rho_0} E_{KL} = \frac{\partial \phi}{\partial \bar{T}_{KL}} \tag{3.23}$$

$$\eta = \frac{\partial \phi}{\partial \theta} \tag{3.24}$$

$$\frac{\partial \phi}{\partial g_k} = 0 \tag{3.25}$$

$$\frac{\partial \phi}{\partial P_{KL}} \dot{P}_{KL} + \frac{\partial \phi}{\partial \kappa} \dot{\kappa} \geq 0 \tag{3.26}$$

In view of Eq.(3.25), g can be excluded from the independent variables of ϕ .

3.5 Stability of Solution

Coleman and Gurtin [12] defined the "attraction domain of constant temperature and strain" and discussed the stability of the solution of differential equation governing the internal state variables. Following the treatment used by Coleman & Gurtin, the stability of the solution of Eq.(3.20) is discussed. From Eq.(3.14), the following equation can be reduced.

$$\dot{\psi} = \frac{\partial \psi}{\partial E_{KL}} \dot{E}_{KL} + \frac{\partial \psi}{\partial \theta} \dot{\theta} + \frac{\partial \psi}{\partial P_{KL}} \dot{P}_{KL} + \frac{\partial \psi}{\partial \kappa} \dot{\kappa} \tag{3.27}$$

Substituting Eqs.(3.14) and (3.27) into Eq.(3.22),

$$(\eta + \frac{\partial \psi}{\partial \theta})\dot{\theta} + \frac{\partial \psi}{\partial g_k}\dot{g}_k + (\frac{\partial \psi}{\partial E_{KL}} - \frac{1}{\rho_0} T_{KL})\dot{E}_{KL}$$

$$- \frac{\partial \psi}{\partial P_{KL}}\dot{P}_{KL} - \frac{\partial \psi}{\partial \kappa}\dot{\kappa} \geq 0 \qquad (3.28)$$

Since $\dot{\theta}$, $\dot{g}$ and $\dot{E}_{KL}$ are given as arbitrary values, these equation must be established.

$$\eta = \frac{\partial \psi}{\partial \theta} \quad , \quad \frac{\partial \psi}{\partial g_k} = 0 \quad , \quad T_{KL} = \rho_0 \frac{\partial \psi}{\partial E_{KL}} \qquad (3.29)$$

Therefore,

$$\dot{\phi} = \frac{1}{\rho_0} E_{KL}\dot{T}_{KL} + \eta\dot{\theta} - \frac{\partial \psi}{\partial P_{KL}}\dot{P}_{KL} - \frac{\partial \psi}{\partial \kappa}\dot{\kappa} \qquad (3.30)$$

If E_{KL} and θ are constant, the following inequality is given

$$- \dot{\psi} = - \frac{\partial \psi}{\partial P_{KL}}\dot{P}_{KL} + - \frac{\partial \psi}{\partial \kappa}\dot{\kappa} \geq 0 \qquad (3.31)$$

When $\psi > 0$, ψ is identical to a Lyapunov function and the solution (E_{KL}, P_{KL}, θ, κ) is Lyapunov stable. If in addition (E_{KL}, P_{KL}, θ, κ) $\rightarrow$ fixed value as $t \rightarrow \infty$, the solution of Eq.(3.20) is called an asymptotically stable in the sense of Lyapunov. In an isothermal relaxation process, the solution

of Eq.(3.19) is stable, but not necessarily stable in isothermal creep process, because there does not exist a Lyapunov function.

3.6 Constitutive Equation for Inelastic Materials

In order to satisfy Eq.(3.26), we assume following internal equations. These equations are so called evolutionary equation governing the internal structures.

$$\dot{P}_{KL} = M^{(1)}_{KLIJ}\frac{\partial \phi}{\partial P_{IJ}} \qquad (3.32) \qquad \dot{\kappa} = M^{(2)}\frac{\partial \phi}{\partial \kappa} \qquad (3.33)$$

The internal variable P_{KL} may be considered to be an inelastic strain tensor. The internal variable κ corresponds to the hardening parameter in the classical theory of plasticity. We postulate that scalar variable κ is determined by

$$\dot{P}_{KL} \quad G_{KL}(T_{KL}, P_{KL}, \kappa, \theta)\dot{\kappa} \qquad (3.34)$$

This equation may be called a hardening rule. Under the condition that P_{IJ} and κ are constant, a function f is defined by

$$f \overset{\text{def}}{\equiv} \int_0^{T_{IJ}} A_{IJ}dT_{IJ} \qquad (P_{IJ}, \kappa = \text{const.}) \qquad \left(A_{IJ} = N_{IJKL}\frac{\partial \phi}{\partial P_{KL}} \right) \qquad (3.35)$$

In elastic-plastic material, the condition that P_{IJ} and κ are constant is physically satisfied in the elastic domain in stress space, because the internal structure remains unchanged in this domain.

$$\text{If} \qquad \frac{\partial A_{IJ}}{\partial \bar{T}_{KL}} = \frac{\partial A_{KL}}{\partial \bar{T}_{IJ}} , \qquad A_{IJ} = \frac{\partial f}{\partial \bar{T}_{IJ}} \tag{3.36}$$

From Eq.(3.32),

$$\dot{P}_{IJ} = M_{IJKL}(N_{KLMN})^{-1}\frac{\partial f}{\partial \bar{T}_{MN}} = Q_{ijkl}\frac{\partial f}{\partial \bar{T}_{KL}} \tag{3.37}$$

where

$$M_{IJKL}(N_{KLMN})^{-1}\frac{\partial f}{\partial \bar{T}_{MN}} = \frac{\partial f}{\partial \bar{T}_{IJ}}$$

In an isothermal process, the strain rate may be expressed by the following equation with consideration of Eqs.(3.23) and (3.34).

$$\frac{1}{\rho_0}\dot{E}_{KL} = \frac{\partial}{\partial \bar{T}_{ST}}\left(\frac{\partial \phi}{\partial \bar{T}_{KL}}\right)\dot{\bar{T}}_{ST} + \frac{\partial}{\partial P_{ST}}\left(\frac{\partial \phi}{\partial \bar{T}_{KL}}\right)\dot{P}_{ST}$$

$$= \frac{\partial}{\partial \bar{T}_{ST}}\left(\frac{\partial \phi}{\partial \bar{T}_{KL}}\right)\dot{\bar{T}}_{ST} + \frac{\partial}{\partial P_{ST}}\left(\frac{\partial \phi}{\partial \bar{T}_{KL}}\right)M_{STMN}(N_{MNUV})^{-1}\frac{\partial f}{\partial \bar{T}_{UV}} \tag{3.38}$$

If p_{KL} equals to the inelastic strain E^{p}_{KL} and ϕ is expressed by

$$\rho_0\phi = E^{vp}_{KL}\, T_{KL} + \frac{1}{2}\gamma_2 T_{KK}T_{KK} + \gamma_1(T_{KJ}T_{KJ}) \tag{3.39}$$

the stress-strain relation is then given by

$$\frac{1}{\rho_0}\dot{E}_{KL} = \gamma_2\dot{\bar{T}}_{KK} + 2\gamma_1\dot{\bar{T}}_{KL} + M_{KLIJ}(N_{IJMN})^{-1}\frac{\partial f}{\partial \bar{T}_{MN}} \tag{3.40}$$

where γ_1 and γ_2 are constant. The complementary energy ϕ of the body is illustarated in Fig.3.1.

3.7 Relation to the Rate Independent Behavior

If $M_{KLIJ}(N_{IJMN})^{-1}$ and f in the Eq.(3.40) are determined, the stress-strain relation can be obtained. One of the effective methods to determine the f-function in dynamic range is to clear the relation between f in equilibrium and that in dynamic range.

In the process of reducing Eq.(3.40), differentiation is performed with respect to the other parameter which increases with time and does not related with time explicitly, the stress-strain relation is then rate independent. In the case where the behavior is rate independent, f is denoted by f_s. Perzyna defined the F-function in the elastic-viscoplastic theory developed originally by himself and gave the relation between f_d and f_s, where f_d and f_s are dynamic and static loading function, respectively. Here, F is defined by

$$F = (f_d - f_s)/f_s \tag{3.41}$$

F = 0 is a static yield condition. In the present study, we define F-function in the sense of generalization of the concept of that developed by Perzyna. F-function may be an arbitrary function if f is equal to f_f only when F = 0.

$$F = F(T_{KL}, P_{KL}, \theta, \kappa) \tag{3.42}$$

Here we must note that f and f_s are not equal to loading function in the sense of Perzyna's theory.

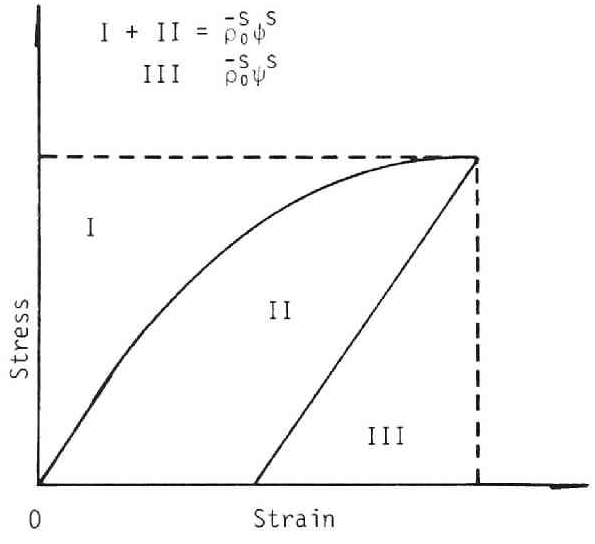

Fig.3.1 Energy function of elastic-viscoplastic body.

3.8 Comparison with Other Theories

Comparing the stress-strain relation of Eq.(3.40), with other theories, we shall discuss the theoretical feature of Eq.(3.40). Now there have been proposed various elastic-viscoplastic theories. At the beginning, the elastic-plastic theory proposed by Perzyna will be discussed in which he proposed the following stress-strain relation in the infinitesimal strain field.

$$\dot{\varepsilon}_{ij} = \frac{1}{2\mu}\dot{s}_{ij} + \frac{1-2\upsilon}{E}\dot{\sigma}_{kk}\frac{1}{3}\delta_{ij} + \gamma(\theta)\langle\Phi(F)\rangle\frac{\partial f}{\partial \sigma_{ij}} \tag{3.43}$$

where ε_{ij} is the strain tensor and σ_{ij} the stress tensor. Moreover,

$$s_{ij} = \sigma_{ij} - \frac{1}{3}\sigma_{kk}\delta_{ij} \quad , \qquad \langle\Phi(F)\rangle = \Phi(F) \quad F > 0$$
$$= 0 \quad F \leq 0$$

The static yield function is given by

$$F = \frac{f_d}{\kappa} - \kappa = 0 \tag{3.44}$$

where $\kappa = \kappa\left(\int_0^{\varepsilon^p_{ij}} \sigma_{ij} d\varepsilon^p_{ij}\right)$ which is the work-hardening parameter.

Starting with the Drucker's postulate of stable inelastic material and adding the assumption of decomposition of strain rate tensor, Perzyna obtained the convexity of the subsequent dynamic loading surface and the normality of the inelastic strain rate vector to the yield surface. After that, he thermodynamically formulated the elastic-viscoplastic body by using the thermodynamics with internal state variables developed by Coleman and Gurtin [12]. In this work, ε^{vp}_{ij} is regarded as the internal state variable. Contrally to the original work described above, Perzyna did not refer to

the normality of the inelastic strain rate vector to the yield surface. Finally, the following relation was obtained.

$$\dot{\varepsilon}_{ij}^{vp} = \gamma(\theta)\langle\Phi(F)\rangle M_{ij}(\varepsilon_{kl},\theta,\sigma_{kl},\kappa) \tag{3.45}$$

The normality of inelastic strain rate vector to the dynamic yield surface must therefore be postulated in order to reduce Eq.(3.43). Conversely, in stead of the normality of ε_{ij}^{vp} to f ,the exact differentiability is postulated in Eq.(3.40). The function$\langle\Phi(F)\rangle$ which is defined by Perzyna does not appear. Differentiating Eq.(3.40) with respect to the parameter which involves time implicitly , then it will be a rate independent stress-strain relation. In Eq.(3.38), $\dot{E}_{KL}^{vp}$ (viscoplastic strain rate tensor) is defined by

$$\frac{1}{\rho_0}\dot{E}_{KL}^{vp} = \frac{\partial}{\partial P_{ST}}\left(\frac{\partial \phi}{\partial T_{KL}}\right)\dot{P}_{ST} \tag{3.46}$$

Integrating the Eq.(3.46) along the path, we get

$$E_{KL}^{vp} = \int_0^{P_{IJ}} \rho_0 \frac{\partial}{\partial P_{ST}}\left(\frac{\partial \phi}{\partial T_{KL}}\right) dP_{ST} \tag{3.47}$$

In an equilibrium state, in the case where the stress tensor is used as an independent variable, the concept of loading surface in classical theory of plasticity must be introduced in order to distinguish between the loading state and unloading state.

In the case of rate independent behavior, the location of f changes only through the intrinsic parameter. The intrinsic time parameter was firstly introduced into the theory of plasticity by Illushin.

From Eq.(3.42), in the isothermal condition,

$$\frac{\partial F}{\partial T_{ij}} dT_{ij} + \frac{\partial F}{\partial \varepsilon_{ij}^{p}} \frac{\partial \varepsilon_{ij}^{p}}{\partial z} dz + \frac{\partial F}{\partial \kappa} \frac{\partial \kappa}{\partial z} dz = 0 \tag{3.48}$$

Therefore,

$$dz = - \frac{- \frac{\partial F}{\partial T_{ij}} dT_{ij}}{\left(\frac{\partial F}{\partial \varepsilon_{ij}^{p}} \frac{\partial \varepsilon_{ij}^{p}}{\partial z} + \frac{\partial F}{\partial \kappa} \frac{\partial \kappa}{\partial z} \right)} \qquad z=z(\varepsilon_{ij}^{p}) \tag{3.49}$$

where, z is an intrinsic time parameter which involves time implicitly. Taking account of Eqs.(3.38),(3.39) and (3.49), plastic strain increment is given by

$$dE_{KL}^{p} = M_{KLIJ} (N_{IJMN})^{-1} \frac{\partial f}{\partial T_{MN}} \cdot - \frac{\frac{\partial F}{\partial T_{AB}}}{\left(\frac{\partial F}{\partial E_{ST}^{p}} \frac{\partial E_{ST}^{p}}{\partial z} + \frac{\partial F}{\partial \kappa} \frac{\partial \kappa}{\partial z} \right)} dT_{AB} \tag{3.50}$$

Therefore, we know the relation between E_{IJ}^{p} and z with regard to the material, stress-strain relation can be obtained by Eq.(3.50).

Valanis obtained the second law of thermodynamics by generalizing the Caratheodory's principle and proved the existence of entropy and and temperature. Using this theory, he derived the stress-strain relation of visco-elastic material, elastic- viscoplastic material and elastic- plastic material by using an intrinsic time scale $z(\zeta)$ aforementioned.
The paramter ζ is given by

$$d\zeta^2 = \bar{\bar{\alpha}}^2 d\xi^2 + \bar{\bar{\beta}}^2 dt^2 \tag{3.51}$$

$$d\xi^2 = P_{ijkl} dE_{ij}^{p} \, dE_{kl}^{p} \tag{3.52}$$

where P_{ijkl}, $\bar{\bar{\alpha}}$ and $\bar{\bar{\beta}}$ are material constants. The type of parameter ξ was firstly introduced by Illushin.[21] Integrating the equation corresponding to the Eq.(3.32) with dz, stress-strain relation is obtained. Consequently, in a Valanis theory, there is no such function that plays a role of the plastic potential. In addition to z, free energy function must be given.

Rice attempted to express the state of material by introducing the internal variables based on a classical non-equilibrium thermodynamics. Internal variables correspond to the micro-structural rearrangement. He manifested a nature of the normality appearing in macroscopic constitutive laws. He assumed that the thermodynamic relation exists between the two different sets of internal variables at the constrained equilibrium state, and defined the flow potential corresponding to the function f in Eq.(3.35).

$$\Omega = \frac{1}{V_0} \int_0^{f'} \xi_i'(f_i', \theta, \xi_j') df_i' \tag{3.53}$$

where ξ_i' is the scalar component of an internal variable, f_i' is a thermodynamic force, and V_0 is a size of volume. In his theory, it is not necessary to add the condition of exact integrability corresponding to Eq.(3.36), becasuse internal variables are considered to be a scalar. Therfore, as a result, the existance of a flow potential Ω was demonstrated as follows;

$$\dot{E}^{p}_{ij} = \frac{\partial \Omega}{\partial S_{ij}} \tag{3.54}$$

where E^{p}_{ij} is a plastic strain tensor and S_{ij} is a Kirchhoff stress tensor. In the theory developed in the present study, not only scalars but also second order tensors are taken into consideration. Although, the plastic strain is caused by the rearrangement of micro-structure which should be treated as an internal state variable, the inelastic strain itself will be treated as an internal state variable herein. For instance, in a latter chapter, a viscoplastic strain is regarded as an internal state variable.

Green & Naghdi [22] developed a theory of elastic-plastic material based on Coleman's thermodynamics and modern non-linear mechanics. This theory is restricted to the case of rate insensitive material. They considered that plastic strain is an internal state variable. Fox [23] also reduced the elastic-plastic theory similar to Green & Naghdi's one. The main distinction between this theory and the author's one is that Green & Naghdi does not explain the relation between plastic potential and the internal energy, but in the author's theory, Eq.(3.35) shows this relation explicitly.

3.9 Conclusions

The energy dissipation is generally observed during the process of deformation. But the theory which can explain the energy dissipation has not been established. Especially, the theory of plasticity does not have rational basis of mechanics. In continuum mechanics, some physical laws exist, for example, balance of linear and angular momentum, mass, energy, and inequality of entropy production. The constitutive equation

which characterizes each material must be compatible with these laws. As long as concerning with the inelastic material, the thermodynamic restriction is very important. In this chapter, thermodynamic restriction for inelastic material was investigated by using the Coleman & Noll's thermodynamics based on the Clausius-Duhem inequality. Also, the concept of the internal state variable was used in order to express the internal energy dissipation, because the state of material cannot be described by the quantity observable on the surface of the material.

(1) The more general constitutive equation for an inelastic material than the elastic-viscoplastic theory proposed by Perzyna is introduced based on the internal variable theory to express phenomena of continua in dynamic state.

(2) The physical relation between a plastic potential and a free or complementary energy function was clarified. The normality rule in the plasticity was also discussed and reduced. The concept of normality is equivalent to the exact differentiability in the proposed theory.

(3) The thermodynamic restriction for inelastic non-linear material was rationally studied based on the Clausius-Duhem inequality. As a result, the internal equations, Eqs.(3.32) and (3.33), governing the structure of material were reduced.

(4) The stability of solutions was discussed following the Coleman & Gurtin's [12] method. Concerning with the equation in this chapter, in the isothermal condition, the solution is stable in relaxation process but necessarily stable or asymptotically stable in creep process.

References for Chapter 3

1) Coleman, B.D. and W. Noll: An Approximation Theorem for Functionals, with Application in Cintinuum Mechanics, Arch. Rational Mech. Anal., Vol.6, 1960, pp.355-370.

2) Coleman, B.D. and W. Noll: The Thermodynamics of Elastic Materials with Heat Conduction and Viscosity, Arch. Rational Mech. Anal. Vol.13, 1963, pp.167-178.

3) Meixner, J. : Processes in Simple Thermodynamic Materials, Arch. Rational, Mech. Anal. Vol.33, 1969, pp.33-53.

4) Truesdell, C.: Rational Thermodynamics, McGraw-Hill, New York, 1969.

5) Müller, I: Die Kärtefunktion, eine universelle Funktion in der Thermodynamik viskoser Wärmeleitender Flüssigkeiten, Arch. Rational Mech. Anal., Vol. 40, 1971, pp.1-36.

6) Valanis, K.C.: Irreversible Thermodynamics of Continuous Media, Springer-Verlag, Wien-New York, 1971.

7) Day, W.A.: The Thermodynamics of Simple Materials with Fading Memory, Springer-Verlag, Berlin-New York, 1972.

8) Nemat-Nasser, S.: On Non-Linear Thermoelasticity and Non-Equilibrium Thermodynamics, Non-Linear Elasticity(ed. by Dicky, R.W.), Academic Press New York-London, 1973. pp.289-338.

9) Coleman. B.D. and D.R. Owen: A Mathematical Foundation for Thermodynamics, Arch. Rational Mech. Anal. Vol.54, 1974, pp.1-104.

10) Biot,M.A. : Theory of Stress-Strain Relations in Anisotropic Viscoelasticity and Relaxation Phenomena, J. Appl. Phys.,Vol.25, 1954, pp.1385-1391.

11) Ziegler, H. : Some Extremum Principle in Irreversible Thermodynamics with Application to Continuum mechanics,Progress in Solid Mechanics,

Vol.IV (ed. by I.N. Sneddon and R.Hill), North-Holland Publ. Co., 1963, pp.83-192.

12) Coleman, B.D. and M.E. Gurtin : Thermodynamics with Internal State Variables, J. Chem. Phys., Vol.47, No.2, 1967, pp.597-613.

13) Perzyna, P. : Thermodynamic Theory of Visco-plasticity, Advanced in Applied Mechanics (ed. by C-S. Yih), Academic Press, New York-London, Vol.II, 1971, pp.313-354.

14) Kratochivil, J.: Thermodynamics of Elastic-Plastic Materials as a Theory with Internal State Variables, J. Appl. Phys. Vol.40, No.8, July, 1969, pp.3207-3218.

15) Kröner,E.: Dislocation : A New Concept in the Continuum theory of Plasticity, J. Math. Phys., Vol.42, 1963, pp.27-37.

16) Mróz, Z.: On the Description of Anisotropic Workhardening, J. Mech. Phys. Solids, Vol.15, 1967, pp.163-175.

17) Lubliner, J.: On the Thermodynamic Foundations of Non-Linear Solid Mechanics, Int. J. Non-Linear Mechanics, Vol.7, 1972, pp.237-254.

18) Rice, J.R.: Inelastic Constitutive Relations for Solids: An Internal Variable Theory and Its Application to Metal Plasticity, J. Mech. Phys. Solids, Vol. 19, 1971, pp.433-455.

19) Mandel, J.: Plasticite Classique et Viscoplasticite, Springer-Verlag, Wien-New York, 1971.

20) Müller, I.: On the Entropy Inequality, Arch. Rational Mech. Anal., Vol.26, 1967, pp.118-141.

21) Illyshin, A.A.: On the Relation between Stresses and Small Deformations in the Mechanics of Continuous Media, Prinkl. Math. Mech., Vol. 18, 1954, pp.641-666.

22) Green, A.E. and P.M. Naghdi: A General Theory of an Elastic-Plastic

Continuum, Arch. Rational Mech. Anal., Vol.18, 1965, pp.251-281.

23) Fox, N.: On the Continuum Theories of Dislocations and Plasticity, Quat. J. Mech. Appl. Math., Vol. 21, 1968, pp.67- 75.

Chapter 4 Theory of Two-Phase Mixture

4.1 General Remarks

In order to analyze the ground motion under dynamic or static loading, the realistic constitutive relation of soil should be obtained. The essential nature of soil is that soil is considered as the multi-phase mixture and has an inelastic property. The purpose of this chapter is to construct the solid-fluid mixture theory for saturated cohesive soil.

Many reserchers treated the saturated soil as the solid-fluid mixture. Biot [1] developed the three-dimensional theory of saturated porous elastic material and applied it to the consolidation problem and the stress wave propagation problem. Ishihara [2] proposed the theory of porous material having the heat effect which is considered as generalization of Biot's theory. His theory was developed by using the linear irreversible thermodynamics on the basis of Onsager's reciprocal theorem. Using the Onsager's relation, he formulated the flow through the porous solid and the heat diffusion. As a result, the obtained theory includes the poro-elasticity and the thermoelasticity proposed by Biot. But, as Truesdell [3] pointed out, Onsager's relation has following defects.

(1) The resolution of entropy production rate to force and flux is not uniquely determined in general.

(2) Onsager's relation is strictly limited to linear process.

From the above reasons, the theory based on the Onsager's relation is too restrictive for continuum mechanics. On the other hand, the non-equilibrium thermodynamic theory proposed by Coleman & Noll [4] is not restricted to the state near the equilibrium state and the linear process. Using this theory Green & Naghdi [5], Ingram & Eringen [6] and Bowen [7] et al. investigated the mixture. Müller [8] proposed the more rational approach to a mixture

by his original thermodynamics based on the modern continuum mechanics developed by Coleman & Noll.

Ishihara[9] clarified the physical meaning of coefficient in the Biot's equation and showed the similarity of Biot's theory to the linear viscoelasticity. From this point of view, Akai & Hori [10] considered that the viscoelastic nature of soil is due to the solid-fluid interaction. But, Ishihara concluded that in the actual situation such as earthquakes, the attenuation of compressional wave due to the friction between the solid (soil skeleton)and the fluid(free water) is close to zero. After all, the inelasticity existing inherently in the solid phase is more important for energy absorption than the friction due to the interaction between soil skeleton and free water during an earthquake. Adachi [11] considered that the soil skeleton was a mixture consisting of elastic solid and two or more fluids, and elastic-plastic solid and viscous fluid. But his theory is waiting for application.

In this chapter, the theory of mixture consisting of elastic fluid and visoelastic-viscoplastic solid is formulated for describing behavior of cohesive soil. The complete constitutive theory is deduced by using the theory proposed in Chapter 3. Up to now, the mechanical nature of principle of effective stress has not been discussed sufficiently. Terzaghi's concept of effective stress is mainly dependent on the limited experimental results rather than rational interpretations. Following the mixture theory, the meaning of effective stress concept can be clearly explained. It may be shown that effective stress concept is available even in dynamic loading. The equations of consolidation are also discussed.

4.2 Theory of Solid-Fluid Mixture

4.2.1 Fundamental Problem of Mixture

The review of the theory of mixture is reported by Truesdell, Atkin & Craine [12] and Bowen.[13] Here, the following two important disputes in the theory of mixture will be discussed.

(1) The definition of total stress

(2) Entropy production inequality

The modern treatment of mixture was firstly tried by Truesdell.[3] He introduced three metaphysical principles.

(1) All properties of the mixture must be produced as mathematical consequences of properties of each constituent.

(2) So as to describe the motion of a constituent, we may, in imagination, isolate it from the rest of the mixture, provided that we allow property for the actions of the other constituents upon it.

(3) The motion of the mixture is governed by the same equations as is a single body.

From the third principle, total stress, total energy and total body force,etc. are defined. Truesdell defined the total stress tensor as follows.

$$t_{ij} = \sum_{\alpha} t_{\alpha ij} - \sum_{\alpha} \rho_{\alpha} u_{\alpha i} u_{\alpha j} \qquad (4.1)$$

t_{ij};total stress tensor acting on the surface of mixture

$u_{\alpha i}$;diffusion velocity vector

$t_{\alpha ij}$;partial stress tensor

From Truesdell to Müller or Green & Naghdi,[14] the theory of mixture has been confirmed by applying the theory to the results in classical thermo-chemistry, for example, Dalton's law. Against the Truesdell's definition, Green & Naghdi defined the total stress by

$$t_{ij} = \sum_a t_{ij}^a \tag{4.2}$$

Green & Naghdi constructed the theory of mixture based on the different primitive concept. As the fumdamental postulate, they took the balance equation not for the several constituents, but for the mixture as a whole. When we face to the boundary value problem including the total stress as the boundary condition, it is important which definition is used.
As Atkin & Craine pointed out, for the general mixture rather than ideal gas, the total stress does not need to be described by Eqs.(4.1) and (4.2). Müller and Bowen [7] criticized the Green & Naghdi's theory,[5] since their theory was not consistent with the calssical thermo-chemical results when it was applied to the ideal gas mixture in equilibrium state. In order to solve the dilemma, Green & Naghdi asserted that the partial stress in the classical theory is different from that in their theory. After that time, they recognized the error and introduced the arbitrary function which did not violate the balance law as a whole in order to be consistent with the classical results. Furthermore, they took the energy equation for several constituents to introduce the arbitrary function.[15] The usefulness of the method with which arbitrary function is introduced is attributed to the thermodynamics developed by them.[16] Müller proposed the theory of mixture that consisted with the result of classical gas mixture and was well motivated physically. His assertion is based on the two important

postultes. One of them is for the independent variable in the constitutive assumption and the other is for the entropy production inequality. Introducing the density gradient as the independent variable, Müller prevents the theory from oversimplifying. This method solved out the dilemma brought about by Bowen.[7] Müller took the entropy flux as the constitutive quantity which was specified by a constitutive equation, not by a conventioanal way expressed by

$$\text{entropy flux} = (\text{heat flux})/(\text{temperature}) \tag{4.3}$$

On the basis of the several principle(equipresence, objectivity, entropy inequality,postulate for entropy supply and constitutive equation for entropy flux), Eq.(4.3) can be derived for a broad class of single material by Müller. Truesdell [3] concluded that the only Müller's theory seemed to satisfy the general principle of modern continuum mechanics. Comparing with the Müller theory, Green & Naghdi's one is less sensitive and has the advantage that total stress can take the form that is applicable to the practical problem. Fundamentally, there is no difference between the basic equations in the Müller's theory and Green & Naghdi's one. In the case of treating the motion of saturated soil, the motion of soil skeletonis more important for engineering problem than that as a single material. So that we need not describe the motion of the assembly of mixture. The author derives the theory of two phase mixture following Green & Naghdi's idea.

4.2.2 Balance equation of two phase mixture

Consider a soil as a mixture of two interacting constituents, each of which is regarded as a continuum. It is assumed that each point is occupied simultaneously by all constituents. A position at the peculiar

particle of constitutent at time τ is denoted by $x_i^{\alpha}(\tau)$.

$$x_i^{(\alpha)} = x_i^{(\alpha)}(X_1^{(\alpha)}, X_2^{(\alpha)}, X_3^{(\alpha)}, \tau) \quad (-\infty < \tau \leq t) \tag{4.4}$$

$$\alpha = s \text{ or } f$$

The indices (f) and (s) denote the fluid phase and solid phase,respectively. X_i^{α} is a reference position of each particle. At time t, any position is occupied by a particle of each constituent.

$$x_i^{(s)} = x_i^{(f)} = x_i \tag{4.5}$$

Balance of mass

It is assumed that a mass of individual constituent is conserved. Then, balance equation for each constituent can be written as follows;

$$\int_S \bar{\rho}^s v_i^s n_i ds + \int_V \frac{\partial \bar{\rho}^s}{\partial t} dv = 0 \tag{4.6}$$

$$\int_S \bar{\rho}^f v_i^f n_i ds + \int_V \frac{\partial \bar{\rho}^f}{\partial t} dv = 0 \tag{4.7}$$

where, ρ^s and ρ^f are the specific mass densities of soil particle and water, respectively. $\bar{\rho}^s$ and $\bar{\rho}^f$ are the mass densities of each continuum constituent (solid and fluid) constituting of the mixture. n is the porosity of the mixture, v_i the component of velocity vector. V the arbitrary volume and S denotes its surface.

Balance of linear momentum

$$\int_S t_{ij}^s n_j ds \quad \int_V (\pi_i + b_i^s) dv = \int_S \bar{\rho}^s v_i^s v_j^s n_j ds + \int_V \frac{\partial}{\partial t}(\bar{\rho}^s v_i^s) dv \tag{4.8}$$

$$\int_S t_{ij}^f n_j ds + \int_V (\pi_i - b_i^f)dv = \int_S \bar{\rho}^f v_i^f v_j^f n_j ds + \int_V \frac{\partial}{\partial t}(\bar{\rho}^f v_i^f)dv \tag{4.9}$$

where t_{ij}^{α} is the partial stress tensor or the stress tensor averaged over a bulk area. Total stress is defined by

$$t_{ij} = t_{ij}^s + t_{ij}^f \tag{4.10}$$

If pore water pressure in the void is expressed by u, Terzaghi's effective stress tensor is denoted by t_{ij}^e which is meaningful under the condition that the water is imcompressible.

$$t_{ij}^e = t_{ij} - u\delta_{ij} = t_{ij}^s - (1-n)u\delta_{ij} \tag{4.11}$$

$$t_{ij}^f = nu\delta_{ij} \tag{4.12}$$

The definition of Terzaghi's effective stress tensor will be discussed further in section 4.4. π_i is the component of interaction force vector arising from the transfer of momentum between constituents. b_i^{α} is the componebt of external body force vector. Total body force b_i is the sum of b_i^s and b_i^f.

From Eqs.(4.10) and (4.11), the linear momentum must be also balanced for mixture as a whole. Using the Eqs.(4.6),(4.7) and (4.13), the local forms of Eqs.(4.10) and (4.11) are denoted as follows if functions in these equations are continuous.

$$\frac{\partial t_{ij}^{e}}{\partial x_j} = \bar{\rho}^{s}\frac{dv_i^{s}}{dt} \quad \frac{\partial (1-n)u\delta_{ij}}{\partial x_j} + \pi_i - \bar{\rho}^{s} b_i^{s} \tag{4.13}$$

$$\frac{\partial t_{ij}^{f}}{\partial x_j} = \bar{\rho}^{f}\frac{dv_i^{f}}{dt} - \pi_i \quad \bar{\rho}^{f} b_i^{f} \tag{4.14}$$

$$\frac{dv_i^{\alpha}}{dt} = \frac{\partial v_i^{\alpha}}{\partial t} + v_j^{\alpha}\frac{\partial v_j^{\alpha}}{\partial x_j} \qquad (\ \alpha \quad s \text{ or } f\ )$$

Balance of angular momentum

Balance equation of angular momentum reffered to a fixed place for individual constituent is assumed to be expressed in this form,

$$\frac{\partial}{\partial t}\int_v e_{ijk}\bar{\rho}^{s} v_i^{s} x_j dv + \int_s e_{ijk}\bar{\rho}^{s} v_i^{s} v_m^{s}\, x_j n_m ds - \int_v e_{ijk}(\pi_i - \bar{\rho}^{s} b_i^{s})x_j dv$$
$$- \int_s e_{ijk} t_{mi}^{s} n_m x_j ds = 0 \tag{4.15}$$

where e_{ijk} is a permutation symbol.

From Eqs.(4.13) and (4.15), we get following equation for solid phase.

$$e_{ijk} t_{ji}^{s} = 0 , \qquad t_{ij}^{s} = t_{ji}^{s} \tag{4.16}$$

Similarly, for fluid phase, Eq.(4.17) is obtained.

$$t_{ij}^{f} = t_{ji}^{f} \tag{4.17}$$

From these results, it can be immediately noted that partial stress for each constituent is symmetric.

Balance of energy

It is sufficient to assume that each constituent has a common temperature for a purpose of the following discussion. We postulate the

balance equation of energy for assembly of mixture which is given by

$$\int_v \frac{\partial}{\partial t}(\bar{\rho}^s\varepsilon^s + \bar{\rho}^s\varepsilon^s + \frac{1}{2}\bar{\rho}^s v_i^s v_i^s + \frac{1}{2}\bar{\rho}^f v_i^f v_i^f)dv + \int_s [(\bar{\rho}^s\varepsilon^s + \frac{1}{2}\bar{\rho}^s v_i^s v_i^s)v_j^s$$

$$+(\bar{\rho}^f\varepsilon^f + \frac{1}{2}\bar{\rho}^f v_i^f v_i^f)v_j^f]n_i ds = \int_s (t_{ij}^s v_i^s + t_{ij}^f v_i^f)n_j ds \qquad (4.18)$$

$$+\int_s (q_i^s + q_i^f)n_i ds + \int_v (\bar{\rho}^s s^s + \bar{\rho}^f s^f)dv + \int_v (\bar{\rho}^s b_i^s v_i^s + \bar{\rho}^f b_i^f v_i^f)dv$$

where ε^α is the internal energy density, q_i^α the heat influx vector and s^α the heat supply.

In the local form, Eq.(4.20) is rewritten by

$$\bar{\rho}^s\frac{d\varepsilon^s}{dt} + \bar{\rho}^f\frac{d\varepsilon^f}{dt} = t_{ij}^s v_{i,j}^s + t_{ij}^f v_{i,j}^f - \bar{\rho}^s v_i^s\frac{dv_i^s}{dt} - \bar{\rho}^f v_i^f\frac{dv_i^f}{dt} + t_{ij,j}^s v_i^s \qquad (4.19)$$

$$+t_{ij,j}^f v_i^f + q_{i,i}^s + q_{i,i}^f + \bar{\rho}^s s^s + \bar{\rho}^f s^f + \bar{\rho}^s b_i^s v_i^s + \bar{\rho}^f b_i^f v_i^f$$

Using the Eqs.(4.13),(4.15) and (4.16), this equation is further rearranged and given by

$$\bar{\rho}^f\frac{d\varepsilon^f}{dt} + \bar{\rho}^s\frac{d\varepsilon^s}{dt} = t_{ij}^e v_{i,j}^s + (1-n)u\delta_{ij}v_{i,j}^s + t_{ij}^f v_{i,j}^f + q_{i,i}^f + q_{i,i}^s \qquad (4.20)$$

$$+\bar{\rho}^f s^f + \bar{\rho}^s s^s - \pi_i(v_i^f - v_i^s) + \bar{\rho}^s b_i^s v_i^s + \bar{\rho}^f b_i^f v_i^f$$

Entropy production inequality

We assume the following entropy production inequality for assembly which is equivalent to one used by Truesdell.

$$\int_V \bar{\sigma} dv = \frac{\partial}{\partial t}\int (\bar{\rho}^s \eta^s + \bar{\rho}^f \eta^f) dv + \int_S (\bar{\rho}^s \eta^s v_i^s + \bar{\rho}^f \eta^f v_i^f) n_i ds$$

$$- \int_S \frac{1}{\bar{\theta}} (q_i^s + q_i^f) n_i ds - \int_V \frac{1}{\bar{\theta}} (\bar{\rho}^s s^s + \bar{\rho}^f s^f) dv \geq 0 \tag{4.21}$$

where η^α denotes the entropy per unit mass, σ the entropy production density of assembly of mixture, and θ the absolute temperature. From Eqs. (4.22) and (4.23), this equation can be expressed in the local form as follows;

$$\bar{\rho}^s \frac{d\eta^s}{dt} + \bar{\rho}^f \frac{d\eta^f}{dt} - \frac{1}{\bar{\theta}} (\bar{\rho}^s \frac{d\varepsilon^s}{dt} + \bar{\rho}^f \frac{d\varepsilon^f}{dt}) + \frac{1}{\bar{\theta}} (t_{ij}^s v_{i,j}^s + t_{ij}^f v_{i,j}^f)$$

$$+ \frac{1}{\theta^2} (q_i^s + q_i^f) \theta_{,i} - \frac{1}{\theta} \pi_i (v_i^f - v_i^s) \geq 0 \tag{4.22}$$

If the body force is neglected, sufficient conditions are given by

$$\theta \bar{\rho}^s \frac{d\eta^s}{dt} - \bar{\rho}^s \frac{d\varepsilon^s}{dt} + t_{ij}^s v_{i,j}^s + \frac{1}{\bar{\theta}} q_i^s \theta_{,i} + \bar{\rho}^f \frac{d\eta^f}{dt} - \bar{\rho}^f \frac{d\varepsilon^f}{dt} + t_{ij}^f v_{i,j}^f$$

$$+ \frac{1}{\bar{\theta}} q_i^f \theta_{,i} \geq 0 \tag{4.23}$$

$$-\pi_i (v_i^f - v_i^s) \geq 0 \tag{4.24}$$

Furthermore, the sufficient condition of Eq.(4.26) is

$$\pi_i = -d(v_i^f - v_i^s) \ , \ (d \geq 0) \tag{4.25}$$

which should be expressed in a more general form by Eq.(4.26)

$$\pi_i = -d^0(v_i^f - v_i^s) - d^1(v_i^f - v_i^s)^3 - \cdots\cdots$$

$$(d^0, d^1, d^2, \cdots\cdots \geq 0) \tag{4.26}$$

From Eqs.(4.25) and (4.26), it is evident that π_i is an invariant for a rigid motion or its superposition.

4.3 Equation of consolidation

The problem of consolidation was firstly formulated as one-dimensional problem by Terzaghi [17] and extended to three-dimension by Rendulic [18], Terzaghi [19] and Davis et al.[20] The noteworthy three-dimensional theory of consolidation was deduced by Biot [21] applying his original theory of a saturated porous elastic solid to the consolidation phenomena. Since them, many investigators used Biot's theory for analyzing the consolidation problem. But, his theory is restricted to a linear formulation. In this section, the governing equations of consolidation applicable to non-linear problem will be shown from a view of a theory of two-phase mixture.

With the aid of Eqs.(4.12) and (4.25), the equation of motion, Eq. (4.14) , becomes

$$\frac{\partial(nu)}{\partial x_j}\delta_{ij} = \bar{\rho}^f \frac{dv_i^f}{dt} + d(v_i^f - v_i^s) - \bar{\rho}^f b_i^f \tag{4.27}$$

If we can neglect the body force and the acceleration, this is reduced to

$$\frac{\partial(nu)}{\partial x_i} = d(v_i^f - v_i^s) \tag{4.28}$$

Furthermore, if ρ^f and ρ^s are constant, one can obtain the following equation from Eqs.(4.6) and (4.7).

$$\{n(v_i^s - v_i^f)\}_{,i} = v_{i,i}^s \tag{4.29}$$

in which it is assumed that the coefficient d in Eq.(4.27) is defined by

$$d = \rho^f g n^2 / k \tag{4.30}$$

Using Eq.(4.30), Eq.(4.28) is rewritten by

$$\frac{1}{\rho^f g} \frac{\partial (nu)}{\partial x_i} = \frac{n^2}{k}(v_i^f \quad v_i^s) \tag{4.31}$$

where k is the permeability coefficient and $\rho^f g$ the weight of water per unit volume.

$n(v_i^f - v_i^s)$ is considered to be the water enflux through the unit surface per unit time, Eq.(4.31) can be replaced to the one-dimensional form which is equal to the Darcy's law, under the consideration that n is constant, and is given by

$$\bar{v}_i = k \cdot i, \qquad i = \frac{\partial u}{\partial x_i} \frac{1}{\rho^f g} \tag{4.32}$$

where v_i is a relative velocity between solid and water.

Differentiating both sides of Eq.(4.31), and using the Eqs.(4.29) and (4.30), one can obtain

$$\frac{1}{\rho^f g}\frac{\partial^2(nu)}{\partial x_i^2} = -\frac{n}{k}v_{i,i}^{s} + \left(\frac{n}{k}\right)_{,i} n(v_i^f - v_i^s) = \frac{n\,d\varepsilon_{kk}^{s}}{k\,dt} + \left(\frac{n}{k}\right)_{,i} n(v_i^f - v_i^s) \tag{4.33}$$

Three equations, Eq.(4.33), the stress-strain relation of solid phase and the equation of motion of solid phase, lead to the governing a consolidation in the general nonlinear form. If n and k are constant, Eq.(4.33) is reduced to, so-called the equation of continuity which is

$$\frac{1}{\rho^f g}\frac{\partial^2 u}{\partial x_i^2} = -\frac{1}{k}\frac{\partial \varepsilon_{kk}^{s}}{\partial t} \tag{4.34}$$

This equation involves both the equation of continuity of mass and the equation of motion of fluid phase.

4.4 Effective stress concept

Terzaghi's effective stress concept plays a great role in soil mechanics and is useful for analyzing the practical problem in soil engineering. But, there has seldom been performed the exact and clear interpretation of this concept. Terzaghi introduced effective stress concept for interpretating nature of soil behavior. Bishiop [23] and Skempton [24] have extended this concept on the basis of data of pore water pressure measured by Rendulic [25] et al. But the rational basis of effective stress concept has not been yet clarified up until now. In this section, the author has tried to explain the physical interpretation of this concept from a point of view of the continuum theory of mixture. The saturated soil is considered to be composed of free water and soil skeleton.

From the Green & Naghdi's theory, the total stress acting on a mixture is sum of the partial stress acting on two phases. Eq.(4.10) is therefore rewritten here by

$$t_{ij} = t^{s}_{ij} + t^{f}_{ij} \tag{4.10}$$

When the cell pressure is acting on the saturated soil, partial stress acting on the fluid phase t^{f}_{ij} is expressed by

$$t^{f}_{ij} = nu\delta_{ij} \tag{4.12}$$

On the other hand, the stress acting on the solid phase t^{s}_{ij} is similarly expressed by

$$t^{s}_{ij} = (1-n)u\delta_{ij} \tag{4.35}$$

Since the assumption has been made that the soil is treated to be saturated, the force action on the solid phase has to be balanced with the force on the fluid phase, when the soil is subjected to only cell pressure. In such this situation, any point in the soil is not in motion.While, a case where the soil is in general stress condtion, the effective stress is defined by

$$t^{e}_{ij} = t_{ij}-(1-n)u\delta_{ij} \tag{4.11}$$

Now, consider the energy balance equation, Eq.(4.20). In Eq.(4.20),

$$t^{s}_{ij}\, v^{s}_{i,j} = [t^{e}_{ij} + (1-n)u_{ij}]v^{s}_{i,j} = t^{e}_{ij}v^{s}_{i,j} + (1-n)uv^{s}_{i,i} \tag{4.36}$$

Under the undrained condition, $v^s_{i,i}=v^f_{i,i}$ such that $\dot{\varepsilon}^s_{ii} = \dot{\varepsilon}^f_{ii}$. If fluid is incompressible, then $\dot{\varepsilon}^f_{ii} = 0$ and $t^s_{ij}\,\dot{\varepsilon}^s_{ij} = t^e_{ij}\,\dot{\varepsilon}^s_{ij}$. From the above discussion, the stress power produced by the term of effective stress only contributes to the entropy production if fluid is incompressible. Further, it should be noted that $(1-n)u\delta_{ij}$ which is the stress component acting on the surface of the solid, does not contribute to net work. That is to say, if the fluid is nearly incompressible, it results in internal constraint. In the case of an unsaturated soil, however, the fluid phase is fairly compressible. Therefore, t^e_{ij}(Eq.(4.11)) does not effectively contribute to the macroscopic deformation. The effective stress can possibly be interpreted as a stress which is a subtruction of the stress$(1-n)\delta_{ij}$ constrained by the fluid from the bulk area averaged solid stress t^s_{ij}. Akai & Tamura [26] determined the pore pressure by accounting the constraining condition together with the balance equation in the numerical study of multi-dimentional consolidation problem. According to the study, pore water pressure was determined as a Lagrangian multipliers.In other words, in saturated soil, bulk surface area averaged fluid stress $nu\delta_{ij}$ constrains the volumetric deformation of solid. But,if there exists no stress tensor $(1-n)\delta_{ij}$, the skeleton constituted by soil particles should be out of constraint. This is a reason of occurrence of the phenomena of quick sand and therefore $(1-n)\delta_{ij}$ is sometimes called the self-supported stress tensor. The effective stress causes the macroscopic deformation of saturated soil. Substituting Eqs.(4.12) and (4.11) into Eq.(4.10), we get the Terzaghi's equation

$$t_{ij} = t^e_{ij} + u\delta_{ij} \tag{4.37}$$

From the above discussion, it is concluded that the effective stress concept should be on the basis of characteristics of soil as a mixture, but not as granular material composed of each particle. In this sence, occurrence of liquifaction could be caused by a lack of interparticle force rather than looseness of the effective stress to zero of which concept has been so far generally accepted.

Nobody has clarified the structure of Terzaghi's effective stress concept. Skempton [24] challenged the generalization of Terzaghi's effective stress equation. From his original observation, he has shown that Terzaghi's effective stress is not strictly true, but is satisfactory adequate only for the saturated soils. Three definitions of effective stress were proposed by him, which are

$$\text{(a)}\quad \sigma' = \sigma - (1 - a_c)u \tag{4.38}$$

$$\text{(b)}\quad \sigma' = \sigma - u \tag{4.39}$$

$$\text{(c)}\quad \sigma' = \sigma - \left(1 - \frac{a_c \tan\psi'}{\tan\phi'}\right)u \qquad \text{For shear strengh} \tag{4.40}$$

$$\sigma' = \sigma - \left(1 - \frac{C_s}{C}\right)u \qquad \text{For volume change} \tag{4.41}$$

where ϕ' is the effective stress angle of shearing resistance, ψ' the intrinsic friction angle, C_s the compressibility of soil particle, C the soil compressibility, a_c the contact surface area, σ the total stress and σ' the effective stress. These equations have been experimentally checked which equation can adequately interpret soil behavior. Skempton concluded that Eq.(4.38) was not valid for representation of effective stress. Eqs.(4.40) and (4.41) interpret approproately experimental results of shear strength and volume change of soil, concrete and rock. Eq.(4.39) is

valid only for saturated soils. These equations for effective stress do not consist with the actual soil behavior in a strict sense and have some defects as follows;

(1) The definition of an effective stress for shear strength is different from that for compression.

(2) The empirical parameters, which are introduced in the reduction of effective stress in order to connect the intergranular force with the external force, are not on physical basis.

(3) Skempton's approach is based on the assumption that Coulomb's strength equation is valid a priori.

From the reason of (3), if stress-strain relation changes, the definition of effective stress may become different, which is not rational.

Almost all considerations of the effective stress expressed by many soil engineers, for example, Lambe,[27] Scott,[28] Mitchell [29] and many soil investigators [30] et al., are not more than the Skempton's work. As seen from the above observations, Skempton's generalization of the effective stress is too restrictive and not rational. An interparticle force of soil is significantly related to the constitutive equation of soil but not to the effective stress essentially. The effective stress is determined depending on motion of a pore fluid. Adachi and Hibiya [31] tried to introduce the interparticle force caused by the suction into the stress-strain relation of an unsaturated soil. This approach may be strictly logical for an investigation on unsaturated soil. Moreover, Lambe's approach that introduced the electric force between particles into the effective stress equation contradicts the author's theory.

As we have discussed in Eq.(4.36), energy equation includes an effective stress as independent variables. Therefore, on the basis of the

principle of equi-presence, all other constitutive functions have to include the term of effective stress as an independent variable. On the contrary, provided that two phases on mixture can be regarded to be compressible comparably each other and coupling between them occurs only in volumetric deformation, stress-strain relation must be expressed by

$$E^{s}_{KK}=\hat{E}^{s}_{KK}(t^{s}_{ij}\ ,\ t^{f}_{ij}\ ,\ \tilde{\alpha}\ )\quad ,\quad E^{f}_{KK}=\hat{E}^{f}_{KK}(t^{s}_{ij},t^{f}_{ij},\ \tilde{\alpha}\ ) \tag{4.42}$$

where $\tilde{\alpha}$ implies other parameters defined in Eq.(3.20). Consequently, the definition of the effective stress concept is deeply related with the selection of independent variables of constitutive function. The Bishiop's effective stress of an unsaturated soil should be therefore reexamined from view point of a theory of mixture.

Kenyon [32] deduced the self-supported stress which he called self-equilibrated stress in his study of an imcompressible solid-fluid mixture. But his theory is restricted to the equilibrium state since he is based on the Müller's theory. In Eq.(4.1), only when soil is equilibrated, Eq.(4.10) is valid. The distinction between the author's and Kenyon's theory is resulted from the difference of the definition of total stress.

4.5 Constitutive theory for a mixture of a viscoelastic-viscoplastic material and an elastic fluid

The principle of objectivity requires that the constitutive equation is invariant under the superposed rigid body motion. In order to satisfy this principle, it is sufficient that all tensorial variables are invariant under such motion. Eq.(4.23) is rewritten by invariant form.

$$-\bar{\rho}^s(\dot{\psi}^s+\eta^s\dot{\theta})+\dot{T}_{KL}\dot{E}^s_{KL}+h^s_i\bar{g}^s_i/\theta\ -\bar{\rho}^f_0(\dot{\psi}^f+\eta^f\dot{\theta})+T^f_{KL}\dot{E}^f_{KL}+h^f_i\bar{g}^f_i/\theta \geq 0 \qquad (4.43)$$

where ψ^α is a partial free energy , T^α_{KL} the second Kirchhoff stress tensor, $\dot{E}^\alpha_{KL}$ the strain rate tensor in Lagragian form,

$$h^\alpha_i = \frac{\bar{\rho}^\alpha_0}{\bar{\rho}^\alpha}F^{-1}_{ij}q^{(\alpha)}_i \quad , \quad \bar{g}^\alpha_i=F^{T(\alpha)}_{ij}\theta,_j$$

and F^α_{ij} the deformation gradient tensor. (α = f or s)

If we introduce the complementary energy density ϕ^α(see Fig.4.1),

$$\phi^\alpha= \frac{1}{\bar{\rho}^\alpha}T^\alpha_{KL}E^\alpha_{KL} - \psi^\alpha \qquad (4.44)$$

Then Eq.(4.43) becomes

$$\bar{\rho}^s_0\dot{\phi}^s-E^s_{KL}\dot{T}^s_{KL}-\bar{\rho}^s_0\dot{\theta}\eta^s+h^s_i\bar{g}^s_i/\theta+\bar{\rho}^f_0\dot{\phi}^f-E^f_{KL}\dot{T}^f_{KL}-\bar{\rho}^f_0\dot{\theta}\eta^f+h^f_i\bar{g}^f_i/\theta \geq 0 \qquad (4.45)$$

Using this equation, a thermodynamic restriction to constitutive equation will be obtained later on. The principle of equi-presence is a rule for a mathematical convienience, but for a physical principle is not always satisfied. The behavior of the solid phase is characterized by seven response functions, while that of the fluid phase by four response functions. The solid constituent(soil particle) is assumed to be imcompressible, on the other hand, a fluid is not incompressible. The bulk averaged soil stress tensor T^s_{IJ} is used as independent variable.

$$\phi^s=\hat{\phi}^s_1(E^{vp}_{KL},\ T^s_{KL},\ \kappa,\ \theta,\ \bar{g}^s_I)+\phi^s_2(E^{ve}_{KL},\ \dot{T}^s_{KL},\ \theta,\ \bar{g}^s_I) \qquad (4.46)$$

$$\phi^f=\hat{\phi}^f(T^f_{KK},\ \theta,\ \bar{g}^f_I) \qquad (4.47)$$

$$\eta^s = \hat{\eta}^s(E^{vp}_{KL},\ E^{ve}_{KL},\ T^s_{KL},\ \kappa,\ \theta,\ \bar{g}^s_I) \tag{4.48}$$

$$\eta^f = \hat{\eta}^f(T^f_{KK},\ \theta\ ,\ \bar{g}^f_I) \tag{4.49}$$

$$E^s_{KL} = \hat{E}^s_{KL}(E^{vp}_{KL},\ E^{ve}_{KL},\ T^s_{KL},\ \kappa,\ \theta,\ \bar{g}^s_I) \tag{4.50}$$

$$E^f_{KL} = \hat{E}^f_{KL}(T^f_{KK},\ \theta,\ \bar{g}^s_I) \tag{4.51}$$

$$h^s_I = \hat{h}^s_I(E^{vp}_{KL},\ E^{ve}_{KL},\ T^s_{KL},\ \kappa,\ \theta,\ \bar{g}^s_I) \tag{4.52}$$

$$h^f_I = \hat{h}^f_I(T^f_{KK},\ \theta,\ \bar{g}^f_I) \tag{4.53}$$

$$\dot{E}^{vp}_{KL} = \hat{\dot{E}}^{vp}_{KL}(E^{vp}_{KL},\ T^s_{KL},\ \kappa,\ \theta,\ \bar{g}^s_I) \tag{4.54}$$

$$\dot{E}^{ve}_{KL} = \hat{\dot{E}}^{ve}_{KL}(E^{ve}_{KL},\ T^s_{KL},\ \theta,\ \bar{g}^s_I) \tag{4.55}$$

$$\dot{\kappa} = \hat{\dot{\kappa}}(E^{vp}_{KL},\ T^s_{KL},\ \kappa,\ \theta,\ \bar{g}^s_I) \tag{4.56}$$

where, E^{vp}_{KL} and E^{ve}_{KL} are the internal state variables corresponding to a viscoplastic strain and a viscoelastic strain, respectively. κ is a scalar parameter which is an internal variable corresponding to hardening parameter. In Eqs.(4.46) and (4.56), it is assumed that the coupling between solid and fluid is not involved. The case when such coupling exists will be discussed later on. The rate equations of ϕ^s and ϕ^f are

$$\dot{\phi}^s = \frac{\partial \phi^s}{\partial T^s_{KL}} \dot{T}^s_{KL} + \frac{\partial \phi^s_1}{\partial E^{vp}_{KL}} \dot{E}^{vp}_{KL} + \frac{\partial \phi^s_1}{\partial \kappa} \dot{\kappa} + \frac{\partial \phi^s_2}{\partial E^{ve}_{KL}} \dot{E}^{ve}_{KL} + \frac{\partial \phi^s}{\partial \theta} \dot{\theta} + \frac{\partial \phi^s}{\partial \bar{g}^s_I} \dot{\bar{g}}^s_I$$

$$\dot{\phi}^f = \frac{\partial \phi^f}{\partial T^f_{KK}} \dot{T}^f_{KK} + \frac{\partial \phi^f}{\partial \theta} \dot{\theta} + \frac{\partial \phi^f}{\partial \bar{g}^f_I} \dot{\bar{g}}^f_I \tag{4.57}$$

Substituting Eq.(4.57) into Eq.(4.45),

$$\left(\frac{\partial\phi^s}{\partial T^s_{KL}} - \frac{1}{\rho^s_0}\dot{E}^s_{KL}\right)\dot{T}^s_{KL} + \frac{\partial\phi^s_1}{\partial E^{vp}_{KL}}\dot{E}^{vp}_{KL} + \frac{\partial\phi^s_2}{\partial E^{ve}_{KL}}\dot{E}^{ve}_{KL} + \frac{\partial\phi^s_1}{\partial\kappa}\dot{\kappa} + \left[\frac{\partial(\phi^s-\phi^f)}{\partial\theta} - \eta^f - \eta^s\right]\dot{\theta}$$

$$+ \frac{\partial\phi^f}{\partial \bar{g}^f_I}\dot{\bar{g}}^f_I + \frac{\partial\phi^s}{\partial \bar{g}^s_I}\dot{\bar{g}}^s_I + \left(\frac{\partial\phi^f}{\partial T^f_{KK}} - \frac{1}{\bar{\rho}^f_0}E^f_{KK}\right)\dot{T}^f_{KK} + (\bar{h}^s_I\bar{g}^s_I + \bar{h}^f_I\bar{g}^f_I)/\theta \geq 0 \qquad (4.58)$$

On the basis of the Coleman's method,[4] we can conclude that

$$\eta^f + \eta^s = \frac{\partial(\phi^f+\phi^s)}{\partial\theta} \qquad (4.59) \qquad E^s_{KL} = \bar{\rho}^s_0\frac{\partial\phi^s}{\partial T^s_{KL}} \qquad (4.60)$$

$$E^f_{KK} = \bar{\rho}^f_0\frac{\partial\phi^f}{\partial T^s_{KK}} \qquad (4.61) \qquad \frac{\partial\phi^f}{\partial \bar{g}^f_I} = 0 \qquad (4.62) \qquad \frac{\partial\phi^s}{\partial \bar{g}^s_I} = 0 \qquad (4.63)$$

$$(h^f_I\bar{g}^f_I + h^s_I\bar{g}^s_I)/\theta \geq 0 \qquad (4.64) \qquad \frac{\partial\phi^s_1}{\partial E^{vp}_{KL}}\dot{E}^{vp}_{KL} + \frac{\partial\phi^s_2}{\partial E^{ve}_{KL}}\dot{E}^{ve}_{KL} + \frac{\partial\phi^s_1}{\partial\kappa}\dot{\kappa} \geq 0 \qquad (4.65)$$

Since the energy dissipation is attributed not only to plastic work but also to viscoelastic work, the inequality (4.65) will be divided into two parts, each of which is therefore assumed to be positive or zero. Resultantly, these inequalities (4.66) and (4.67) correspond to a sufficient condition of Eq.(4.65).

$$\dot{E}^{vp}_{KL}\frac{\partial\phi^s_1}{\partial E^{vp}_{KL}} + \frac{\partial\phi^s_1}{\partial\kappa}\dot{\kappa} \geq 0 \qquad (4.66) \qquad \dot{E}^{ve}_{KL}\frac{\partial\phi^s_2}{\partial E^{ve}_{KL}} \geq 0 \qquad (4.67)$$

We also postulate

$$\dot{E}^{vp}_{KL} = M_{KLIJ}\frac{\partial \phi^{s}_{1}}{\partial E^{vp}_{IJ}} \tag{4.68}$$

$$\dot{\kappa} \quad G_{KL}\dot{E}^{vp}_{KL} \tag{4.69}$$

$$\dot{E}^{ve}_{KL} = \bar{\eta}_{KLMN}\frac{\partial \phi^{s}_{2}}{\partial E^{ve}_{MN}} \tag{4.70}$$

Eq.(4.68) shows that $\dot{E}^{vp}_{KL}$ is not generally normal to the complementary energy function ϕ^{s}_{1} . Eq.(4.69) indicates that $\dot{\kappa}$ is a function of only the rate of viscoplastic strain. In this sense, κ corresponds to the strain hardening parameter used in the classical theory of plasticity. Complementary energy densities are assumed as follows for further discussion later on.

$$\bar{\rho}^{s}_{0}\phi^{s} \quad E^{vp}_{KL}T^{s}_{KL} + E^{ve}_{KL}T^{s}_{KL} + G(T^{s}_{IJ}) - \gamma^{1}_{IJKL}E^{ve}_{IJ}E^{ve}_{KL} \tag{4.71}$$

$$\gamma^{1}_{IJKL} = a^{1}\delta_{IJ}\delta_{KL} + b^{1}(\delta_{IK}\delta_{JL} + \delta_{IL}\delta_{JK})$$

$$\bar{\rho}^{f}_{0}\phi^{f} = (T^{f}_{KK})^{2}m_{f}/6 \tag{4.72}$$

where $a^{(1)}, b^{(1)}$ and m_f are the material constants. From Eqs.(4.60) and (4.71), we obtain

$$E^{s}_{KL} = E^{vp}_{KL} + E^{ve}_{KL} + \frac{\partial G}{\partial T^{s}_{KL}} \tag{4.73}$$

Similarly, from Eqs.(4.61) and (4.72),

$$E^{f}_{KK} = num_{f} \tag{4.74}$$

where u is a pore pressure and m_f is an intrinsic compressibility of a fluid.

Now, it is described again that we consider a satulated soil. m_f is extremely small compared to the compressibility of soil skeleton in general. In the following discussion, m_f is assumed to be zero, that is, fluid is supposed to be incompressible. Consequently, as discussed in section 4.4, we must use the effective stress tensor T^e_{IJ} in stead of the bulk area averaged solid stress tensor T^s_{IJ}.

The viscoelastic strain which is assumed to be Voigt type is introduced by taking Eq.(4.75) as the explicit description of Eq.(4.70).

$$\dot{E}^{ve}_{KL} = \bar{\eta}_{KLMN} \left(T^e_{MN} - \gamma^1_{MNIJ} E^{ve}_{IJ}\right) \tag{4.75}$$

If $\bar{\eta}_{KLMN}$ is a fourth order isotropic tensor, then it is given by

$$\bar{\eta}_{KLMN} = a^{(2)}\delta_{KL}\delta_{MN} + b^{(2)}\left(\delta_{KM}\delta_{LN} + \delta_{KN}\delta_{LM}\right) \tag{4.76}$$

Eq.(4.75) becomes

$$\dot{E}^{ve}_{KL} = 3a^{(2)}T^e_m\delta_{KL} + 2b^{(2)}s_{KL} - 3\tau^{(1)}E^{ve}_{KL} - 2\tau^{(2)}e^{ve}_{KL} \tag{4.77}$$

$$\tau^{(1)} = 3a^{(1)}a^{(2)} + 2a^{(1)}b^{(2)} + 2b^{(1)}a^{(2)} \tag{4.78}$$

$$\tau^{(2)} = 2b^{(1)}b^{(2)}$$

$$e_{KL} = E_{KL} - \frac{1}{3}E_{MM}\delta_{KL}, \qquad T^e_m = \frac{1}{3}T^e_{KK} \tag{4.79}$$

$$s_{KL} = T^e_{KL} - T_m\delta_{KL}$$

Finally, Eq.(4.73) is reduced to

$$\dot{E}^{s}_{KL}=\dot{E}^{vp}_{KL}+\left(\frac{\partial G}{\partial T^{e}_{KL}}\right)^{\cdot}+(3\hat{a}^{(2)}\dot{T}^{e}_{m}-3\hat{\tau}^{(1)}\dot{E}^{ve}_{MM})\delta_{KL}+(2\hat{b}^{(2)}\dot{S}_{KL}-2\hat{\tau}^{(2)}\dot{e}^{ve}_{KL}) \tag{4.80}$$

The explicit form of $\dot{E}^{vp}_{KL}$ has been already discussed in Chapter 3. The evolutionary equation governing $\dot{E}^{vp}_{KL}$ is given by the second term of Eq.(3.39).

The complementary energy density ϕ of a viscoelastic-viscoplastic body is illustrated in Fig.4.1. When both the soil particle and fluid are compressible, following relations must be given under the condition that the coupling between solid and fluid influences the volumetric strain only.

$$\begin{aligned} E^{s}_{IJ} &= \hat{E}^{s}_{IJ}(T^{f}_{IJ},T^{s}_{IJ},E^{vp}_{IJ},E^{ve}_{IJ},\ \theta,\ \bar{g}^{s}_{I},\ \kappa) \\ E^{f}_{KK} &= \hat{E}^{f}_{KK}(T^{f}_{KK},T^{s}_{KK},E^{vp}_{KK},E^{ve}_{KK},\ \theta,\ \bar{g}^{f}_{I},\ \kappa) \end{aligned} \tag{4.81}$$

The deformation of a solid phase is strongly related to the deformation of a fluid. For example, Biot takes the linear relation Eq.(4.82) in place of Eq.(4.81).

$$\begin{aligned} E^{s}_{KK} &= \frac{1}{(k_c\alpha_b-\alpha_c)}\{[(1-n)u+T^{e}_{m}]k_c-nu\alpha_c\} \\ E^{f}_{KK} &= \frac{1}{(k_c\alpha_c-\alpha_c)}\{nu\alpha_b-[(1-n)u+T^{e}_{m}]\alpha_c\} \end{aligned} \tag{4.82}$$

where α_b, α_c and k_c are the material constants.[22] The case when an internal constrain exists is a special case as two-phase mixture. Most generally, however, the coupling, prescribed by such as Eq.(4.81), exists and such

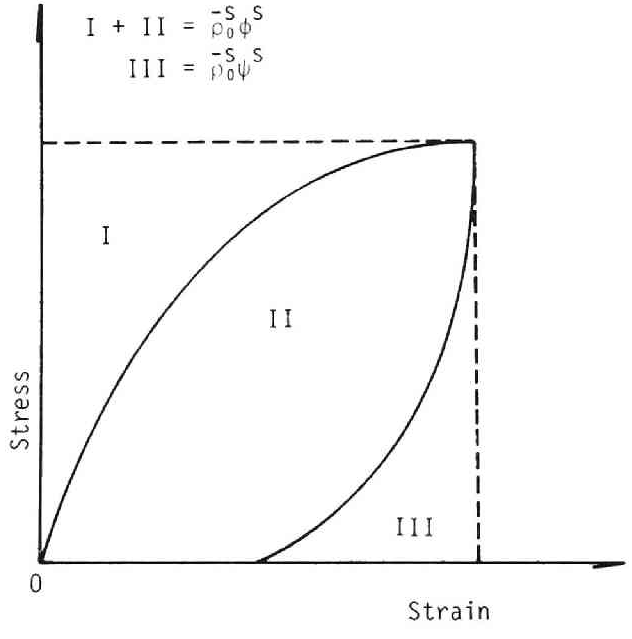

Fig.4.1 Energy function of viscoelastic-viscoplastic body.

case will be of interest in the theory of mixture. There must exist a relative velocity between solid and fluid phase and this term should be taken as an independent variable in derivation of the constitutive equations. From a thermodynamic restriction,[33] and/or a property of wave phenomena,[34] however, the first order term of relative velocity vanishes deductively under a condition with a special assumption. Moreover, higher order terms of the relative velocity than the second order is neglected from the consideration.

4.6 Conclusion

In this chapter, the nature of soil as a multi-phase mixture has been treated as a mixture constituting of the solid and fluid phase. A saturated soil was mainly taken in consideration. A fundamental theory of two-phase mixture was developed and the constitutive theory proposed for a mixture of a viscoelastic-viscoplastic material and an elastic fluid will be employed to analyze the one-dimensional stress wave propagation problem through saturated cohesive soil in Chapter 6. The main conclusions obtained throughout in Chapter 4 are listed below.

(1) The fundamental equations governing the solid-fluid mixture were clearly described, based on the Green & Naghdi's theory for an aim of application to saturated soil.

(2) Using the theory of mixture of solid and fluid, the exact meaning of Terzaghi's effective stress concept was made clear. As a result, it can be seen that the only stress power deduced by an effective stress contributes to the entropy production if a fluid is incompressible. The effective stress concept is deeply dependent on the form of the pore fluid motion. An interparticle force (or stress) is related with the constitutive equation of soil

but not with the effective stress.

(3) The general equations governing the consolidation which is applicable to non-linear analysis were deduced from a theory of two-phase mixture

(4) The constitutive theory for a mixture of a viscoelastic-viscoplastic material and an elastic fluid was deduced, using the theory of mixture and an internal state variable theory.

References for Chapter 4

1) Biot, M.A.: Mechanics of Deformation and Acoustic Propagation in Porous Media, J. Appl. Phys., Vol.33, 1962, pp.1482-1498.

2) Ishihara, K.: Theory of Consolidation of a Porous Material with Heat Effect Based on the Irreversible Thermodynamics, Trans. of JSCE, No.113, Jan., 1965, pp.28-42.

3) Truesdell, C. : Rational Thermodynamics, New York, McGraw-Hill, 1969.

4) Coleman, B.D. and W. Noll: Thermodynamics of Elastic Materials with Heat Conduction and Viscosity, Arch. Rational Mech. Anal., Vol.13, 1963, pp.167-178.

5) Green, A.E. and P.M. Naghdi: A Dynamical Theory of Interacting Continua, Int. J. Eng. Sci.,Vol.3, 1965, pp.231-241.

6) Eringen, A.C. and J.D.Ingram: A Continuum Theory of Chemically Reacting Media-I, J.Eng. Sci., Vol.3., 1965, pp.197-212.

7) Bowen, R.M. : Toward a Thermodynamics and Mechanics of Mixtures, Arch. Rational Mech. Anal., Vol.24, 1967, pp.370-403.

8) Müller, I.: A Thermodynamic Theory of Mixtures of Fluids, Arch. Rational Mech. Anal., Vol.28, 1968, pp.1-39.

9) Ishihara, K. : Approximate Forms of Wave Equation for Water-Saturated Porous Materials and Related Dynamic Modulus, Soils and Foundations, Vol.10, No.4, 1970, pp.10-38.

10) Akai, K. and M. Hori : Considerations of Wave Characteristics in Soil Assumed as a Viscoelastic Material, Proc. JSCE, No.221, Jan., 1974, pp.81-91.

11) Adachi, T.: Consideration of Constitutive Equation of Soil Material, Preprint 27th Conf. JSCE, 1972, PP.333-336 (in Japanese).

12) Atkin, R.J. and R.E. Craine: Continuum Theory of Mixtures(Basic Theory and Historical Development), Q. J. Mech. Appl. Math., Vol.29, 1976, pp.209-244.

13) Bowen, R.M.: Continuum Physics(ed. by E.Eringen), Vol.III(Mixtures and EM Field Theories), Academic Press, New York-London, 1976.

14) Green, A.E. and P.M. Naghdi: Remarks on a Paper by R.M.Bowen, Arch. Rational Mech. Anal., Vol.27, 1967, pp.175-180.

15) Green, A.E. and P.M.Naghdi: Entropy Inequalities for Mixtures, Quart. J. Mech. Appl., Vol.24, 1971, pp.473-485.

16) Green, A.E. and P.M.Naghdi: On Continuum Thermodynamics, Arch. Rational Mech. Anal., Vol.43, 1972, pp.352-378.

17) Terzaghi, K.:'Die Berechnung der Durchlässigkeitsziffer des Tones aus dem Verlauf der hydrodynamischen Spannungserscheinungen', reprinted in From Theory to Practice in Soil Mechanics, J. Wiley & Sons., New York, 1923, pp.133-146.

18) Rendulic, L.: 'P renziffer and Poren Wasserdruck in Tonen', Der Ba ingenieur, Vol.17, 1936, pp.559-564.

19) Terzaghi, K. : Theoretical Soil Mechanics, J. Wiely & Sons., New York, 1943, pp.11-15.

20) Davis, E.H. and Poulos, H.G.: Triaxial Testing and Three-Dimensional settlement Analysis, Proc. 4th Aust.-N.Z. Conf. Soil Mech. and Fndn. Engng., 1965, pp.233-243.

21) Biot, M.A.: General Theory of Three-Dimensional Consolidation, J. Appl. Phys. Vol. 12, 1941, pp.155-164.

22) Ishihara, K.: Fundamentals of Soil Dynamics, Kajima Pub., 1976, pp. 50- 69 (in Japanese).

23) Bishiop,A.W.: The Principles of Effective Stress, Norwegian Geotechnical Institute Pub., No.32, 1960, pp.1-5.

24) Skempton, A.W. : Effective Stress in Soils, Concrete and Rocks, Pore Pressure and Suction in Soils, London, Butterworth, 1961, pp.4-16.

25) Rendulic, L. : Ein Grundgesetz der Tonmechanik und sein experimenteller Beweis, Bauingenieur, Vol.18, 1937, pp.459-467.

26) Akai, K. and T. Tamura: An Application of Nonlinear Stress-Strain Relations to Multi-Dimensional Consolidation Problems, Disaster Prevention Research Institute Annuals, No.19.B-2, Kyoto Univ., 1976, pp.15-29 (in Japanese).

27) Lambe, T.W. and R.V. Whitman: Soil Mechanics, John Wiley & Sons Inc., 1969, pp.241-250.

28) Scott, R.F.: Principle of Soil Mechanics, Addison-Wiesley Pub. Company Inc., 1963, pp.163-166.

29) Mitchell, J.K. : Fundamentals of Soil Behavior, John Wiley & Sons Inc., 1976, pp.186-196.

30) Yamaguchi, H.: Mechanics of Soil, Kyoritsu Pub. Company Inc., Tokyo, 1976, pp.7-9 (in Japanese).

31) Adachi, T. and K. Hibiya: Consideration of Deformation Mechanism of Unsaturated Soil, Preprint 10th Annual Meeting of JSSMFE, 1975, pp. 209-212 (in Japanese).

32) Kenyon, D.E. : The Theory of an Incompressible Solid-Fluid Mixture, Arch. Rational Mech. Anal., Vol. 62, 1976, pp.131-147.

33) Green, A.E. and T.R.Steel: Constitutive Equations for Interacting Continua, Int. J. Engng. Sci., Vol.4, 1966, pp.483-500.

34) Toki, K. and T.Sato: One-Dimensional Acceleration Waves in a Mixture of 2 Phases, Theoretical and Applied Mechanics, Vol.22, 1974, pp.89-102.

Chapter 5 Stress-Strain Relation of Cohesive Soil

5.1 General remarks

In order to analyze a dynamic behavior of a ground or a soil-structure interaction quantitatively, the stress-strain relation of soil has to be made clear. Recently, many investigators have used the stress-strain curves of soil in a simple form. Kondner [1] and Hardin & Drnevich [2), 3)] formulated a hyperbolic stress-strain relation of soil which involves two parameters. But the hyperbolic stress-strain relation can not explain the hysterisis loop of reserved loading. To compensate this difficulty, the Ramberg-Osgood [4)] curve was introduced by Constantious et al. [5)], Streeter et al. [6)] and Richart & Wylie [7)]. Finn, Lee & Martin [8)] used a Masin's curve to present a stress-strain curve of sand. These stress-strain curves described above are independent of strain rate.

For clays, a strain rate effect is important(at high rate of strain). Therefore, it is necessary to get a stress-strain relation of clay which can explain the rate effect in soil dynamics. The theoretical formulations of constitutive relation of soil materials have been conducted by assuming the various models for soil material; viscoplastic model, elasto-plastic model, elasto-viscoplastic model, compacting and locking model. For cohesive soil,it is pointed out by various researchers[9)]that dynamic behaviors in the comparatively wide range of frequency can reasonably interpreted using a three-parameter visco-elastic model.

Generally, it is well known that there occur inelastic deformation and energy dissipation of soil, depending upon the stress or strain level, during stress wave propagation. To describe these characters, various dissipative models are proposed by Salvadori et al. [10)], Seaman [11)] and

Heierli et al.[12] The theoretical formulation of stress wave propagation problem accompanied with the inelastic deformation of material was firstly developed for the metal bar in various ways. These are the roughly divided into two theories; the strain rate dependent theory and the strain rate independent theory. The later was mainly developed by Karman et al.[13] Taylor[14] and Rakhmatulin. On the contrary, Sokolowskii and Malvern[15] developed the longitudinal wave propagation theory(which is called "SM" theory), accounting for strain rate dependency. This "SM" theory was then generalized by Cristescu[16] and Lubliner.[17] Parkin[18] applied this theory to the stress wave propagation test through sand which was carried out by Whitman.[19] Perzyna,[20],[21] developed the three dimensional elastic-viscoplastic theory which is equivalent to a generalized body proposed by Cristescu et al.. Adachi and Okano[22] used the Perzyna's theory to describe the dynamic stress-strain relation of cohesive soil. It should be noted, however, that Perzyna's theory of elastic-viscoplasticity is not sufficient to be applied to the dynamic plasticity of clay. The dynamic behavior of clay includes both high strain rate behavior and comparatively low strain ones. In other words, the constitutive relations for cohesive soil should be able to interprete dynamic behavior in a wide range of strain and strain rate.

From the results of Chapter 2, it is clear that the cohesive soil includes the viscoelastic-viscoplastic nature. In Chapter 3, the general thermodynamic constitutive theory of inelastic material has been developed. Therefore, in this chapter, the author will deduce the more elaborated stress-strain relation for cohesive soil, based on the results obtained in Chapter 2 and 3.

5.2 Developement of constitutive equation for a normally consolidated clay

In a following developement, we consider infinitesimal strain and isothermal condition. ε_{ij} is the strain tensor, ε_{ij}^{vp} the viscoplastic strain tensor and σ_{ij} the stress tensor. Deviatoric strain is denoted by e_{ij} and deviatoric stress tensor by s_{ij}, these are given by

$$e_{ij} = \varepsilon_{ij} - \frac{1}{3}\varepsilon_{kk}\delta_{ij} \quad , \quad s_{ij} = \sigma_{ij} - \frac{1}{3}\sigma_{kk}\delta_{ij}$$

The second invariant of deviatoric stress tensor is denoted by

$$J_2 = \frac{1}{2}s_{ij}s_{ij}$$

There does not exist the exact and complete theory for stress-strain relation of fully saturated clay in equilibrium state. Roscoe's original theory [23] and Burland's modified energy theory [24] are not sufficient to explain the behavior of fully saturated clay, but can explain the behavior of saturated clay in equilibrium to some extent. Following the study by Adachi et al. at the first step, we will use the Roscoe's original theory to construct the constitutive equation of clay, which includes the rate effect. Adachi and Okano [22] extended the Roscoe's original energy theory to the three-dimensional case. The extended yield function is given by

$$f_s = \sqrt{2J_2} + M^* \sigma'_m \ln(\sigma'_m/\sigma'_{my}) = 0 \qquad (5.1)$$

where σ'_{ij} is the effective stress tensor, M^* the value of $\sqrt{2J_2}/\sigma'_m$ at critical state and σ'_{my} the hardening parameter. By the way, the yield condition of Von-Mieses asserts that the material yields and flows plastically when the elastic energy reaches some critical quantity.

$$f_s = \frac{1}{2} s_{ij} s_{ij} - \kappa = 0 \tag{5.2}$$

The yield condition Eq.(5.1) is regarded as the extension of Von-Mieses. Corresponding to Eq.(5.2), Eq.(5.1) is then replaced by

$$f_s = 2J_2 - [M^* \sigma'_m \ln(\sigma'_m/\sigma'_{my})]^2 = 0 \tag{5.3}$$

Eq.(5.3) may be physically explained as follows. Function f must be connected with the energy function since f is defined by Eq.(3.35). When the yield function Eq.(5.3) is used, the obtained results should be identical to those by using Eq.(5.1) as plastic potential.

According to the result of Chapter 3, $f = f(F, T_{KL}, P_{KL}, \theta, \kappa)$, and F-function may be arbitrary if f is equal to f_s only when F = 0. Fig.5.1 depicts procedure to determine f. From this figure, f is therefore given by

$$f = s_{ij} s_{ij} - [M^* \sigma'_m \ln(\sigma'_m/\sigma'_{my}) - F]^2 = 0 \tag{5.4}$$

$$F = \bar{\alpha}(\varepsilon^{vp}_{ij})(\sqrt{2J_2}^{(d)} - \sqrt{2J_2}^{(s)}) \tag{5.5}$$

In this figure, $\bar{\alpha}$ is

$$\bar{\alpha} = \frac{\sqrt{2J_2}(P_1) - \sqrt{2J_2}(P_3)}{\sqrt{2J_2}(P_1) - \sqrt{2J_2}(P_2)} \tag{5.6}$$

Where

$$\sqrt{2J_2}(P_3) + M^* \sigma'_m(P_3) \ln[\sigma'_m(P_3)/\sigma'_{my}] = 0 \tag{5.7}$$

$$\sqrt{2J_2}(P_2) + M^* \sigma'_m(P_2) \ln[\sigma'_m(P_2)/\sigma'_{my}] = 0 \tag{5.8}$$

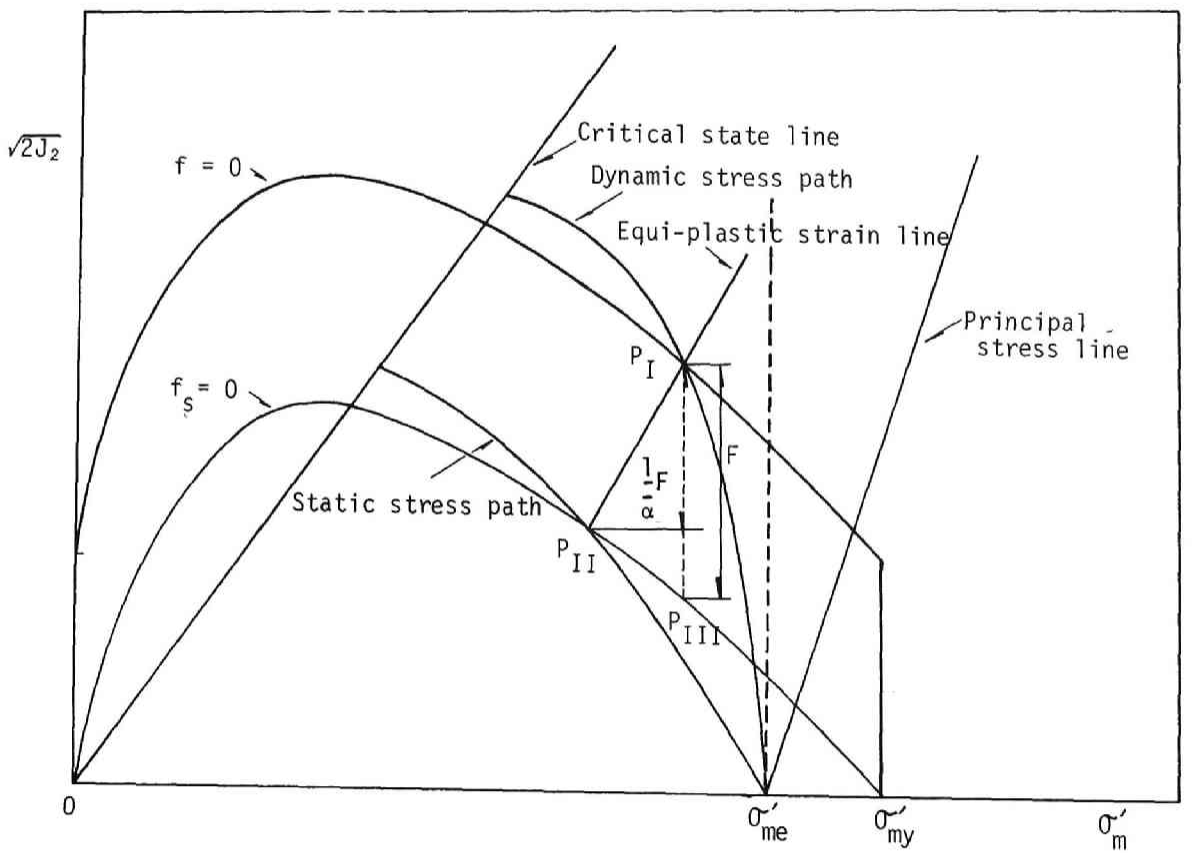

Fig.5.1 Manner to determine f-function.

The point P_1 has the plastic strain equivalent to the point P_2. From the Eqs.(5.7) and (5.8), we obtain

$$\sqrt{2J_2}(P_3)=\frac{\sigma'_m(P_3)}{\sigma'_m(P_2)}\sqrt{2J_2}(P_2) - M^*\sigma'_m(P_3)\ln\frac{\sigma'_m(P_3)}{\sigma'_m(P_2)} \tag{5.9}$$

F is obtained from Eqs.(5.5),(5.6) and (5.9) as;

$$F = \sqrt{2J_2}(P_1)- \frac{\sigma'_m(P_1)}{\sigma'_m(P_2)}\sqrt{2J_2}(P_2) + M^*\sigma'_m(P_1)\ln[\sigma'_m(P_3)/\sigma'_m(P_2)] \tag{5.10}$$

In view of Eqs.(5.3), (5.4) and (5.10),

$$\frac{\partial f}{\partial \sigma_{ij}} = 2S_{ij}- 2(M^*\sigma'_m\ln\{\sigma'_m/\sigma'_{my}\}- F)(1+\ln\{\sigma'_m/\sigma'_{my}\})M^*\frac{1}{3}\delta_{ij}$$

$$=\sqrt{2S_{ij}}- 2\sqrt{2J_2}\left(M^*- \frac{\sqrt{2J_2}(s)}{\sigma'_m(s)} + M^*\ln\{\sigma'_m/\sigma'_m(s)\}\right)\frac{1}{3}\delta_{ij} \tag{5.11}$$

From Eqs.(3.37) and (3.38), we can get

$$\dot{\varepsilon}^{vp}_{ij}= O_{ijkl}\frac{\partial f}{\partial \sigma_{kl}} \tag{5.12}$$

in which, O_{ijkl} and N_{ijkl} are postulated as an isotropic tensor and they are expressed by

$$O_{ijkl}=M_{ijmn}(N_{mnkl})^{-1}=X\delta_{ij}\delta_{kl}+ Y(\delta_{ik}\delta_{jl}+\delta_{il}\delta_{jk}) \tag{5.13}$$

$$N_{ijkl}=A\delta_{ij}\delta_{kl} + B(\delta_{ik}\delta_{jl} +\delta_{il}\delta_{jk}) \tag{5.14}$$

$$A = \frac{1}{3}\left\{- \frac{2}{3\sigma'_{in}}(M^*\ln\{\sigma'_m/\sigma'_{my}\}- F)(\ln\{\sigma'_m/\sigma'_{my}\})+1)-2\right],B=1$$

In Eq.(5.13), we also postulate;

$$X = (\beta_2 - \beta_1)/6\sqrt{2J_2}\ , \quad Y = \beta_1/4\sqrt{2J_2} \tag{5.15}$$

where β_1 and β_2 are arbitrary functions.

In this case, M_{ijkl} is reduced as

$$M_{ijkl} = P\delta_{ij}\delta_{kl} + Q(\delta_{ik}\delta_{jl} + \delta_{il}\delta_{jk}) \tag{5.16}$$

$$P = (3A+2)X + 2AY,\quad Q = 2Y$$

Substituting Eq.(5.14) into Eq.$(3.36)_2$, A_{ij} is obtained,

$$A_{ij} = 2s_{ij} - \frac{2}{3}M^*(M^*\sigma'_m \ln\{\sigma'_m/\sigma'_{my}\} - F)(\ln\{\sigma'_m/\sigma'_{my}\}+1)\delta_{ij} \tag{5.17}$$

Therefore,

$$\frac{\partial A_{ij}}{\partial \sigma_{mn}} = \frac{\partial A_{mn}}{\partial \sigma_{ij}}$$

Then A_{ij} satisfies the exact differentiability condition, Eq.$(3.36)_1$.

From Eq.(3.39),

$$\dot{\varepsilon}^{vp}_{ij} = M_{ijkl}(N_{klmn})^{-1}\frac{\partial f}{\partial \sigma_{mn}} = (3P+2Q)\sigma'_m \delta_{ij} + 2QS_{ij} \tag{5.18}$$

Using Eq.(3.26), (3.38) and Eq.(5.18), we get

$$\begin{aligned}\dot{\varepsilon}^{vp}_{ij}\frac{\partial \phi}{\partial \varepsilon^{vp}_{ij}} &= \beta_2 M^*(\ln\{\sigma'_m/\sigma'_{my}\}+1)\sigma'_m + \sqrt{2J_2}\beta_1 \\ &= \beta_2(F-\sqrt{2J_2}) + \sigma'_m M^*\beta_2 + \sigma'_m M^*\beta_2 + \sqrt{2J_2}\beta_1 \\ &= F\beta_2 + \sigma'_m M^*\beta_2 + \sqrt{2J_2}(\beta_1 - \beta_2)\end{aligned} \tag{5.19}$$

If β_1 and β_2 are positive function, Eq.(5.20) will be sufficient condition of Eq.(3.26), because F is positive.

$$\beta_1-\beta_2 \geq 0 \tag{5.20}$$

From Eqs.(4.80) and (5.18), the stress-strain relation is finally obtained as follows:

$$\dot{\varepsilon}_{ij}=\overline{\left(\frac{\partial g}{\partial \sigma_{ij}}\right)}\ +(2b^2 S_{ij}-2\tau^{(2)}e^{ve}_{ij})\ +\ (3a^{(2)}\sigma'_m\ 3\tau^{(1)}\varepsilon^{ve}_{kk})\delta_{ij}+\ \frac{S_{ij}}{\sqrt{2J_2}}\beta_1$$
$$+\frac{1}{3}\delta_{ij}\beta_2\{M^*-\ \frac{\sqrt{2J_2}}{\sigma'_m(s)}\ +M^*\ln[\sigma'_m/\sigma'^{(s)}_m]\} \tag{5.21}$$

In the case of conventional axi-symmetric compression,

$$s_{11}=\ \frac{2}{3}(\sigma'_{11}-\sigma'_{22})=\ \frac{2}{3}q,\quad e_{11}=\varepsilon_{11}\ ,\quad \sigma'_m=\ \frac{1}{3}\sigma'_{kk}$$

$$S_{ij}/\sqrt{2J_2}=\sqrt{\frac{2}{3}}\ ,\qquad \dot{\varepsilon}_{11}-\ \frac{2}{3}(\dot{\varepsilon}_{11}-\dot{\varepsilon}_{22})$$

From the Eq.(5.21), the stress-strain relation in undrained axi-symmetric triaxial compression is expreesed by

$$\dot{e}_{11}=\gamma_1\dot{S}_{11}\ +\sqrt{\frac{2}{3}}\beta_2+(\frac{4}{3}b^{(2)}q-2\tau^{(2)}e^{ve}_{11}) \tag{5.22}$$

If viscoelastic volume change is zero, taking the condition of $\dot{\varepsilon}_{kk}=0$ into consideration,

$$\gamma_2\dot{\sigma}'_m\ +\beta_2(M^*\ \ \frac{\sqrt{2J_2}(s)}{\sigma'_m(s)}\ +\ M^*\ln\{\sigma'_m/\sigma'^{(s)}_m\})=0 \tag{5.23}$$

where the assumption has been made as

$$\frac{\dot{\partial g}}{\partial \sigma_{ij}} = \gamma_1 \dot{S}_{ij} + \frac{1}{3}\dot{\sigma}'_m \gamma_2 \delta_{ij} \tag{5.24}$$

5.3 Phenomenological nature of parameters without a viscoelastic effect

We examine a degree of approximation of Eqs.(5.22) and (5.23) for the experimental results of undrained axi-symmetric triaxial test. In the further consideration, the viscoelastic strain is not taken in discussion for a simplicity. Under these considerations, the stress-strain relation is then given by

$$\dot{e}_{11} = \gamma_1 \dot{S}_{11} + \sqrt{\frac{2}{3}}\beta_2 \tag{5.25}$$

Fig.5.2 shows the relation between the viscoplastic strain rate and $\sqrt{\frac{2}{3}}(\sqrt{2J_2} - \sqrt{2J_2^{(s)}})/\sigma'_m$ in semi-log scale, which is obtained by rearranging the results of the undrained creep test.[25] It is evident from Fig.5.2 that $(q-q_s)/\sigma'_m$ increases in proportional to the logarithm of strain rate when the amount of strain is equal. Therefore, β'_2 may possibly be taken as

$$\beta_1 = C_0(\varepsilon_{11}^{vp})\exp\{\frac{m(\varepsilon_{11}^{vp})}{\sigma'_{me}}(q-q_s)\} \tag{5.26}$$

$$\ln\dot{\varepsilon}_{11}^{vp} = \ln\sqrt{\frac{2}{3}}C_0 + \frac{m}{\sigma'_{me}}(q-q_s) \tag{5.27}$$

Experimental equation in the stress relaxation test, proposed by Murayama et al.,[26] is given by

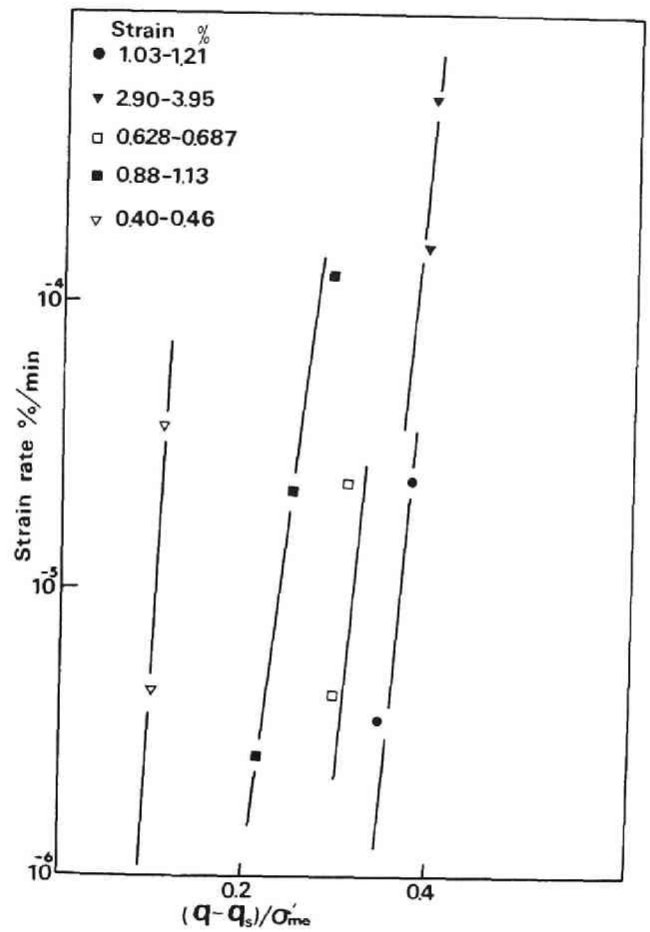

Fig.5.2 Relationship between strain-rate and $(q-q_s)/\sigma'_{me}$.

$$q_r(\varepsilon_{11},t)-q_r(\varepsilon_{11},t_0) = -\beta(\varepsilon_{11})\log(t/t_0) \tag{5.28}$$

where q_r is the deviator stress at time t when the total strain is maintained unchanged and $\beta(\varepsilon_{11})$ is the rate of relaxation, equivalent to $dq_r/d\log(t)$. Substituting Eq.(5.28) into Eq.(5.25) and assuming $q_r(\varepsilon_{11},t_0) = q_s$, we get

$$-\frac{2}{3}\gamma_1\frac{\beta}{2.303}\frac{1}{t} + \frac{2}{3}C_0\exp\{\frac{m}{\sigma'_{me}}\frac{\beta}{2.303}\ln(t/t_0)^{-1}\} = 0 \tag{5.29}$$

The condition to satisfy Eq.(5.29) is obtained by

$$\frac{m}{\sigma'_{me}}\frac{\beta}{2.303} = 1 \tag{5.30}$$

$$\frac{2}{3}\gamma_1\frac{\beta}{2.303} = C_1 t_0, \qquad C_1=\sqrt{\frac{2}{3}}C_0 \tag{5.31}$$

From Eq.(5.30), β increases proportionally to the consolidation pressure σ'_{me}. These results coincide with the stress relaxation test results. In the strain rate controlled shear test indicated by Fig.5.3 which shows the correlation between q and $\log\dot{\varepsilon}_{11}$, it is clearly noticed that the slope σ'_{me}/m increases as the strain increases and becomes constant. The intercept C_1 in Fig.5.2 decreases as the strain increases, even for the same values of $(q-q_s)/\sigma'_{me}$. The rate of reduction becomes small as the increase of strain. The following empirical equation is a special case of Eq.(5.25) which has been proposed by Yong & Japp [27] into consideration for dynamic loading triaxial test with constant strain rate neglecting the elastic strain rate.

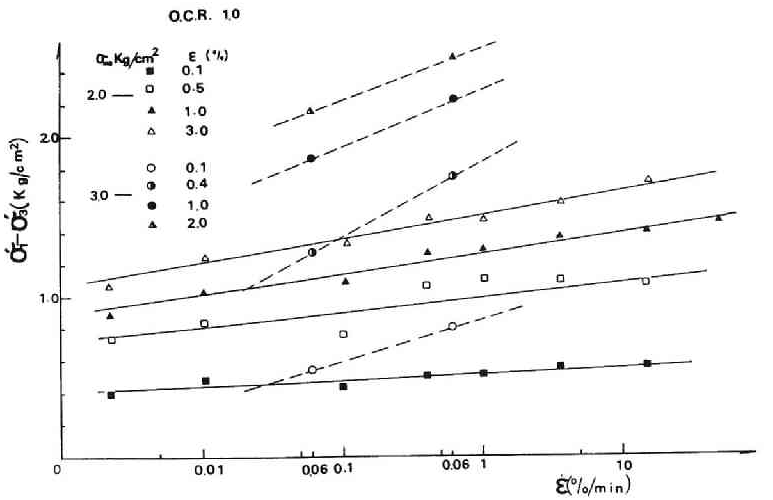

Fig.5.3 Relatioship between deviator stress and logarithm of strain-rate.

$$q(\varepsilon_{11},\dot{\varepsilon}_{11})-q(\varepsilon_{11},\dot{\varepsilon}_{11(0)})=\alpha(\varepsilon_{11})\log(\dot{\varepsilon}_{11}/\dot{\varepsilon}_{11}^{(0)}) \tag{5.32}$$

Akai et al.[28] show that Eqs.(5.28) and (5.32) are equivalent, resulting in equality of $\alpha(\varepsilon_{11})$ in Eq.(5.32) and β in Eq.(5.28) which has been approximately accepted from the experiment. Consequently, they derive the empirical equation given by Singh & Mitchell [29] for undrained creep deformation. Eq.(5.25) satisfies these results.

Discussion is now made on Eq.(5.23). This equation which governs the variation of a mean effective stress σ'_m was obtained by assuming that volumetric strain rate is zero under undrained condition. The pore-water pressure can be approximately assessed by this equation. Substituting Eq.(5.28) into Eq.(5.23), we obtain

$$\begin{aligned}\gamma_2\dot{\sigma}'_m &= -\beta_2(F)(M^* - \frac{\sqrt{2J_2}(s)}{\sigma'_m(s)} + M^*\ln\{\sigma'_m/\sigma'_m(s)\}\\ &= -C_2\exp\{\frac{m}{\sigma'_{me}}\frac{\beta}{2.303}\ln(t/t_0)^{-1}\}\\ &= -C_2\bar{t}^{t_0}\end{aligned} \tag{5.33}$$

where $$\frac{m}{\sigma'_{me}}\frac{\beta}{2.303} = 1$$

$$C_2=C_0\ (M^*\ \frac{\sqrt{2J_2}(s)}{\sigma'_m(s)} + M^*\ln\{\sigma'_m/\sigma'_m(s)\})$$

Therefore, provided that C_2/γ_2 is determined only by strain, Eq.(5.33) can be integrated as

$$\sigma'_m = -\bar{A}\ln(t/t_0) + \sigma'_{m(0)} \tag{5.34}$$

where, as a result, $C_2 = \frac{\gamma_2 \bar{A}}{t_0}$. $\bar{A}$ is determined from the test as an inclination of the stress path in the effective mean principal stress-deviator stress plane. As a special case, when a relaxation test is performed, the stress path is parallel to the principal stress line. Then, in view of Eqs.(5.34) and (5.28), $\dot{\sigma}'_m : q = 1 : 3$. Therefore, $\bar{A}$ can be expressed by $\bar{A} = \frac{1}{3} \frac{\beta}{2.303}$. According to Eq.(5.31) and the relations of β and $\bar{A}$ given above, C_1 is given by

$$C_1 = \frac{1}{t_0} \frac{2^{\gamma_1 \beta}}{6.909} = \frac{2^{\gamma_1} C_2}{\gamma_2} \tag{5.35}$$

For practical usage of Eqs.(5.23) and (5.25), the parameters which are regarded to be determined are γ_1, γ_2, β , σ'_{me} , M^*, λ, κ and e_0(initial void ratio). λ and κ denote the slope of e-log σ'_m line for consolidation test and swelling test, respectively. Using these parameters, the dynamic stress-strain relation and stress path for normally consolidated clay can be determined. The test results by Akai et al. [28] and Murayama et al. [26] show that $\alpha(\varepsilon_{11})$ and $\beta(\varepsilon_{11})$ take approximately the values of 0.2 kg/cm^2 and 0.14 to 0.17 kg/cm^2, respectively, for clay samples consolidated under 2 kg/cm^2. Taking these results into consideration, it is probable that the value of m is in a range between 23.0 to 33.0 computed by Eq.(5.30)

5.3 Discussion

Fig.5.4 represents the effective stress path under triaxial compression test on a normally consolidated clay carried out by Richardson and Whitman .[30] This figure indicates that the strain-rate influences significantly the effective stress path and the pore water pressure developement. These effect of strain-rate to stress path will be discussed on the basis

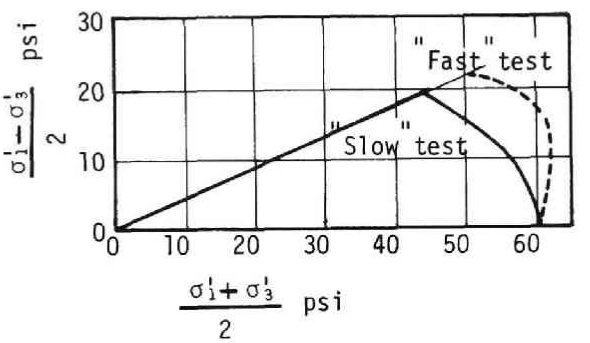

Fig.5.4 Average stress path under triaxial compression test on a normally consolidated clay (after Richardoson and Whitman 1963[30]).

of author's theory. Figs.5.5 and 5.6 show a theoretical effective stress path under the strain-rate controlled triaxial compression test on a normally consolidated clay, calaulated by using Eqs.(5.23) and (5.25). The calculation was carried by using a Runge-Kutta's method, in which the relation $\gamma_2=\kappa/[(1+e_0)\sigma'_m]$ was assumed, considering the swelling curve, e-lnσ'_m line. From these figures, it may be noted that the effect of strain rate can be reasonably assessed by author's theory. In Fig.5.6, the equilibrium stress path can be given by the Roscoe's original theory.[23] After all it may be concluded that the dynamic stress-strain-pore pressure relation of a normally consolidated clay can be completely described by solving Eqs.(5.23) and (5.25) at the same time.

Fig.5.7 shows the relation between the deviator stress and the rate of increase of pore water pressure due to an effect of dilatancy, which has been obtained from the triaxial test with constant stain rate.[31] From this figure, phenomenological relation may be deduced.

$$\log\Delta\dot{u} = \log\Delta\dot{u}_0 + \bar{\delta}\,(\sigma_1-\sigma_3) \tag{5.36}$$

where, $\bar{\delta}$ denotes the slope of line in Fig.5.7 and depends on the magnitude of strain.

Under the condition of a triaxial compression test, we have

$$\sigma'_m = \sigma'_{me} + \frac{1}{3}(\sigma_1-\sigma_3) - u \tag{5.37}$$

Therefore, the time rate of a mean effctive stress is given by Eq.(5.38).

$$\dot{\sigma}'_m = \dot{\sigma}'_{me} + \frac{1}{3}\dot{q} - \dot{u} = \frac{1}{3}\dot{q} - \dot{u} = -\Delta\dot{u} \tag{5.38}$$

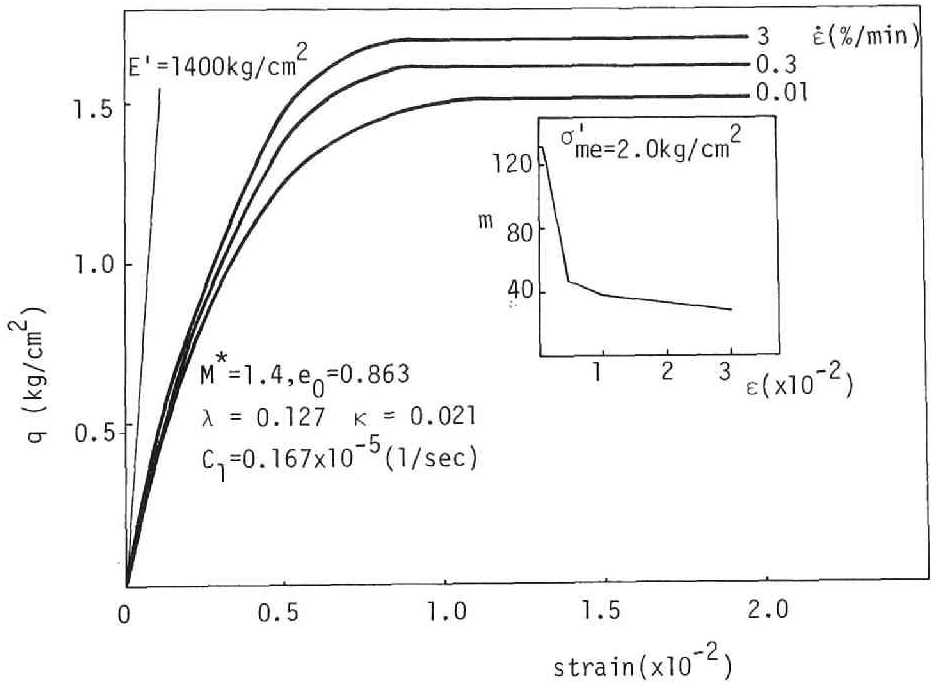

Fig.5.5 Calculated results of stress-Strain relation of strain-rate constant triaxial compression test.

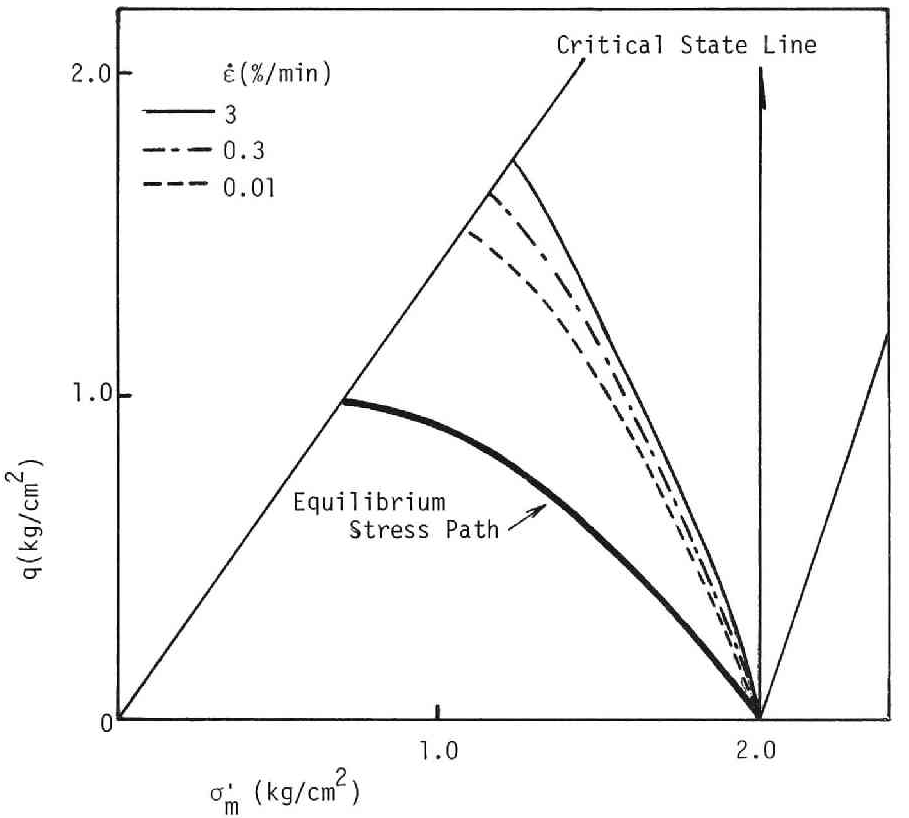

Fig.5.6 Calculated results of stress path of strain-rate constant triaxial compression test.

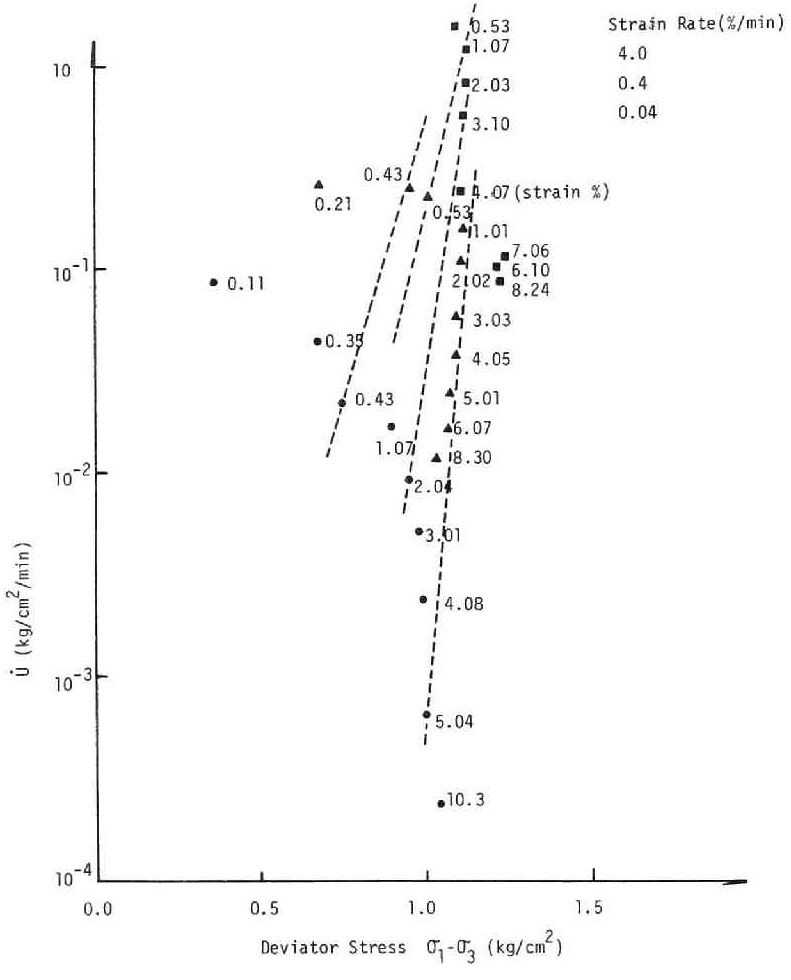

Fig.5.7 Relationship between rate of excess pore water pressure and deviator stress.

where, $\overline{\Delta \dot{u}}$ is a rate of increase of pore water pressure due to a dilatancy. By the way, substituting Eq.(5.38) into Eq.(5.23),

$$\Delta \dot{u} = \Delta \dot{u}_0 \exp\left(\frac{m}{\sigma'_{me}} q\right) \tag{5.39}$$

So that,

$$\ln \Delta \dot{u} = \ln \Delta \dot{u}_0 + \frac{m(\varepsilon_{11})}{\sigma'_{me}} q \tag{5.40}$$

It is evident that this relation is equivalent to Eq.(5.36).

Now, we will perform a parametric study and consider a correlation of the parameters, one m/σ'_{me} for the pore water pressure developement expressed by Eq.(5.40) which corresponds to the empirical relation Eq.(5.36) and the other for the shear stress and strain relation expressed by Eq.(5.27) corresponding to the empirical relation Eq.(5.32). It should be again noted that Eqs.(5.27) and (5.40) are expressed in natural logarithmic form, while those empirical equations are expressed in common logarithmic form. From the experimental results, $\bar{\delta}$ and α can be determined as 7.8 at ε=1.07% from Fig.5.7 and 10, from Fig.5.8,respectively. Taking the correspondence Eq.(5.36) to Eq.(5.40) and Eq.(5.32) to Eq.(5.27) into consideration, the value of m/σ'_{me} in Eq.(5.40) becomes therefore to be 18(7.8x2.303) and one in Eq.(5.27) to be 23(10x2.303). Consequently, a conclusion may then be drawn that the parameters which have been individually determined from the pore water pressure development and the shear stress-strain relation are identical each other with relatively high correlation. That is to say, although an assumption has been made that the functions β_1 and β_2 are identical and relevant equations for pore water pressure and the shear stress-strain relation have been deduced, it could be noted from the parametric study above discussed that this assumption is moderately consistent with the experimental results.

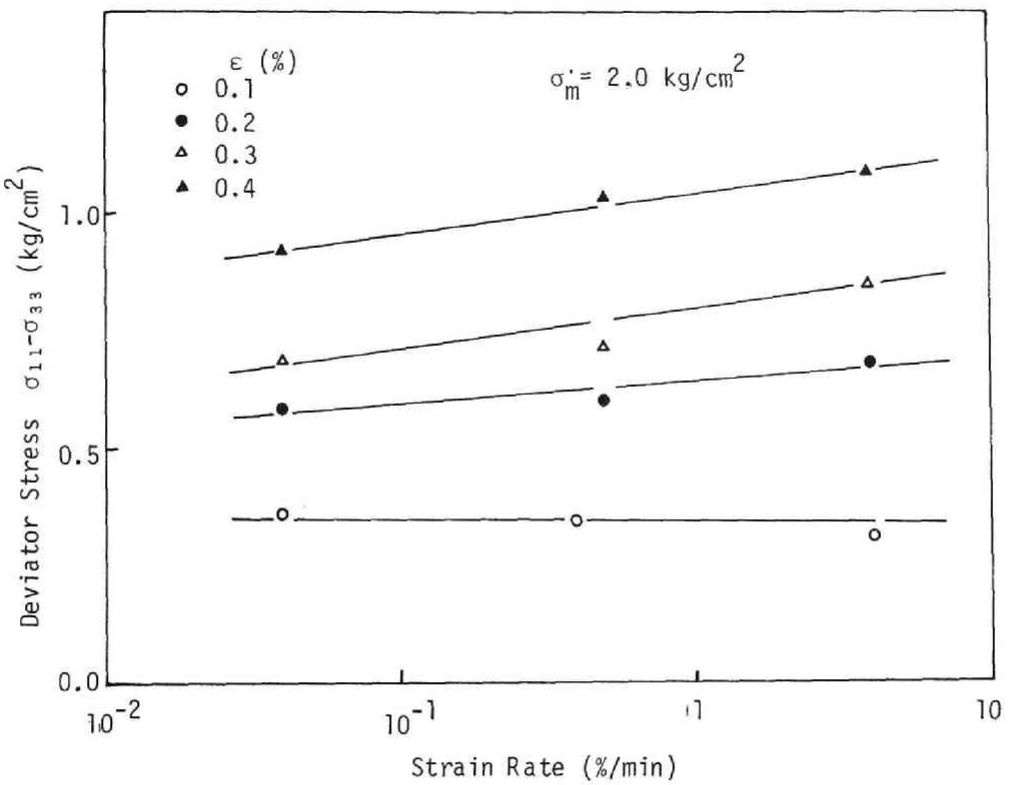

Fig.5.8 Relationship between deviator stress and logarithm of strain rate.

On the other hand, Matsui et al. [32] deduced the phenomenological relation governing the development of excess pore water pressure due to a repeated loading, using Singh & Mitchell's method.[29]

$$\ln\dot{\Delta u} = \ln\dot{\Delta u}_{(t,\tau_{d0})} + \alpha'\tau_d \tag{5.41}$$

where, τ_d is the maximum shear stress and $\dot{\overline{\Delta u}}$ the rate of increase of pore water pressure. Since τ_d is exactly corresponding to q, Eq.(5.41) is also equivalent to Eq.(5.40). Until now, the viscoelastic nature in the most general stress-strain relation, Eq.(5.22) has been neglected in the above discussion. But, generally, it is noted that clayey soil exhibits the viscoelastic behavior as a following discussion.

The various dynamic loading tests on clay samples have been so far carried out by many investigators. According to test results by Kondner & Ho ,[33] Nishigaki & Hirobe(especially for water content =43.4 %),[34] Saito & Goto,[35] it can be noted that shear modulus becomes large as the frequency increases and the damping characteristics also depend on the frequency. Kondner & Ho [33] and Hori [36] reported that the viscoelastic nature of cohesive soil can be approximately expressed by the linear spring-Voigt model. On the other hand, the test results of Krizek & Franklin,[37] Nishigaki and Hirobe(especially for water contant= 84.4 %),[34] Kovas et al.,[38] Parmelee et al.,[39] Hara,[40] Hampton & Wetzel [41] and Vey & Strauss [42] show that the shear modulus and the damping characteristics do not depend on the frequency. The difference of the experimental results between two groups may be able to be explained from a view point of the consideration by Ishihara.[43] Generally, the shear modulus and the damping characteristics of soil do not depend on the magnitude of frequency under the con-

dition such that the strain is below 10^{-3} but are influenced when the strain is over 10^{-3}. However, detail inspection of test conditions and used soil sample of the investivations listed above reveals that general trend can also be seen that soil with high water content does not depend on the frequency. This fact is consistent with the report by Osaki [44] in which he stated that the shear modulus and damping characteristics of soft clay do not depend on the frequency.

From the above discussion, it is concluded that stress-strain relation of clay will be necessary to include the viscoelastic nature. Then, Eq.(5.21) is considered to be more realistic than Eq.(5.25) for elastic-viscoplastic behavior. The parameters which are encountered in the viscoelastic component of stress-strain relation, Eq.(5.22), will be estimated in Chapter 6, considering the wave propagation phenomena.

5.5 Conclusion

In this chapter, the author was mainly concerned with the development of the stress-strain relation of normally consolidated clay. The proposed theory is based on the thermodynamic theory of inelastic material investigated in Chapter 3. The stress-strain relation has been obtained for an elastic-viscoplastic-vicoplastic body, considering various strain rate effects. The phenomenological nature of parameters included in the proposed theory is examined by various types of test (undrained strain rate controlled triaxial test, undrained creep test and a stress relaxation test), neglecting viscoelastic characteristics of soil. The proposed stress-strain relation of clay will be used in Chapters 6 and 7.The main obtained conclusions are as follows.

(1) The stress-strain relation of a normally consolidated clay is deduced, using a general thermodynamic theory of inelastic material. The proposed theory is satisfied with a thermodynamic restriction.

(2) In static state, the author used the Roscoe's original theory as a stress-strain relation. Using a proposed theory, the stress path under the undrained condition can be predicted. That is to say, the development of pore water pressure can be estimated.

(3) The proposed stress-strain relation can explain the dynamic behavior of normally consolidated clay in various tests; undrained creep test, stress relaxation test and undrained strain rate controlled triaxial compression test.

(4) The viscoelastic and viscoplastic property of clay is considered in formulating the stress-strain relation of clay. The viscoelastic property may be expressed by a linear Voigt viscoelastic body from the test results shown in Chapter 2.

(5) The general pattern of the stress path under the relaxation test highly depends on the parameters used in stress-strain relation. For adequately predicting the stress path, the parameter has therefore to be adequately determined.

References for Chapter 5

1) Kondner, R.L.: Hyperbolic Stress-Strain Response: Cohesive Soils, J. SMFD, Proc. ASCE, Vol.89, No.SM1, 1963, pp.115-143.

2) Hardin, B.O. and V.P. Drnevich : Shear Modulus and Damping in Soils: Measurement and Parameter Effects, J. SMFD, Proc. ASCE, Vol.98, No.SM6, 1972, pp.603-624.

3) Hardin, B.O. and V.P. Drnevich: Shear Modulus and Damping in Soils: Design Equations and Curves, J. SMFD, Proc. ASCE, Vol.98, SM7, 1972, pp.667-692.

4) Ramberg, W. and W.T. Osgood: Description of Stress-Strain Curves by Three Parameters, Tech. Note 902, Adv. Comm. for Aeronautics, 1943.

5) Constantious, I.V., J.M. Rosset and J.T. Christian: A Comparison of Linear and Exact Non-Linear Analysis of Soil Amplification , Proc. 5th WCEE, 1973, pp.1806-1815.

6) Streeter, V.L. E.B.Wylie and F.E. Richart, Jr.: Soil Motion Computations by Characteristics Method, J.GED, Proc. ASCE, Vol.100, No.GT3, 1974, pp.247-263.

7) Richart,F.E., Jr. and E.B. Wylie: Influence of Dynamic Soil Properties on Response of Soil Masses, Symp. Struc. and Geotech. Mech., U. of Ill., Urbana, Ill,Oct.,1975, pp.2-5.

8) Finn, W.D.L., K.W. Lee and G.R.Martin : An Effective Stress Model Liquefaction , J. GED, Proc. ASCE, Vol.103, No.GT6, June, 1977, pp.517-533.

9) Kondner, R.L. and M.K. Ho: Energy Dissipation of a Cohesive Soil by the Fourier Transformation of Stress Relaxation Response, Trans. Soc. of Rheology, Vol.9 Part 1, 1965, pp.145-157.

10) Salvadori, M.G., R. Shàlak and P. Weidlinger: Waves and Shocks in Locking and Dissipative Media, Proc. ASCE, Vol.86, NO.EM2, 1960, pp. 77-105.

11) Seaman, L.: One-Dimensional Stress Wave Propagation in Soils, Stanford Research Inst., AD-632106, DASA 1757, 1966, pp.19-40.

12) Heilerli, W.: Inelastic Wave Propagation in Soil Columns, Proc. ASCE, Vol.88, No. SM6, 1962, pp.33-63.

13) Karman, Th. and P.Duwez: The Propagation of Plastic Deformation in Solids, J. Appl. Phys., Vol.21, 1950, pp.987-993.

14) Taylor, G.I.: Scientific Papers(ed. by G.K. Bachelor), Cambridge Univ. Press, Vol.II, 1958, p.467.

15) Malvern, L.E.: Plastic Wave Propagation in a Bar of Material Exhibiting a Strain Rate Effect, Quart. Appl. Math.,Vol.8, 1951, pp.405-411.

16) Cristescu, N.: Dynamic Plasticity, North-Holland Publ. Co., Amsterdam, 1968, pp.101-140.

17) Lubliner, J.: A Generalized Theory of Strain Rate Dependent Plastic Wave Propagation in Bars, J. Mech. Phys. Solid, Vol.12, 1964, pp.59-65.

18) Parkin, B.R.: Theory Compared with Experiments on Column, Discussion: Implications of an Elementary Theory, Impact Waves in Sand Symposium, Trans. ASCE, Vol.127, 1962, pp.1270-1334.

19) Whitman, R.V.: The Behavior of Soils under Transient Loadings, Proc. 4th Inst. Conf. Soil Mech. and Found. Engng., Vol.1, 1957, pp.207-212.

20) Perzyna, P.: The Constitutive Equations for Work-Hardening and Rate-Sensitive Plastic Materials, Proc. Vibrational Problems, Warsaw, Vol.4, No.3, 1963, pp.281-290.

21) Perzyna, P.: Thermodynamic Theory of Visco-Plasticity, Advanced in

Applied Mechanics(ed. by C-S.Yih), Academic Press, New York-London, Vol.II, 1971, pp.313-354.

22) Adachi, T. and M. Okano: A Constitutive Equations for Normally Consolidated Clay, Soils and Foundations, Vol.14, No.4, 1974, pp.55-73.

23) Roscoe, K.H. and J.B. Burland: On the Generalized Stress-Strain Behavior of 'Wet Clay', Engineering Plasticity, Cambridge Univ. Press, 1968, pp.535-609.

24) Burland, J.B.: The Yielding of Clay, Correspondence, Geotechnique, Vol.15, 1965, pp.211-214.

25) Okano, M.: Study on Deormation of Fully Saturated Clay from a View of Viscoplasticity, M.S. Thesis, Kyoto Univ., 1972.

26) Murayama, S., H.Sekiguchi and T.Ueda: Stress Relaxation of Clays, Proc. Kansai Regional Meeting of JSCE, 1972, pp.III-1 (in Japanese).

27) Yong, R.N. and R.D. Yapp: Stress-Strain Behavior of Clays in Dynamic Compression, Vibrational Effects on Earthquakes on Soils and Foundations, ASTM STP, 450, 1969, pp.233-262.

28) Akai, K., T.Adachi and N. Ando: A Stress-Strain-Time Relation of Saturated Clay, Proc. JSCE, No.225, April, 1974, pp.53-61 (in Japanese).

29) Singh, A. and J.K. Mitchell: General Stress-Strain-Time Function for Soils, Proc. ASCE, Vol.94, SM1, 1968, pp.21-46.

30) Richardson, A.M. and R.V. Whitman: Effect of Strain Rate upon Undrained Shear Strength of a Saturated Remoulded Fat Clay, Geotech., Vol.13, No.4, 1963, pp.310-324.

31) Yoneda, O.: Fundamental Study on the Stress-Strain Relation of a Saturated Clay, M.S. Thesis, Kyoto Univ., 1977 (in Japanese).

32) Matsui,T., H. Ohara and T. Ito: Effects of Dynamic Stress History on Mechanical Characteristics of Saturated Clays, Proc. JSCE, No.257, 1977, pp.41-51(in Japanese).

33) Kondner, R.L. and M.M.K. Ho: Viscoelastic Response of a Cohesive Soil in the Frequency Domain, Trans. Soc. of Rheology, Vol.9, Part 2, 1965, pp.329-342.

34) Nishigaki, Y. and T. Hirobe: Characteristics of Hyaterisis of Osaka Diluvial Clays, Preprint, 8th Annual Meeting of JSSMFE, 1973, pp.359-362 (in Japanese).

35) Saito, J. and Y. Goto: Consideration on the Measurement of Elastic Moduli of Soil, 7th Annual Meeting of JSSMFE, 1972, pp.277-280 (in Japanese).

36) Hori, M.: Fundamental Study of Wave Propagation Characteristics through Soils, Doctor Thesis, Kyoto Univ., 1974.

37) Krizek, R.J. and A.G. Franklin : Energy Dissipation in a Soft Clay, Proc. Int. Symp. Wave Propagation and Dynamic Properties of Earth Material, Univ. New Mexico, 1967, pp.293-304.

38) Kovas, W.D.,H.B. Seed and C.K. Chan : Dynamic Moduli and Damping Ratios for a Soft Clay, Proc. ASCE, No.SM1, 1971, pp. 59-75.

39) Parmelee, R.A., J. Penzien, C.F. Scheffey, H.B. Seed and G.R. Thiers: Seismic Effects on Structures Supported on Piles Extending through Deep Sensitive Clays, Report No.64- 2, Inst. of Eng. Res., Univ. of California Barkley, California, 1964.

40) Hara, A. : Dynamic Characteristics of Ground and its Application, Proc. Symp. 2nd. Ground Motion, JSAE, 1973, pp.33-39 (in Japanese).

41) Hampton, D. and R.A. Wezel: Stress Wave Propagation in Confined Soils, Proc. Int. Symp. on Wave Propagation and Dynamic Properties of Earth Materials, 1967, pp.433-442.

42) Vey, E. and L.V. Strauss: Stress-Strain Relationships in Clay due to Propagating Stress Wave, Proc. Int. Symp. on Wave Propagation and

Dynamic Properties of Earth Materials, 1967, pp.575-586.

43) Ishihara, K. : Fundamentals of Soil Dynamics, Kajima Pub., 1976 , pp.1-230(in Japanese).

44) Osaki, T.: Review of Dynamic Analysis, Tsuchi to Kiso, Vol.22, No.3, 1974, pp.1-5 (in Japanese)

Chapter 6 Analytical Study on One-Dimensional Stress Wave Propagation through Cohesive Soil

6.1 General Remarks

Generally, it is well known that there exist inelastic deformation and energy dissipation depending upon the stress or strain level during stress wave propagation through soil. In order to describe these wave characteristics various dissipative models have been so far proposed. Salvadori et al.[1), 2)] investigated the attenuation of a plane wave in certain types of compacting and locking medium. Heierli [3)] calculated the one-dimensional stress wave propagation in hysteretic material by the step by step method. Seaman [4)] proposed the visco-elastic compacting model and the S-hysteretic model. Comparing the experiment with the calculated results, he concluded that tanδ model which exhibited the frequency-independent dissipation well predicted the attenuation of peak stress during wave propagtion in clay and the viscoelastic compacting model was appropriate for sand. Vey & Strauss [5)] proposed the non-linear Voigt model for clay from the experimental stress-strain relations. Hampton & Wetzel [6)] performed the experimental study through EPK clay and Ottawa sand, and the theoretical models were also proposed. They reported that a linear hysteretic model is appropriate for Ottawa sand and a constant tanδ viscoelastic model for EPK clay.

The theoretical formulations of stress wave propagtion problem associated with the inelastic deformation have been developed for the metal bar in various ways. These are divided into two theories; the strain rate dependent theory and the strain rate independent theory. The strain rate independent theory was mainly developed by Karman & Duwez,[7)] Taylor [8)] and Rakumatulin. On the contrary, Sokolovskii and Malvern [9)] independently

developed the theory of the propagation of longitudinal plastic wave in bar which was called "SM" theory. They concerned the influence of the strain rate for stress wave propagation problem.Malvern employed the constitutive equation as follows(for loading part).

$$\sigma = f(\varepsilon) + \hat{A}\ln(1 + \hat{B}\frac{d\varepsilon^p}{dt}) \quad (\hat{A} \geq 0,\ \hat{B} \geq 0) \tag{6.1}$$

$\sigma=f(\varepsilon)$ is the static stress-strain relationship. ε^p is the plastic component of strain rate. $\hat{A}$ and $\hat{B}$ are arbitrary physical parameters.

From Eq.(6.1), it is seen that the plastic strain rate depends on the difference between the dynamic stress and static stress. Later on, this "SM" theory was generalized by Cristescu [10] and Lubliner [11] as follows.

$$\frac{\partial\sigma}{\partial t} = \hat{F}(\sigma,\varepsilon)\frac{\partial\varepsilon}{\partial t} + \hat{G}(\sigma,\varepsilon) \tag{6.2}$$

where $\hat{F}$ and $\hat{G}$ are arbitrary functions.

Parkin [12] applied this theory to the stress wave propagation test through sand which was carried out by Whitman . Perzyna and Bejda [13), 14] used the three-dimensinal elastic-viscoplastic model for analyzing the stress wave propagation problem, which was developed by Perzyna.[15), 16] Adachi & Okano [17] developed the more general elastic-viscoplastic theory extended on the basis of the Perzyna's theory and applied to the normally consolidated clay.

On the other hand, the wave propagation phenomena through the viscoelastic body were theoretically studied by many investigators. For example, Lee & Kanter,[18] Glauz & Lee,[19] Morrison,[20] Lee & Morrison [21] treated the simple Voigt model, Maxwell model and a four-or three-element model.

Akai & Hori [22] obtained the theoretical model by Laplace transformation technique. Akai & Hori [23] also considered the wave characteristics through soil from the point of view of viscoelasticity. In this chapter, fully saturated clay is assumed to be a mixture of elastic-viscoplastic body and incompressible fluid, or of viscoelastic-viscoplastic body and incompressible fluid.

The energy dissipation during wave propagation is considered to be due to an internal friction of soil. It is important to explain the nature of the internal friction of soil. Ishihara [24] showed that the attenuation of compressional wave due to the internal friction between elastic solid and elastic fluid is very small in a realistic range of frequency as beforementioned in Chapter 4. In this chapter, it will be examined how the internal friction is caused by the interaction between elastic-viscoplastic body and incompressible fluid. Numerical results will be given by using the method of characteristics.

6.2 Method of Characteristics

By the method of characteristics, the original system of first order partial differential equations can be transformed into a system involving characteristic coordinates by which the differentiation becomes considerably simplified. Accordingly to Courant & Hilbert,[25] the characteristic lines play a role as wave fronts. These are the lines across which solution of partial differential equation suffers discontinuities. We shall discuss the one-dimensional wave propagation in the material which is expressed by the following constitutive equation.

$$\frac{\partial \sigma}{\partial t} = f(\sigma,\varepsilon)\frac{\partial \varepsilon}{\partial t} + g(\sigma,\varepsilon) \tag{6.3}$$

where ε denotes the total strain and σ the axial stress. A thin bar is considered of which the lateral inertia can be neglected. The coordinate of any particle is X in Lagrangian form and x in current coordinate. The displacement of particle $\bar{u}$ is then defined by

$$\bar{u} = X - x \tag{6.4}$$

The strain ε is given by

$$\varepsilon = 1 - \frac{\partial x}{\partial X} \tag{6.5}$$

Since the strain ε is defined by $\frac{\partial \bar{u}}{\partial X}$, ε is taken as positive value in compression. As particle velocity is given by $v = \frac{\partial x}{\partial t}$, then we obtain

$$-\frac{\partial \varepsilon}{\partial t} = \frac{\partial v}{\partial X} \tag{6.6}$$

Along the curve $\bar{\psi} = 0$ which implies the wave front, the interior derivatives of v, σ and ε are continuous. Accordingly, we can take the derivatives as follows.

$$\begin{aligned} dv &= \frac{\partial v}{\partial t}dt + \frac{\partial v}{\partial X}dX \\ d\varepsilon &= \frac{\partial \varepsilon}{\partial t}dt + \frac{\partial \varepsilon}{\partial X}dX \\ d\sigma &= \frac{\partial \sigma}{\partial t}dt + \frac{\partial \sigma}{\partial X}dX \end{aligned} \tag{6.7}$$

When we neglect the body force, the equation of motion becomes

$$-\frac{\partial \sigma}{\partial t} = \rho_0 \frac{\partial v}{\partial t} \tag{6.8}$$

Eqs.(6.3),(6.6) and (6.8) construct quasi-linear partial differential equations. From Eqs.(6.3),(6.6),(6.7) and (6.8), we can express them in a matrix form.

$$D\ W = Z \tag{6.9}$$

$$W=\begin{vmatrix} 0,\rho_0, & 0, & 0, & 1, & 0 \\ 1, & 0, & 0, & 1, & 0, & 0 \\ 0, & 0, & 0,-f, & 0, & 1 \\ dX,dt, & 0, & 0, & 0, & 0 \\ 0, & 0,dX,dt, & 0, & 0 \\ 0, & 0, & 0, & 0,dX,dt \end{vmatrix} \qquad D=\begin{vmatrix} \partial v/\partial X \\ \partial v/\partial t \\ \partial \varepsilon/\partial X \\ \partial \varepsilon/\partial t \\ \partial \sigma/\partial X \\ \partial \sigma/\partial t \end{vmatrix} \qquad Z=\begin{vmatrix} 0 \\ 0 \\ g \\ dv \\ d\varepsilon \\ d\sigma \end{vmatrix}$$

The solution as a wave is obtained only when det(D)=0. In case when det(D)=0, the uniquely determined solution is then determined. Solving det(D)=0, we obtain,

$$dX = 0, \qquad dX/dt = \pm\sqrt{\frac{f(\sigma,\varepsilon)}{\rho_0}} \tag{6.10}$$

Along these characteristics, there exist the following differential relations.

$$\text{Along } dX = 0, \qquad d\sigma = f(\sigma,\varepsilon)d\varepsilon + g(\sigma,\varepsilon)dt \tag{6.11}$$

$$\text{Along } dX/dt = \pm C, \qquad d\sigma = \rho_0 dv \mp g(\sigma,\varepsilon)dt \tag{6.12}$$

where $C = \sqrt{\frac{f(\sigma,\varepsilon)}{\rho_0}}$.

The most simplest method to solve the above ordinary differential equations, Eqs.(6.11) and (6.12), is a numerical integration.

6.3 One-dimentional Wave Equation

Bar wave propagation can be observed under the condition such that the lateral displacement is not confined and wave length is very small compared to the diameter of the bar. The boundary condition is therefore given by stress condition. Stress condition under the wave propagation test using the special triaxial cell is as follows.

$$\sigma_{ij} = \begin{vmatrix} \sigma_{11}, & 0, & 0 \\ 0, & \sigma_{22}, & 0 \\ 0, & 0, & \sigma_{33} \end{vmatrix} \qquad (\sigma_{22}=\sigma_{33}) \tag{6.13}$$

As σ_{33} is constant under the undrained condition, the equation of motion in one-dimentional case is

$$\begin{aligned} \frac{-f}{\rho_0}\frac{dv_1^f}{dt} + \frac{-s}{\rho_0}\frac{dv_1^s}{dt} &= \frac{\partial\sigma_{11}}{\partial X} = \frac{\partial}{\partial X}(s_{11}+\sigma_m) \\ &= \frac{\partial}{\partial X}(\frac{2}{3}q + \sigma_m' + u) \\ &= \frac{\partial}{\partial X}(\frac{2}{3}q + \sigma_{me}' + \frac{1}{3}q - u + (1-n)u + nu) \\ &= \frac{\partial}{\partial X}(q + \sigma_{me}') = \frac{\partial q}{\partial X} \qquad (q=\sigma_{11}-\sigma_{22}) \end{aligned} \tag{6.14}$$

where σ_{me}' is a consolidation pressure. Rewriting the Eq.(6.14),

$$\frac{\partial(\sigma_{11}^s - \sigma_{33}^s - \sigma_{11}^f)}{\partial X} + \frac{\partial\sigma_{11}^f}{\partial X} = \frac{-f}{\rho_0}\frac{\partial v_1^f}{\partial t} + \frac{-s}{\rho_0}\frac{\partial v_1^s}{\partial t} \tag{6.15}$$

$$\sigma_{11}^f = nu$$

The equations of motion for each constituent are denoted by

For solid phase $$\frac{\partial q}{\partial X} = \frac{-s}{\rho_0}\frac{dv_1^s}{dt} + \frac{\partial(nu)}{\partial X} + \pi_1 \tag{6.16}$$

For fluid phase $$\frac{\partial(nu)}{\partial X} \quad \frac{-f}{\rho_0}\frac{dv_1^f}{dt} - \pi_1 \tag{6.17}$$

$$\pi_1 = -d(v_1^f - v_1^s) \tag{6.18}$$

These Eqs.(6.16)to(6.18) are obtained from the Eqs.(4.13),(4.14) and (4.25). In case when v_1^s is equal to v_1^f, the equation of motion becomes

$$\frac{\partial q}{\partial X} = \rho_0 \frac{\partial v^s}{\partial t} \qquad (\rho_0 = \bar{\rho}_0^s + \bar{\rho}_0^f) \tag{6.19}$$

When bar wave propagates through the linear elastic body under the condition of $\varepsilon_{kk}=0$, the wave equation in the direction of X-axis is discussed as follows. In the case of $\varepsilon_{kk}=0$, $\varepsilon_{ij}=e_{ij}$. Then,

$$\sigma_{ij} = 2\bar{\mu} e_{ij} = s_{ij}. \tag{6.20}$$

The stress-strain relation in the direction of X-axis is given by

$$e_{11} = \frac{1}{2\bar{\mu}} s_{11} = \frac{1}{2\bar{\mu}} \frac{2}{3} q = \frac{1}{3\bar{\mu}} q = \frac{1}{3G} q \tag{6.21}$$

Since $\nu=0.5$ under the condition of $\varepsilon_{kk}=0$,

$$E' = 2G(1+\nu) = 3G \tag{6.22}$$

Using Eq.(6.22), Eq.(6.21) becomes

$$\varepsilon_{11} = e_{11} = \frac{1}{E'} q \tag{6.23}$$

From Eqs.(6.6),(6.8) and (6.23), the wave equation in the direction of X can be obtained as

$$E' \frac{\partial^2 v}{\partial X^2} = \rho_0 \frac{\partial^2 v}{\partial X^2} \tag{6.24}$$

Therefore, wave velocity C is given by

$$C = \sqrt{\frac{E^{\tau}}{\rho_0}} \tag{6.25}$$

According to Ishihara,[26] if v_1^f is not assumed to be not equal to v_1^s and the frequency range is from 1 cps to 30 cps, the interaction term π_1 is predominant rather than inertia term $\bar{\rho}_0 dv_1^f/dt$. The form of the motion becomes for consolidation phenomenon. Therefore, in the ordinay range of frequency, a motion of soil becomes wave for phenomenon only if v_1^s is equal to v_1^f in case of the saturated elastic porous material.

The pulse observed in the stress wave propagation test carried by author has the several hundred frequency. It is necessary to examine the effect of interaction term in case of one-dimendional stress wave propagation. Provided that the water is incompressible and cohesive soil is modelled by an elastic-viscoplastic body developed in Chapter 5, we have

$$|d(v_1^f - v_1^s)| = 1.48 \times 10^3 (\text{kg/m sec}^4) \ , \ \bar{\rho}_0^f \frac{dv_1^f}{dt} = 1.19 \times 10^4 (\text{kg/m sec}^4)$$

$$\bar{\rho}_0^s \frac{dv_1^s}{dt} = 3.71 \times 10^4 (\text{kg/m sec}^4)$$

At this time, permeability coefficient k is 2.14×10^{-4} cm/sec and Eq.(4.30) is accounted. The stress-strain relation employed for the calculation is as follows.

$$\frac{\partial \varepsilon_{11}}{\partial t} = \frac{1}{E'}\frac{\partial q}{\partial X} + C_1 \exp\left[\frac{m}{\sigma'_{me}}(q-q_s)\right] \tag{6.26}$$

$$\frac{\partial \sigma'_m}{\partial t} = \frac{C_2}{\gamma_2} \exp\left[\frac{m}{\sigma'_{me}}(q-q_s)\right] \tag{6.27}$$

The finite difference method is used herein, for a calculation, combined with the method of characteristics. In this case, interaction term is not necessarily predominant than inertia term. However, the attenuation of stress wave is almost independent on permeability no matter how it is. When k is 2.14×10^{-4}cm/sec , $|v_1^s - v_1^f|$ is about 10^{-5} m/sec. Taking the above discussion into account, we can postulate that v_1^s is equal to v_1^f. Therefore, the equation of motion is given by Eq.(6.19). When we can assume that the volumetric strain is zero, Eq.(5.21) becomes in the form of one-dimensional.

$$\dot{\varepsilon}_{11} = \frac{1}{E'}\dot{q} + \left(\frac{4}{3}b^{(2)}q - 2\tau^{(2)}e_{11}^{ve}\right) + \sqrt{\frac{2}{3}}\beta_1(F) \tag{6.28}$$

(for viscoelastic-viscoplastic state)

$$\dot{\varepsilon}_{11} = \frac{1}{E'}\dot{q} + \sqrt{\frac{2}{3}}\beta_1(F) \tag{6.29}$$

(for elastic-plastic state)

Furthermore, if viscoelastic volume strain is zero,

$$\gamma_2 \dot{\sigma}'_m + \beta_2\left[M^* - \frac{\sqrt{2J_2}^{(s)}}{\sigma'^{(s)}_m} + M^* \ln\{\sigma'_m/\sigma'^{(s)}_m\}\right] = 0 \tag{6.30}$$

From the results in Chapter 5, functions β_1 and β_2 are given by

$$\sqrt{\frac{2}{3}}\beta_1(F) = C_1 \exp\left[\frac{m}{\sigma'_{me}}(q-q_s)\right] \tag{6.31}$$

$$\beta_2(F) = \bar{C}_1 \exp\left[\frac{m}{\sigma'_{me}}(q-q_s)\right] \tag{6.32}$$

The parameter m, $\bar{C}_1$, C_1 are considered to generally depend on the value of strain, which can be determined by the strain rate constant triaxial compression test.

We also postulate that the behavior is purely elastic or viscoelastic if $f_s<0$ (f_s is a yield fuction)

$$\dot{\varepsilon}_{11} = \frac{1}{E'}\dot{q} + \sqrt{\frac{2}{3}}\beta_1(F) \quad \text{(for elastic-viscoplastic material)} \tag{6.33}$$

$$\dot{\varepsilon}_{11} = \frac{1}{E'}\dot{q} + \left(\frac{4}{3}b^{(2)}q \quad 2\tau^{(2)}e_{11}^{ve}\right) + \sqrt{\frac{2}{3}}\beta_1(F) \tag{6.34}$$

(for viscoelastic-viscoplastic material)

Eqs.(6.6),(6.19) and (6.26) are forming the quasi-linear partial diffential equations. The characteristics are therefore given by

$$dX_1 = 0, \qquad dX_1/dt = \pm\sqrt{\frac{E'}{\rho_0}} = \pm C \tag{6.35}$$

Along which, the following differential relations exist;

$$\text{Along } dX_1 = 0, \qquad d\varepsilon_{11} = \frac{1}{E'}dq + \left(\frac{4}{3}b^{(2)}q - 2\tau^{(2)}e_{11}^{ve}\right)dt + \sqrt{\frac{2}{3}}\beta_1(F)dt \tag{6.36}$$

$$\text{Along } dX_1/dt = \pm C, \quad dv_1 = \mp\frac{1}{\rho_0 C}dq - \left[\left(\frac{4}{3}b^{(2)}q - 2\tau^{(2)}e_{11}^{ve}\right) + \sqrt{\frac{2}{3}}\beta_1(F)\right]E'dt \tag{6.37}$$

For an elastic-viscoplastic material,the second terms of the right hand side of Eqs.(6.36) and (6.37) are eliminated.

6.4 Numerical Results and Discussion

Differential relations(e.g.Eqs.(6.36) and (6.37)) are integrated along the characteristics by the Massau's method. At first, the one-

dimensional stress wave propagation through elastic-viscoplastic body descrived by Eqs.(6.29) and (6.30) are examined. Table 6.1 lists the parameters used in the calculations. Fig.6.1 shows the variation in the shape of wave during propagating. The shape of wave in the neighbourhood of the peak stress becomes round as the wave advances. The rise time, which is defined as the difference in arrival time of wave front and peak stress, increases as the wave shape collapses. From Fig.6.1, the induced attenuation of peak stress is great in the first part of rod and then gradually becomes constant. Fig.6.2 shows the stress-strain relations depicted during wave propagation. The type of the stress-strain relation is bilinear in behavior and hysteretic type dissipation is predominant. The area of hysterisis loop becomes small as maximum stress decreases. The dynamic stress path is shown Figs.6.3 and 6.4 in which the former corresponds to Fig.6.1.Fig.6.4 is the case where C_2/γ_2 is larger than that in Fig.6.3. Fig.6.5 shows the stress-strain relation obtained in the stress wave propagation test. The stress-strain relation is bilinear type in loading part and coincides with the result of Fig. 6.2. But, in the unloading part, Fig.6.2 differs from the experimental result. This fact may be associated with elastic property of cohesive soil. Fig.6.6 shows the experimental results of the variation in the shape of wave travelling through the cohesive soil. The peak stress attenuates about 40 percent of the total in the first 23 cm from the end of the specimen. The wave shape in the neighbourhood of peak stress becomes round and the rise time becomes large as the wave travels further distance. Figs.6.7 to 6.9 represent the calculated results which have been obtained by using the same input surface stress as Fig.6.6. The stress-strain relationship in Fig.6.8 also differs from the experimental results

Young's Modulus $E' = 1.4 \times 10^7 (kg/m^2)$
Density $\bar{\rho}_0 = 1.963 \times 10^2 (kg\ sec^2/m^4)$
Slope of e-ln σ'_m line of consolidation test $\lambda = 0.127$
Slope of e-ln σ'_m line of swelling test $\kappa = 0.0214$
Value of $\sqrt{\frac{2}{3}}(\sigma_{11}-\sigma_{33})/\sigma'_m$ at critical state $M^* = 1.300$

Table 6.1 Parameters used in numerical calculation.

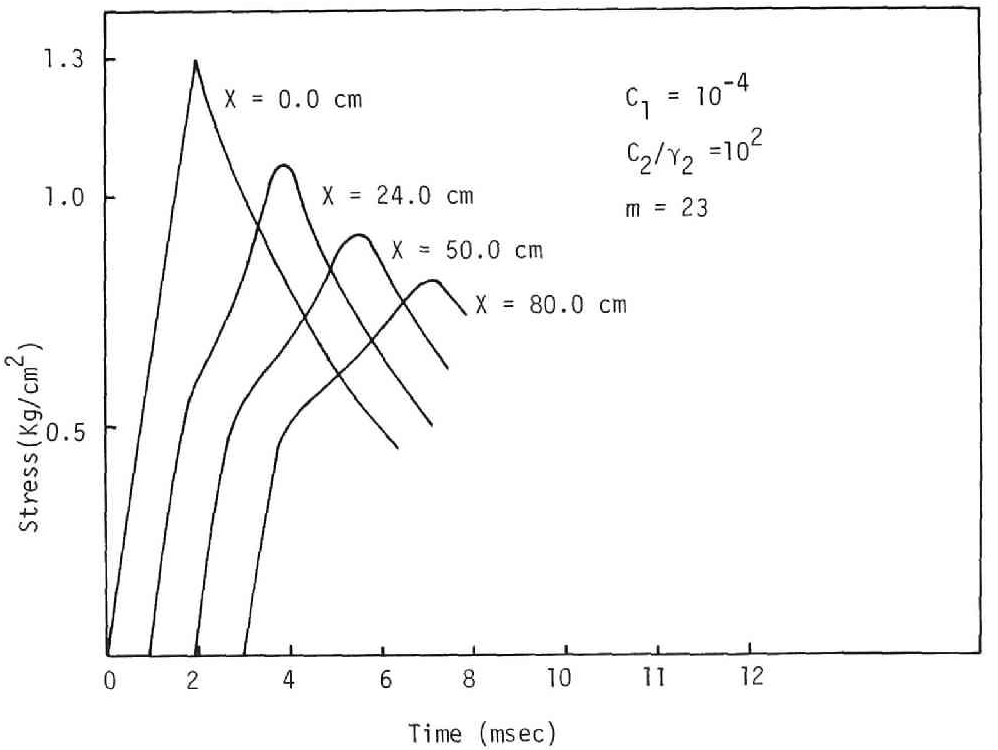

Fig.6.1 Stress wave propagation(calculated results).

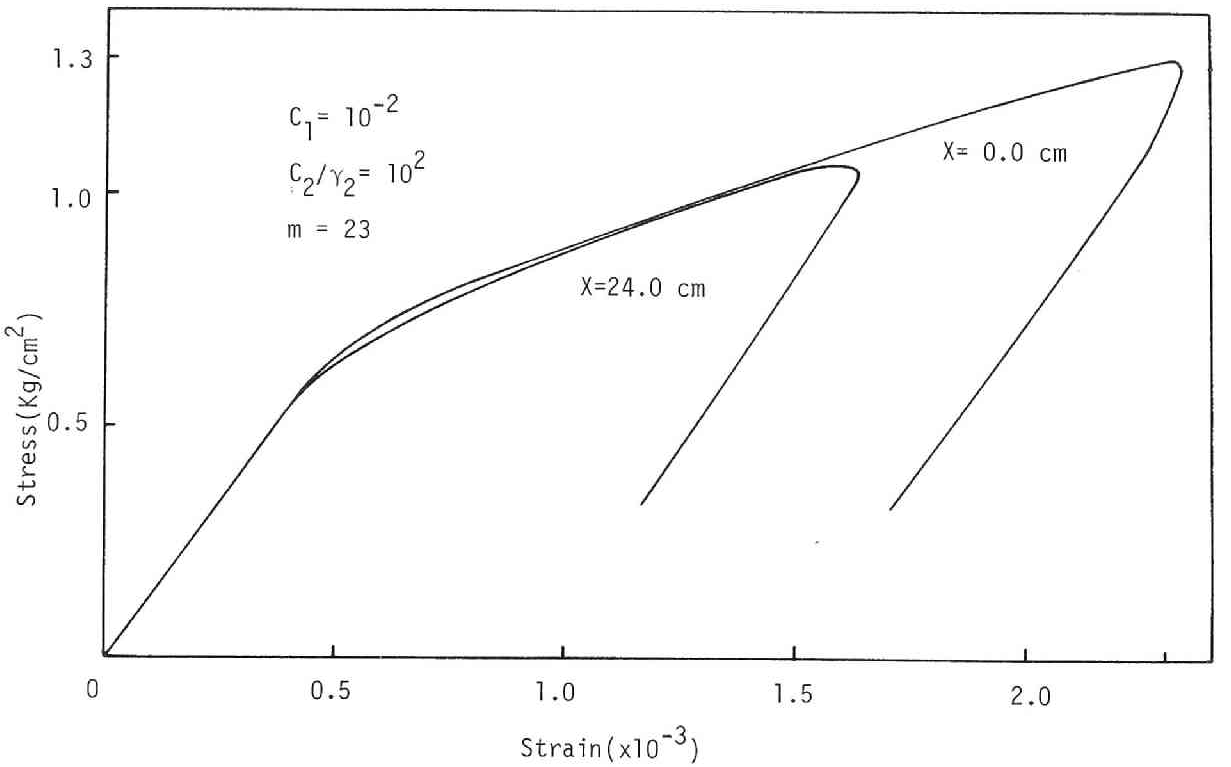

Fig.6.2 Stress-strain relation(calculated results).

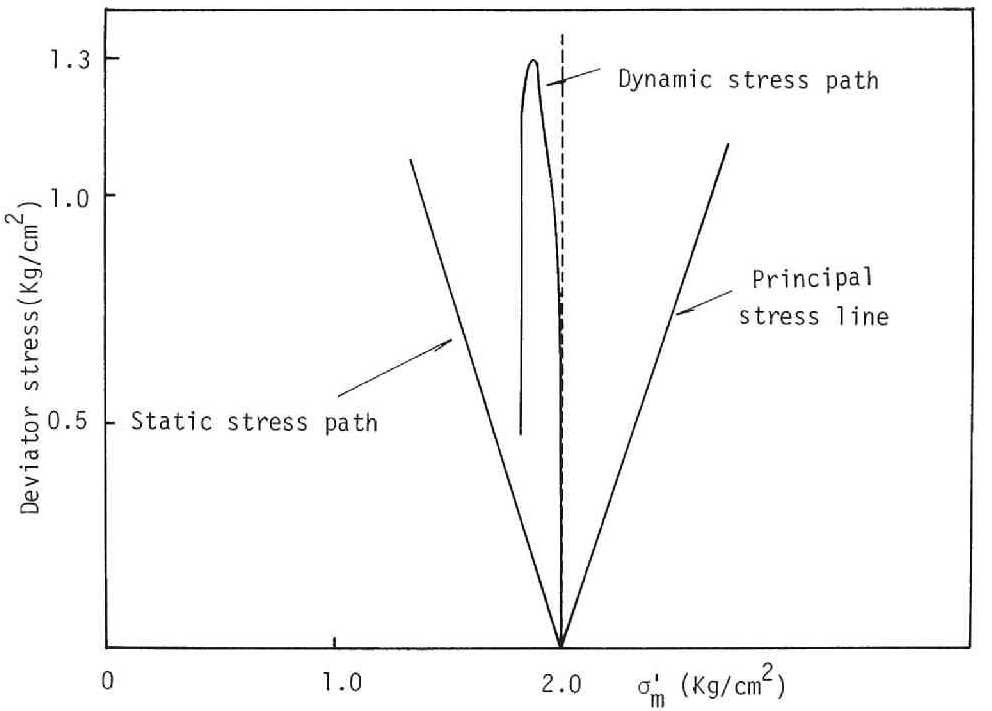

Fig.6.3 Stress path(calculated result).

Fig.6.4 Stress path(calculated result).

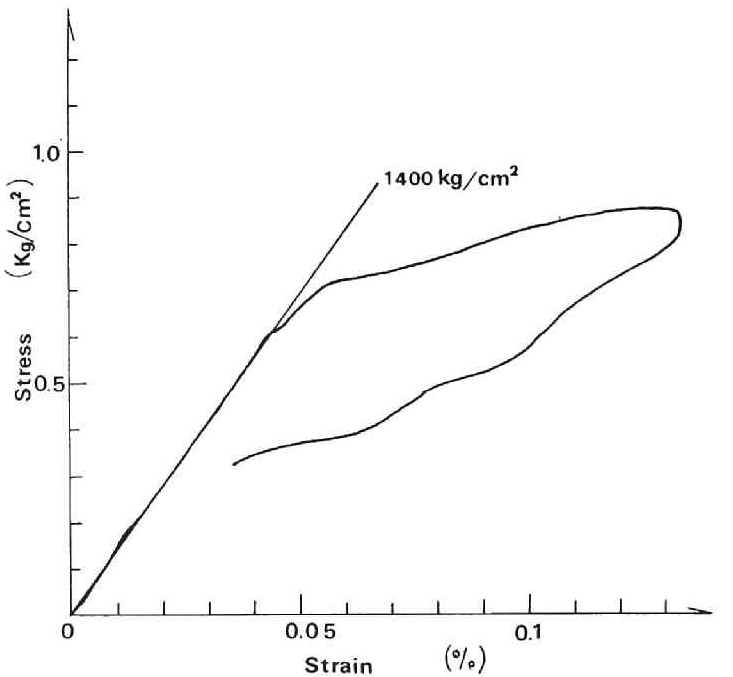

Fig.6.5 Stress-strain relation(experimental result).

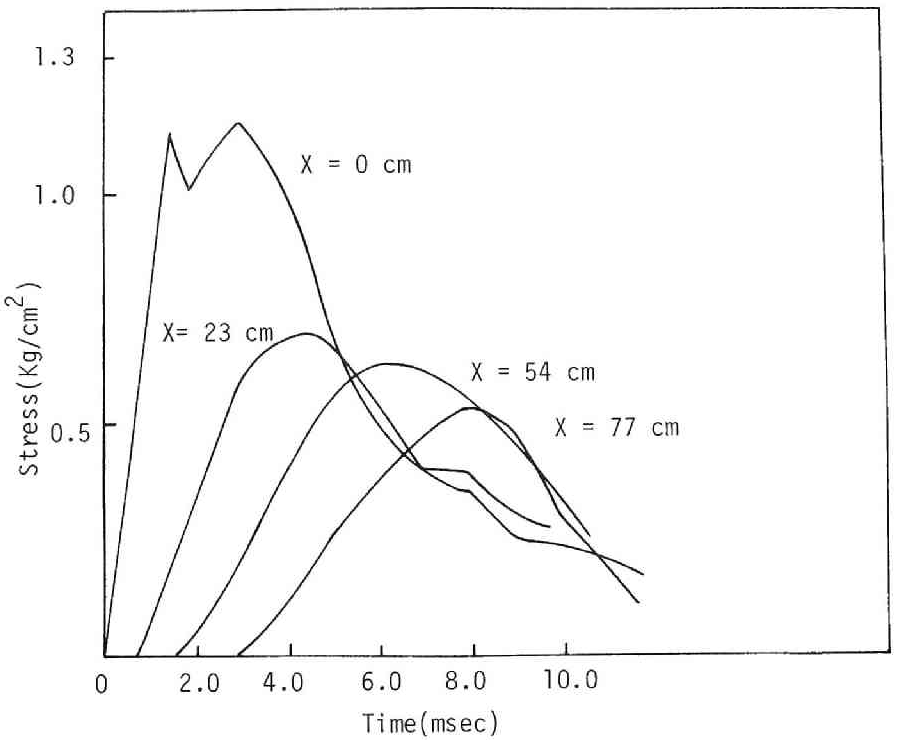

Fig.6.6 Stress wave propagation(experimental result).

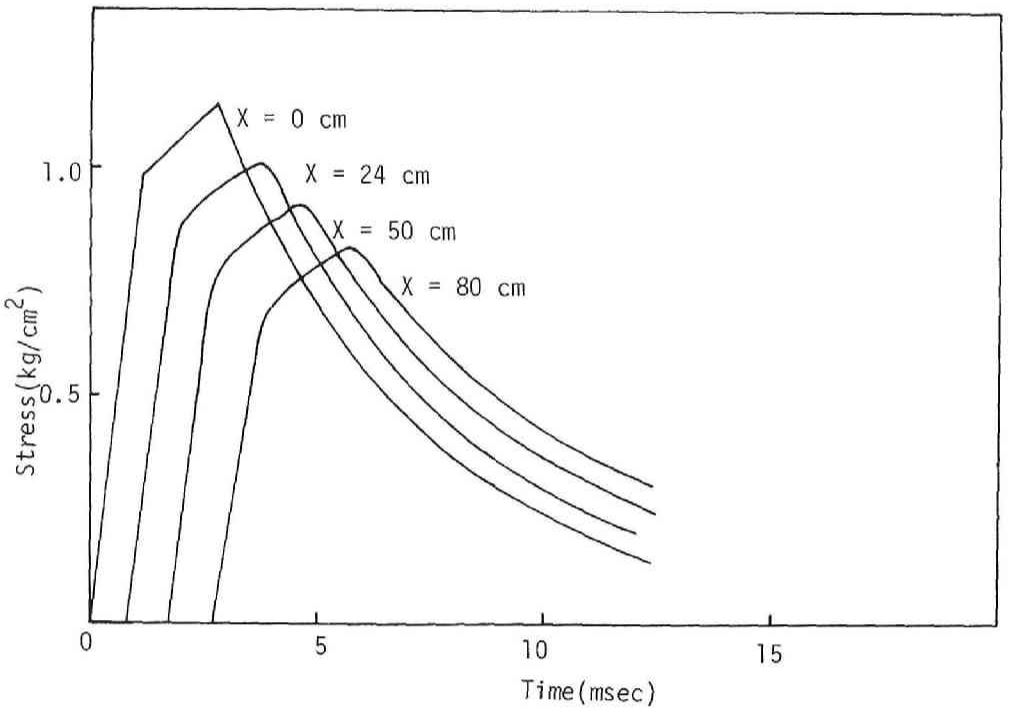

Fig.6.7 Stress wave propagation(calculated results).

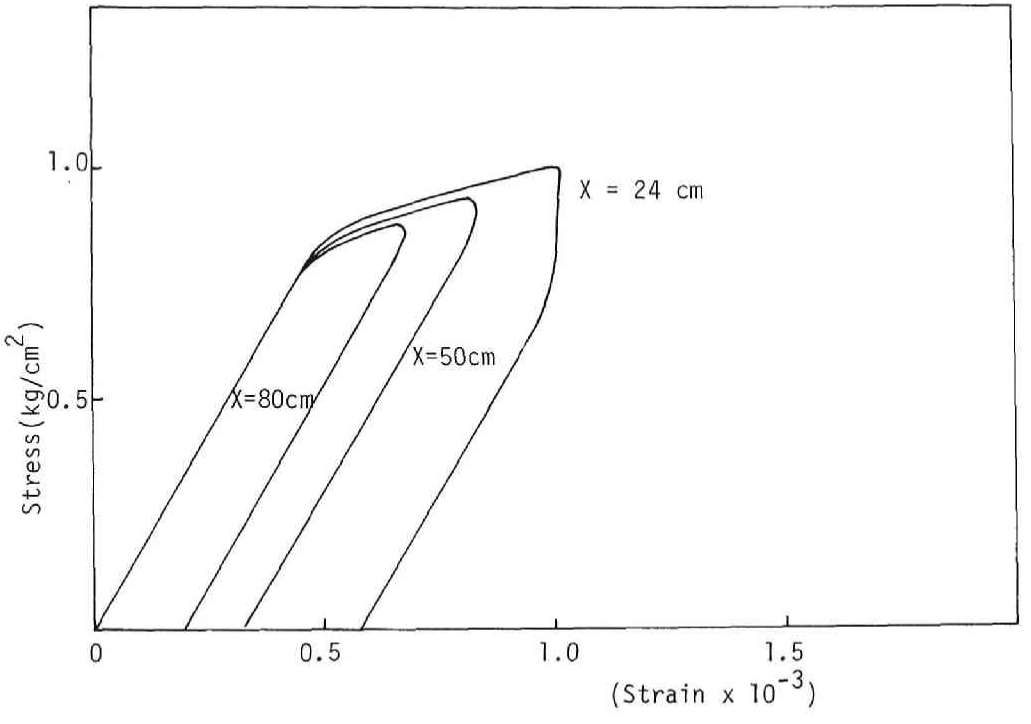

Fig.6.8 Stress-strain relation(calculated results).

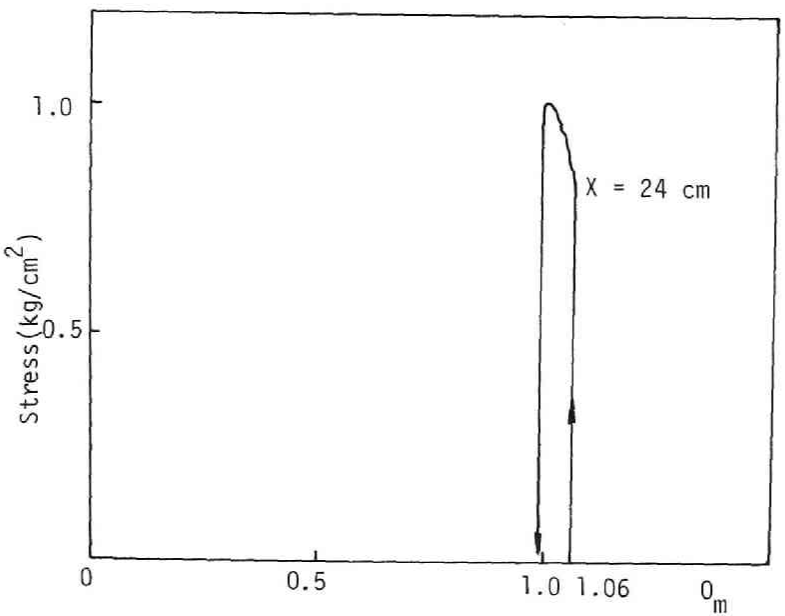

Fig.6.9 Stress path(calculated results).

in unloading part. Fig.6.9 shows the stress path corresponding to Fig.6.6.

Taking the experimental results shown in Chapter 2 into account, we will introduce the viscoelastic effect in order to describe the behavior in unloading part. From the results of Fourier transformation of stress wave, it is concluded that the viscoelastic property of cohesive soil is described by a linear spring-Voigt model in the range of the frequency less than 100 cps. The visco-elastic parameters in Eq.6.28, $E(=\frac{3\tau^{(2)}}{2_b^{(2)}})$ and $\mu(=\frac{4}{3}b^{(2)})$, can be determined according to Akai & Hori [23] who concluded in their investigation that the physical behavior of soil is visco-elastic in the strain level of 10^{-4} - 10^{-3} and soil can be assumed as a lineat spring-Voigt model in wide frequency range. The viscoelastic parameter $\bar{k}=(E/E')$ and relaxation time constant $\tau(=1/E\mu)$ take the value of 0.1-0.5 and $(1\text{-}5)\times10^{-2}$ sec, respectively. E' is the Young's modulus of free spring and E is the elastic modulus of Voigt part in the model. $1/\mu$ is the viscosity coefficient. Table 6.2 shows the employed parameters in the calculation. The parameters m and C_1 used in the calculation are determined from the strain-rate controlled triaxial compression test, as below

$$
\begin{aligned}
&m = -1400\varepsilon_{11} + 37 \qquad (\varepsilon_{11} \leq 10^{-2}) \\
&m = 23 \qquad\qquad\qquad (\varepsilon_{11} \geq 10^{-2}) \\
&\bar{k} = 0.32\ , \qquad \tau = 1.03 \times 10^{-2}(\text{sec}) \qquad\qquad (6.38) \\
&\bar{C}_1 = [1.8\times10^{-14}\times(10^2\times\varepsilon_{11})^{3.06} + 10^{-17}]\exp[mq_s/\sigma'_{me}](\varepsilon_{11} \leq 10^{-2}) \\
&\bar{C}_1 = [1.8\times10^{-14} + 10^{-17}]\exp[mq_s/\sigma'_{me}](\varepsilon_{11} \geq 10^{-2})
\end{aligned}
$$

Fig.6.10 shows the variation of the shape during the wave propagation through the viscoelastic-viscoplastic bar. Comparing Fig.6.10 with Fig.6.7,

Young's Modulus $E' = 1.73 \times 10^7 (kg/m^2)$
density $\bar{\rho}_0 = 196.3\ (kg/m^2 sec^2)$
Slope of e-ln σ'_m line of consolidation test $\lambda = 0.127$
Slope of e-ln σ'_m line of swelling test $\kappa = 0.0214$
Value of $\sqrt{\frac{2}{3}}(\sigma'_{11}-\sigma'_{33})/\sigma'_m$ at critical state $M^* = 1.300$
Consolidation pressure $\sigma'_{me} = 1.06 (kg/cm^2)$
Void ratio $e_0 = 0.77$
$\bar{k}(=E/E') = 0.32$, $\mu = 1.75 \times 10^{-5} (1/sec/kg/m^2)$
$\bar{C}_1/2\gamma_2 = 10 \times C_1\ (kg/m^2/sec)$

Table 6.2 Parameters used in numerical calculation.

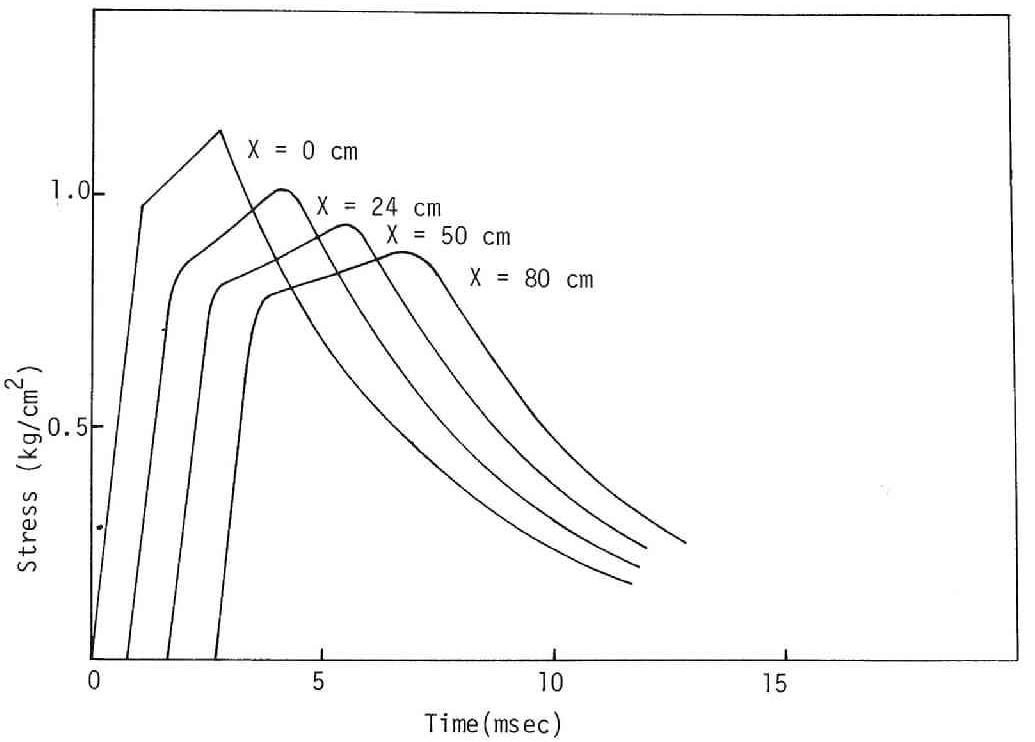

Fig.6.10 Stress wave propagation(calculated results).

the tendency of peak stress attenuation is similar between these two cases. The rise time becomes large as the wave propagates in these figures. Fig.6.11 shows the stress-strain relations. In Fig.6.11 and 6.8, the stress-strain relation is bilinear and the type of dissipation is hysteretic, but in Fig.6.11, the viscoelastic effect of Voigt type can be recognized, that exhibits delayed elastic component of strain. The feature shown in Fig.6.12 in unloading part may then be described by this model. The combination of the viscoplastic model and the linear spring-Voigt model is very effective model for interpretating the behavior of cohesive soil. Fig.6.12 shows the dynamic stress path corresponding to Fig.6.10. Fig.6.13 and 6.14 are the calculated results, where the model has not the viscoelastic component and the other parameters are same as in Fig.6.10. It is seen in Fig.6.14 that the hysterisis loop is very small and in Fig.6.13, that the peak stress attenuation is smaller than that in Fig.6.10. The model which has not the viscoelastic component is not sufficient for describing the dynamic behavior of cohesive soil. Figs.6.15 to 6.17 show the results of wave propagation test through the compacted Kaolin clay, carried by Vey & Strauss.[5] The stress-strain relation in Fig.6.17 is similar to that of Fig.6.11. The attenuation of the peak stress and the feature of the rise time are also similar to the calculated results as is shown in Fig.6.1 and/or Fig.6.10.

6.5 Conclusion

In the present chapter, the one-dimensional stress wave propagation through a saturated cohesive soil is studied and the numerical calculation is carried by integrating the differential equation along the characteristics. The stress-strain relations of cohesive soil developed in

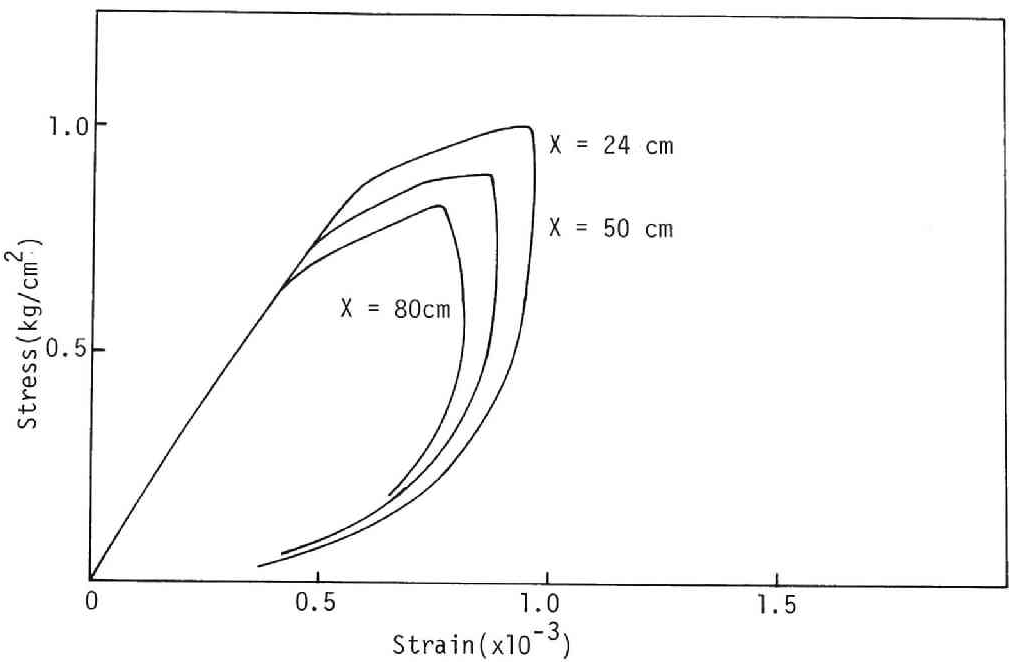

Fig.6.11 Stress-strain relation(calculated results).

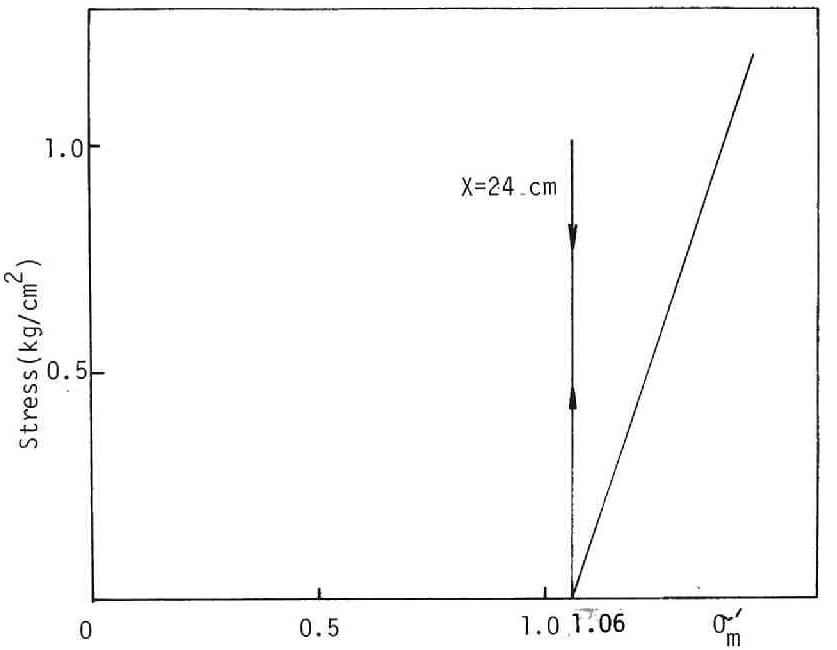

Fig.6.12 Stress path(calculated results).

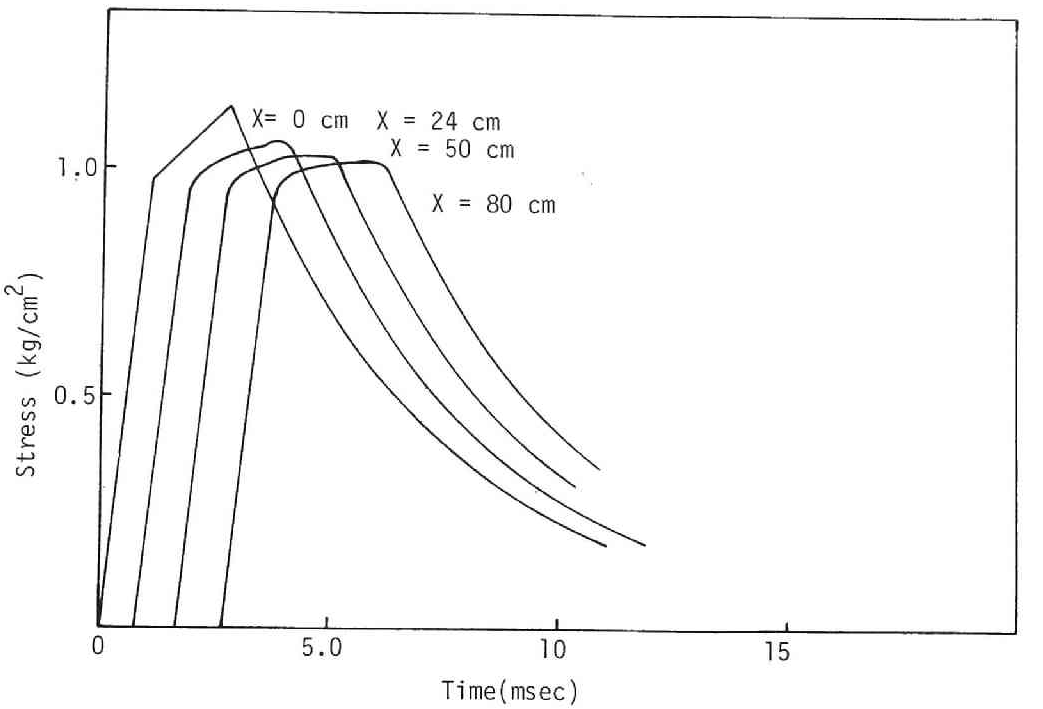

Fig.6.13 Stress wave propagation(calculated results).

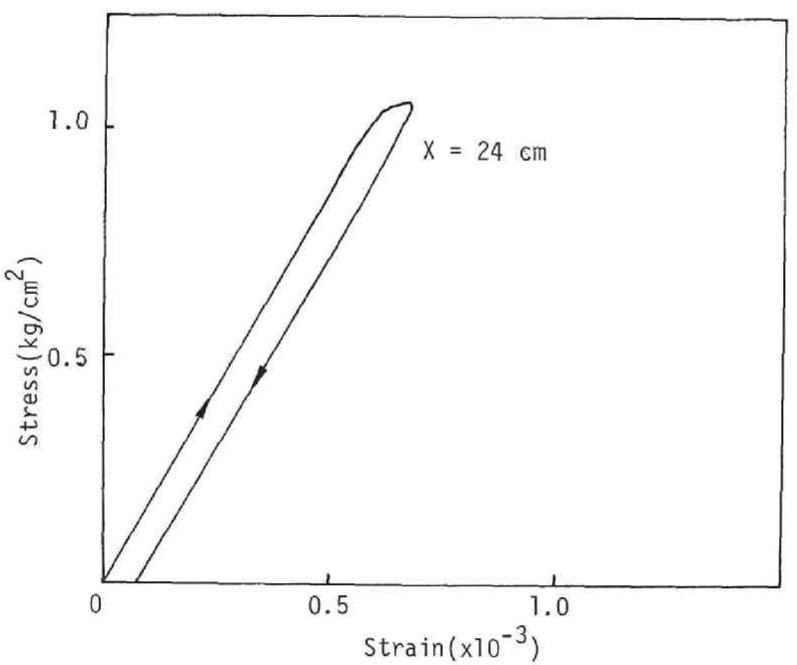

Fig.6.14 Stress-strain relation(calculated results).

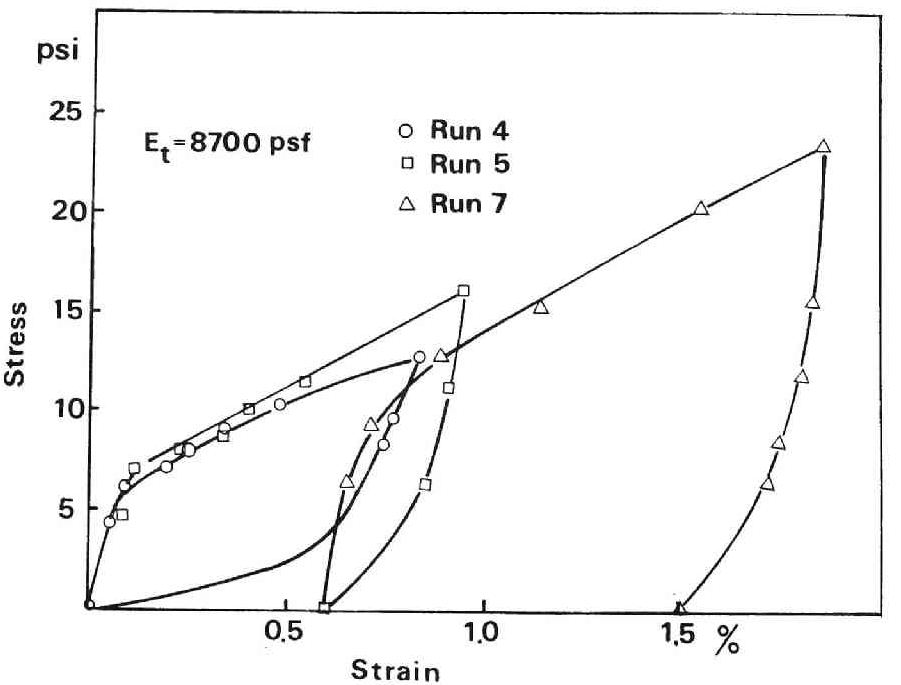

Fig.6.15 Dynamic stress-strain relation(after Vey & Strauss[5]).

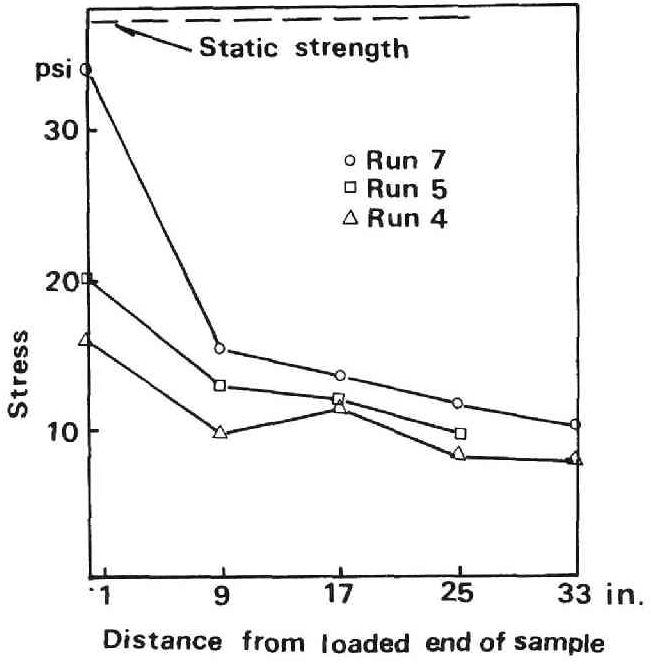

Fig.6.16 Typical peak stress attenuation(after Vey & Strauss[5]).

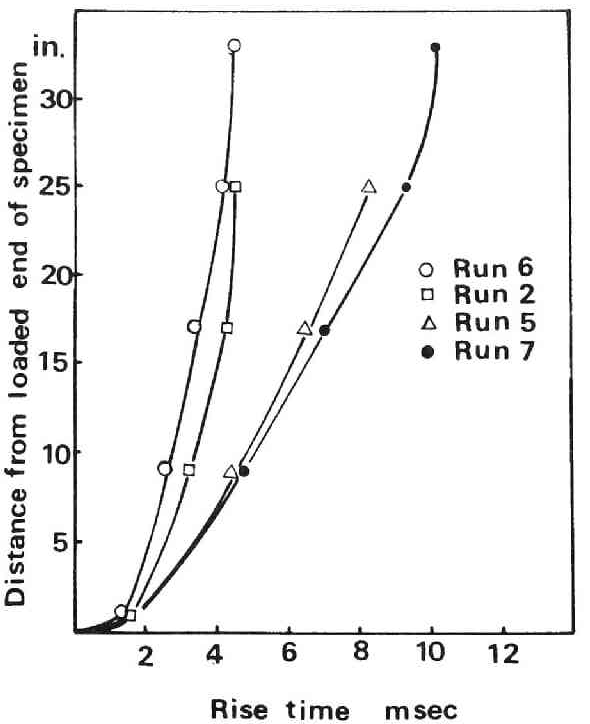

Fig.6.17 Distance from loaded end of specimen versus rise time to peak stress(after Vey & Strauss[5]).

Chapter 5 are used. Moerover, the effect of internal friction due to the interaction between solid and fluid is examined by taking the theory of mixture proposed in Chapter 4 into account. In order to clarify the wave characteristics through soil, many mechanical models have been proposed, for example, viscoelastic model, elasto-plastic model, compacting model or locking model. But, except the Biot's study of the saturated porous elastic material, the model on the basis of the theory of mixture has not been proposed. In this chapter, the pore water pressure, which is developed during the wave propagation through saturated soil, can be estimated by the proposed model. The dynamic effective stress path can also be presumed. The stress-strain relation proposed is preferred to elastic-viscoplastic relation. The main conclusions obtained are as follows.

(1) In the ordinary range of frequency between 1 cps to 100 cps, we may be able to postulate that v_1^f is equal to v_1^s in the equation of motion, taking into account the wave characteristics through the two-phase mixture constituting the elastic-viscoplastic solid and incompressible fluid.

(2) The hysteretic type energy dissipation is predominant and the stress-strain relation is bilinear in behavior at the wave propagation through an elastic-viscoplastic cohesive soil. The calculated results show that this model is not sufficient to completely describe the behavior in unloading part.

(3) The stress-strain relation obtained by the stress wave propagation test exhibits the delayed elastic property. In order to describe this property of soil, it is adequate to introduce the viscoelastic-viscoplastic stress-strain relation. The viscoelastic component is represented by a linear spring-Voigt

model, considering the results of Fourier transformation of stress wave. The viscoelastic parameters $\bar{k}$ and $1/E\mu$ are determined based on the Akai & Hori's study.[23] It is appropriate that $\bar{k}$ and $1/E\mu$ takes the value of 0.1-0.5 and $1\text{-}5\times10^{-2}$(sec), respectively. The parameters m and C_1 are determined by the strain-rate constant triaxial compression test. These parameters depend on the level of strain. From the calculated results, it is seen that the viscoelastic-viscoplastic model can feasibly describe the wave propagation characteristics through cohesive soil.

(4) The tendency that the peak of the stress-strain relation becomes round results from the viscoplastic effect, in the calculation the values of $\bar{k}$ and $1/E\mu$ are taken as 0.32 and 1.03×10^{-2}(sec), respectively.

(5) Using the two models, elastic-viscoplastic model and viscoelastic-viscoplastic model, the dynamic stress-path can be presumed taking the effect of dilatancy into account.

References for Chapter 6

1) see ref. 10) in Chapter 5

2) see ref. 4) in Chapter 2

3) see ref. 12) in Chapter 5

4) see ref. 11) in Chapter 5

5) see ref. 42) in Chapter 5

6) see ref. 41) in Chapter 5

7) see ref. 13) in Chapter 5

8) see ref. 14) in Chapter 5

9) see ref. 15) in Chapter 5

10) see ref. 16) in Chapter 5

11) see ref. 17) in Chapter 5

12) see ref. 18) in Chapter 5

13) Beida, J.: Propagation of Two-Dimensional Stress Wave in an Elastic/Visco-plastic Material, Proc. 12th Int. Congress of Appl. Mech., Stanford Univ., August 1968, pp.121-134.

14) Perzyna, P. and J. Beida: The Propagation of Stress Wave in a Rate Sensitive and Work-Hardening Plastic Medium, Archwum Mechaniki Stosowanej, 6.,16, 1964, pp.1215-1244.

15) see ref. 20) in Chapter 5

16) see ref. 21) in Chapter 5

17) see ref. 22) in Chapter 5

18) Lee, E.H. and I.Kanter: Wave Propagation in Finite Rods of Viscoelastic Material, J. Appl.Phys., Vol.24, 1953, pp.1115-1122.

19) Glauz, R.D. and E,H, Lee: Transient Waves Analysis in a Linear Time-Dependent Material, J. Appl. Phys., Vol.25, 1954, pp.947-953.

20) Morrison, J.A.: Wave Propagation in Rods of Voigt Material and Visco-elastic Materials with Three-Parameter Models, Q.Appl. Math., Vol.14, 1956, pp.153-169.

21) Lee, E.H. and J.A. Morrison: A Comparison of the Propagation of Longitudinal Waves in Rods of Viscoelastic Materials, J. Polymer Sci., Vol. 14, 1956, pp.93-110.

22) Akai,K. and M.Hori: Analytical Study on Stress Wave Propagation in Viscoelastic Materials Subjected to Spike Pulse, Proc. of JSCE, No.195, Nov., 1971, pp.101-108.

23) see ref. 10) in Chapter 4

24) Ishihara, K.: Propagation of Compressional Waves in a Saturated Soil, Proc. Int. Symp. Wave Propagation and Dynamic Properties of Earth Materials, Univ. New Mexico, 1967, pp.451-467.

25) Courant, R. and D. Hilbert: Methods of Mathematical Physics, Vol.II, Partial Differential Equations, Intersience Publ., New York, 1962.

26) see ref. 22) in Chapter 4

Chapter 7 Dynamic Response of Layered Cohesive soil

7.1 General Remarkes

Facing with the problem of dynamic analysis of ground during earthquakes, these four following factors are considered to be important.

(1) Constitutive equation of soil composing the ground

(2) Boundary conditions(the geological conditions of site in question)

(3) Type of seismic wave

(4) Method of analysis

This chapter treats the influence of non-linear soil behavior on the dynamic response of layered soil on the basis of the results of Chapter 5.

The constitutive equations using for describing the dynamic behavior of soil are as follows; linear elasticity, non-linear elasticity, visco-elasticity and simple elastic-plasticity. The convienient stress-strain relation developed by Ramberg-Osgood is also used by many investigators.[1),2)] On the other hand, the dynamic property of soil has been examined in detail and the constitutive equation that includes the effect of dilatancy is now being established in soil mechanics. Therefore, it is required and of interest to apply these refined constitutive theory to the practical problem. Finn[3)] developed the stress-strain relation of sand and applied it to the liquifaction of sand. Sato[4)] examined the non-linear effect of soil on the motion of the ground during the seismic wave propagation. But, the cohesive soil has seldom been dealt with by investigators. Generally, the local geological condition is often inspected in detail. Therefore, one-dimensional horizontally layered system of the ground is rather easily investigated. Furthermore, two-or three-dimensional model of ground must be included in the dynamic analysis in future, When we deal with the wave which has the component of the short period, the dynamic response is sensitive to

the local geological system in a surface layer of ground.

To analyze the dynamic behavior of soil deposit in the case when the soil can be described by a unique constitutive equation, the two types of methods of analysis exist. One is to describe the soil system as the multi-degree of freedom. Idriss & Seed[5] used a shear beam as a discrete system for computing the ground vibration. This method is called a lumped mass method. This simple method, however, is rather hard to express the geometrical dissipation. The other method[6),7)] is to get a solution by integrating a differential relation along the characteristics of partial differential equations. The well used multiple reflection theory of wave is based on this characteristics method. This method is restricted to the linear elastic system. The general characteristic method is available for non-linear analysis and time to be required for computation is relatively short. When the geological condition is complicated and the constitutive equation is not unique, the finite element method is available for analysis. The analysis by the finite element method has a difficulty in determing a boundary condition.

The seismic waves are mainly devided into two types; surface waves and body wave. Which is predominant depends on the complicated mechanism of propagation of sismic wave. Until now, many investigators have been dealing with shear wave propagating in surface layer upward from the base rock. Recently, the surface wave is recognized to be important during earthqukes[8)]. But, the problem of surface wave will not be treated in this chapter.

The many seismic records were obtained on the surface of the ground, but the record of base rock motion is little. In order to design an underground structure, it is necessary to estimate the strain, velocity or stress under the ground. In this chapter, the author aims to determine strain, stress and velocity in the layered cohesive soil calculated from

the surface motion of ground. The stress-strain relation developed in Chapter 5 is extended to K_0-consolidated condition. The pore-water pressure is also calculated.

7.2 Ground Model and Equation of Motion

The dynamic response of horizontally layered system, which is composed of elastic layers and saturated clay layers, will be concerned in this chapter. Shearing stresses are set up by horizontal motions imposed at the base of soil layer as shown in Fig.7.1. The clay layer is initially K_0-consolidated. Fig.7.2 shows the initial stress conditions, where $\sigma'_{ij(0)}$ is the initial effective stress. The material property of each layer is assumed to be constant. As the boundary condition, the shear stress at the ground surface is zero and the velocity records at the surface are given. It is important to determine the value of the stress, velocity and strain in the ground, from the gound surface records. Initial stress condition is given as follows.

$$\sigma'_{ij(0)} \quad \begin{vmatrix} \sigma'_{11(0)}, & 0 & , & 0 \\ 0 & , & K_0\sigma'_{11(0)}, & 0 \\ 0 & , & 0 & , K_0\sigma'_{11(0)} \end{vmatrix} \tag{7.1}$$

From Eq.(7.1), initial mean effective stress $\sigma'_{m(0)}$ is expressed by

$$\sigma'_{m(0)} = \frac{1}{3}(1+2K_0)\sigma'_{11(0)} \tag{7.2}$$

Similarly, an initial deviatoric stress $s_{ij(0)}$ is

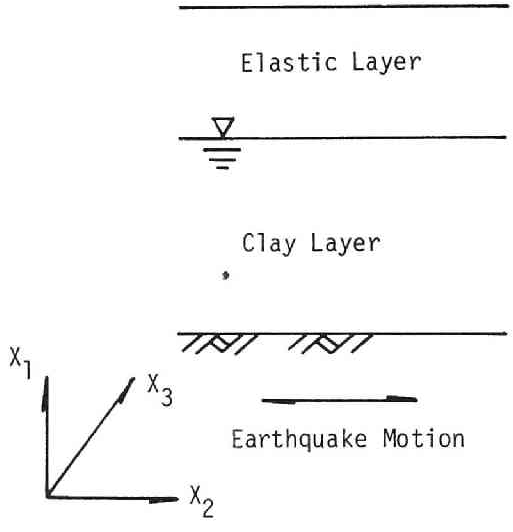

Fig.7.1 Model of soil layers.

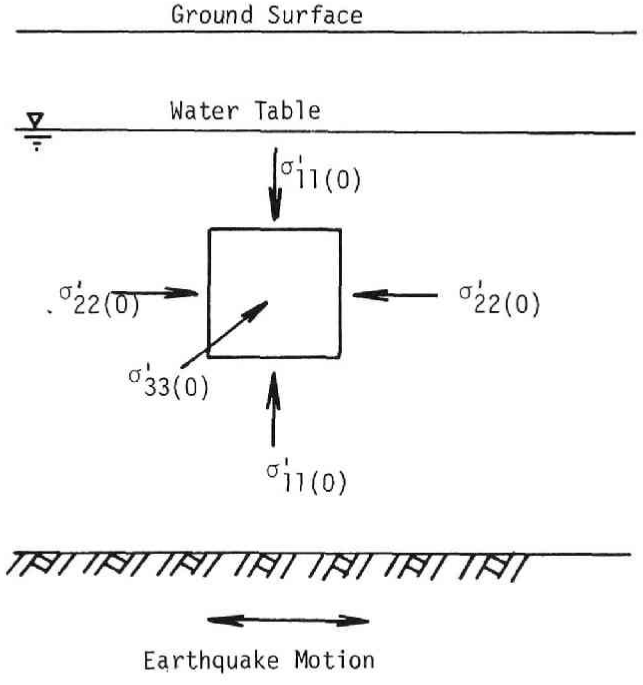

Fig.7.2 Stress condition.

$$s_{ij(0)} = \begin{vmatrix} \frac{2}{3}(1-K_0)\sigma'_{11(0)}, & 0 & , & 0 \\ 0 & , \frac{1}{3}(K_0-1)\sigma'_{11(0)}, & & 0 \\ 0 & , & 0 & , \frac{1}{3}(K_0-1)\sigma'_{11(0)} \end{vmatrix} \qquad (7.3)$$

$$\sqrt{2J_{2(0)}} = \sqrt{s_{ij(0)}s_{ij(0)}} = \sqrt{\frac{\sigma'_{11(0)}}{9}[(2-2K_0)^2+2(K_0-1)^2]} \qquad (7.4)$$

in which, J_2 is the second invariant of deviatoric stress. The stress condition during the shear wave transmission is given by

$$\sigma_{ij} = \sigma_{ij(0)} + \Delta\sigma_{ij} \qquad (7.5)$$

$$\sigma'_m = \sigma_{ij(0)} + \Delta\sigma'_m \qquad (7.6) \qquad s_{ij} = s_{ij(0)} + \Delta s_{ij} \qquad (7.7)$$

The equation of motion and the kinetic relation between the strain and the displacement are expressed by Eqs.(7.8) and (7.9), respectively. As we have discussed in Chapter 4, the effect of saturation of soil only influences the density $\rho(= \bar{\rho}^s + \bar{\rho}^f)$.

$$\rho\frac{\partial v_2}{\partial t} = -\left(\frac{\partial\sigma_{21}}{\partial X_1} + \frac{\partial\sigma_{22}}{\partial X_2} + \frac{\partial\sigma_{23}}{\partial X_3}\right) \qquad (7.8)$$

$$-\varepsilon_{12} = \frac{1}{2}\left(\frac{\partial u_2}{\partial X_1} + \frac{\partial u_1}{\partial X_2}\right) \qquad (7.9)$$

where, strain tensor ε_{ij} is taken positive in compression and the body force is neglected, v_i; velocity vector, u_i; displacement vector, σ_{ij}; stress tensor. Since derivative components in X_2 and X_3 direction in the above equations may be negligibly small in one-dimensional analysis,

Eqs.(7.8) and (7.9) are approximated by Eqs.(7.10) and(7.11).

$$\rho \partial v_2/\partial t = -\partial \sigma_{21}/\partial X_1 \qquad (7.10) \qquad -\varepsilon_{12} = \frac{1}{2}\frac{\partial u_2}{\partial X_1} \qquad (7.11)$$

7.3 Stress-strain Relation of Soil

The elastic layers are modelled by linear elastic body expressed by

$$\sigma_{ij} = \bar{\lambda}\varepsilon_{kk}\delta_{ij} + 2\bar{\mu}\varepsilon_{ij} \qquad (7.12)$$

where $\bar{\lambda}$ and $\bar{\mu}$ are Lamé's constants.

When $\varepsilon_{kk} = 0$, $\sigma_{ij} = 2\mu\varepsilon_{ij}$. (7.13)

In the saturated clay layers, the stress-strain relation is presented by elastic-viscoplastic or viscoelastic-viscoplastic body. We extend the stress-strain relation written by Eq.(5.21) to anisotropically consolidated state, and it can be expressed by the following relation in K_0-consolidated state.

$$\dot{\varepsilon}_{ij} = \gamma_1 s_{ij} + \frac{1}{3}\gamma_2 \dot{\sigma}'_m \delta_{ij} + \beta_1 \frac{s_{ij}}{\sqrt{2J_2}} + \beta_2 [M^* - \frac{\sqrt{2J_2}(s)}{\sigma'_m(s)} + M^* \ln\{\sigma'_m/\sigma'_m(s)\}]\frac{1}{3}\delta_{ij} \qquad (7.14)$$

Deduction of Eq.(7.14) is now given as follows. The Roscoe's original theory extended to three-dimensional problem is also formally extended to anisotropic consolidated state for the purpose of using in equilibrium state. Static yield function is given by

$$f_s = \pm(\eta^* - \eta^*_{(0)}) + M^* \ln(\sigma'_m / \sigma'_{my}) = 0 \tag{7.15}$$

where $\eta^*_{(0)} = \sqrt{2J_{2(0)}}/\sigma'_{m(0)}$. The plus or minus sign of Eq.(7.15) corresponds to active or passive state, respectively.

Hardening rule is expressed by

$$\sigma'_m = \sigma'_{me} \exp[\frac{1+e}{\lambda-\kappa}\varepsilon^p_{kk}] \tag{7.16}$$

As we postulate that de= 0 during the wave propagation, the equation is obtained in equilibrium state according to Adachi & Okano [9] as follows;

$$\lambda \frac{d\sigma'_m}{\sigma'_m} = - \frac{\lambda-\kappa}{M^*} d\eta^* \tag{7.17}$$

$$d\varepsilon^p_{kk} = \frac{\lambda-\kappa}{1+e}[\frac{1}{M^*} d\eta^* + \frac{d\sigma'_m}{\sigma'_m}] \tag{7.18}$$

The plastic volumetric strain increment is given by Eq.(7.18). From the Eqs.(7.17) and (7.18), we obtain under the condition of $\eta^* = \eta^*_{(0)}$ when $\varepsilon^p_{kk} = 0$,

$$\pm(\eta^* - \eta^*_{(0)}) = \frac{(1+e)\, M^*}{(\lambda-\kappa)\kappa} \varepsilon^p_{kk} \tag{7.19}$$

From Eqs.(7.17) and (7.19), σ'_m can be determined by

$$\sigma'_{m(s)} = \sigma'_{me} \exp[-\frac{(1+e)}{\kappa}\varepsilon^p_{kk}] \tag{7.20}$$

Finally, $\sqrt{2J_2}$ is determined by Eqs.(7.16),(7.19) and (7.20).

$$\sqrt{2J_2}^{(s)} = [\frac{\sqrt{2J_2}(0)}{\sigma'_{m(0)}} \pm \frac{(1+e)}{(\lambda-\kappa)\kappa}\varepsilon^p_{kk}]\sigma'_{m(s)} \tag{7.21}$$

Therefore, the static stress path in the $\sqrt{2J_2}$-σ'_m space can be determined by Eqs.(7.20) and (7.21), corresponding to the value of plastic strain. Next, the f-function in Eq.(5.12) which is considered to be a dynamic yield function will be determined as the same manner in Chapter 5. Fig.7.3 shows the function f in the $\sqrt{2J_2}$-σ'_m space. F is given by Eq.(7.22) corresponding to Fig.7.3.

$$f = \sqrt{2J_2} - \eta^*_{(0)}\sigma'_m + M^*\sigma'_m \ln(\sigma'_m/\sigma'_{my}) - F = 0 \tag{7.22}$$

From the constitutive theory of elastic-viscoplastic body in Chapter 5, the dynamic stress-strain relation is expressed by

$$\dot{\varepsilon}_{ij} = \frac{1}{2G}\dot{s}_{ij} + \frac{1}{3}\gamma_2\dot{\sigma}'_m\delta_{ij} + O_{ijkl}\frac{\partial f}{\partial \sigma_{kl}} \tag{7.23}$$

The elastic strain rate is given by

$$\dot{\varepsilon}^e_{kk} = \gamma_2\dot{\sigma}'_m \tag{7.24}$$

Taking account of e-logσ'_m curve of the consolidation, γ_2 is given by

$$\gamma_2 = \frac{\kappa}{(1+e)\sigma'_m} \tag{7.25}$$

O_{ijkl} in Eq.(7.23) is given by Eq.(5.13), but in this chapter O_{ijkl} is assumed to be as

$$O_{ijkl} = \frac{\beta_2}{4\sqrt{2}}(\delta_{ik}\delta_{jl} + \delta_{il}\delta_{jk}) \tag{7.26}$$

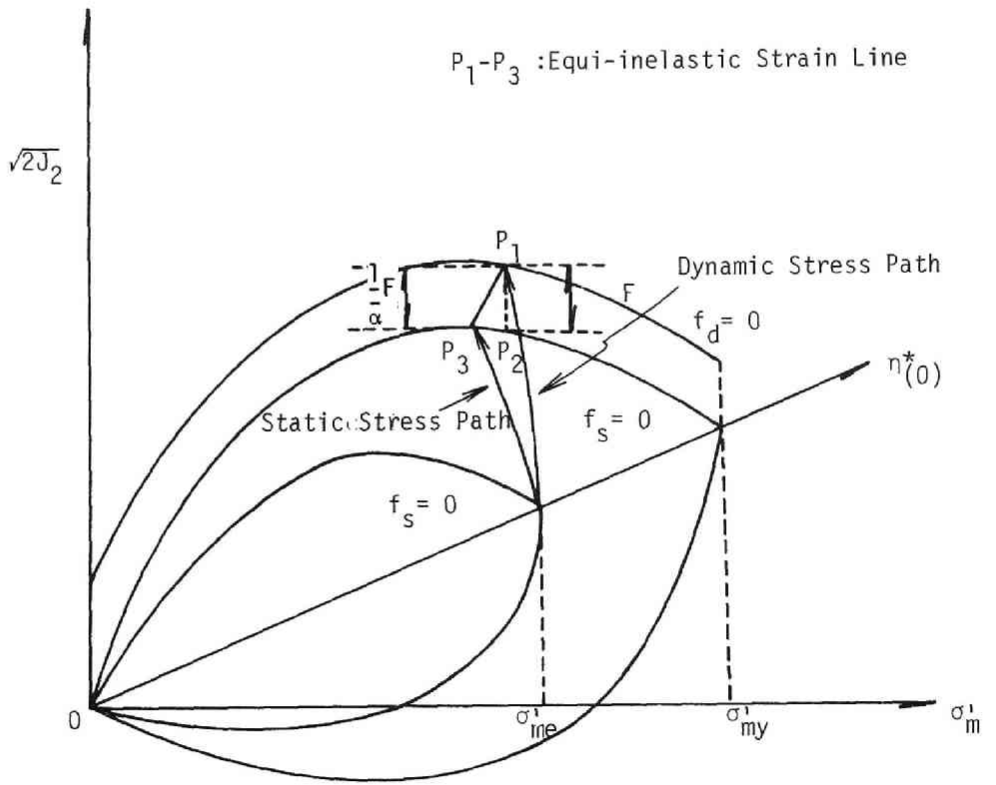

Fig.7.3 Manner to determine f-function.

Differentiating Eq.(7.22) with respect to the stress tensor, we obtain

$$\frac{\partial f}{\partial \sigma_{ij}} = \frac{s_{ij}}{\sqrt{2J_2}} + [M^* \frac{\sqrt{2J_2^{(s)}}}{\sigma'_m} + M^* \ln\{\sigma'_m/\sigma'^{(s)}_m\}]\frac{1}{3}\delta_{ij} \qquad (7.27)$$

The explicit expression of Eq.(7.23) can be rewritten by substituting this equation into Eq.(7.23) and taking the relation of Eqs.(7.25) and (7.26),

$$\dot{\varepsilon}_{ij} = \frac{\kappa}{(1+e)\sigma'_m}\dot{\sigma}'_m + \frac{1}{2G}\dot{s}_{ij} + \frac{s_{ij}}{\sqrt{2J_2}}\beta_1 + \beta_1[M^* \frac{\sqrt{2J_2^{(s)}}}{\sigma'^{(s)}_m} + M^* \ln\{\sigma'_m/\sigma'^{(s)}_m\}]\frac{1}{3}\delta_{ij} \qquad (7.28)$$

where

$$\beta_1 = C_1 \exp[m\frac{(q-q_s)}{\sigma'_{me}}] \qquad (7.29)$$

The form of β_1 corresponds to Eq.(5.26) in Chapter 5.

From Eq.(7.28), we obtain

$$\frac{\partial \varepsilon_{12}}{\partial t} = \frac{1}{2G}\frac{\partial \sigma'_{12}}{\partial t} + \beta_1(F)\frac{s_{ij}}{\sqrt{2J_2}} \qquad (7.30)$$

$$\frac{\partial \varepsilon_{kk}}{\partial t} = \frac{\kappa}{(1+e)\sigma'_m}\frac{\partial \sigma'_m}{\partial t} + \beta_1(F)[M^* - \frac{\sqrt{2J_2^{(s)}}}{\sigma'^{(s)}_m} + M^* \ln\{\sigma'_m/\sigma'^{(s)}_m\}] \qquad (7.31)$$

Since Eqs.(7.10),(7.11) and (7.30) formulate the system of quasi-linear hyperbolic partial differential equations, the characteristics exist. Along the characteristics, these differential relations are given by

$$\text{Along } dX/dt = \pm C, \quad d\sigma'_{12} = \mp \rho C dv_2 - 2G\beta_1 (F) \frac{\sigma'_{12}}{\sqrt{2J_2}}\, dt \tag{7.32}$$

$$\text{Along } dX/dt = 0, \quad d\varepsilon_{12} = \frac{1}{2G} d\sigma'_{12} + \beta_1 \frac{\sigma'_{12}}{\sqrt{2J_2}} dt \tag{7.33}$$

$$C = \sqrt{\frac{G}{\rho}}$$

Fig.7.4 shows the characteristic net. When the particle velocity at two points, B_0 and B_1, on the boundary of the bed rock are known, the stress and strain at C_0 can be determined by the differential relations along the lines; B_0-B_1 and C_0-B_1. The stress, strain and velocity at point C_2 can be obtained by solving the three differential relations along the lines(A_1-C_2, C_1-C_2, B_2-C_2).

Along the line A_1-C_2, the relation is given

$$\sigma'_{12(C_2)} - \sigma'_{12(A_1)} = \rho_0 C(v_{2(A_2)} - v_{2(A_1)}) - 2G\beta_1 \frac{\sigma'_{12}}{\sqrt{2J_2}} (t_{(C_2)} - t_{(A_1)}) \tag{7.34}$$

Along the line C_1-C_2,

$$\varepsilon_{12(C_2)} - \varepsilon_{12(C_1)} = \frac{1}{2G} (\sigma'_{12(C_2)} - \sigma'_{12(C_1)}) + \beta_1 \frac{\sigma'_{12}}{\sqrt{2J_{2(C_1)}}} (t_{(C_2)} - t_{(C_1)}) \tag{7.35}$$

Along the line B_2-C_2,

$$\sigma'_{12(C_2)} - \sigma'_{12(B_2)} = -\rho_0 C(v_{2(C_2)} - v_{2(C_1)}) - 2G\beta_1 \frac{\sigma'_{12}}{\sqrt{2J_{2(B_2)}}} (t_{(C_2)} - t_{(B_2)}) \tag{7.36}$$

From Eqs.(7.34) and (7.36), $\sigma'_{12(C_2)}$ and $v_{2(C_2)}$ are determined and $\varepsilon_{12(C_2)}$ is obtained by Eq.(7.35). Conversely, if the stress, strain and velocity at points A_1,A_2 and C_1 are known, the stress, strain and velocity at point C_2 can be obtained theoretically. By the same manner, the underground motion can be presumed from the surface motion.

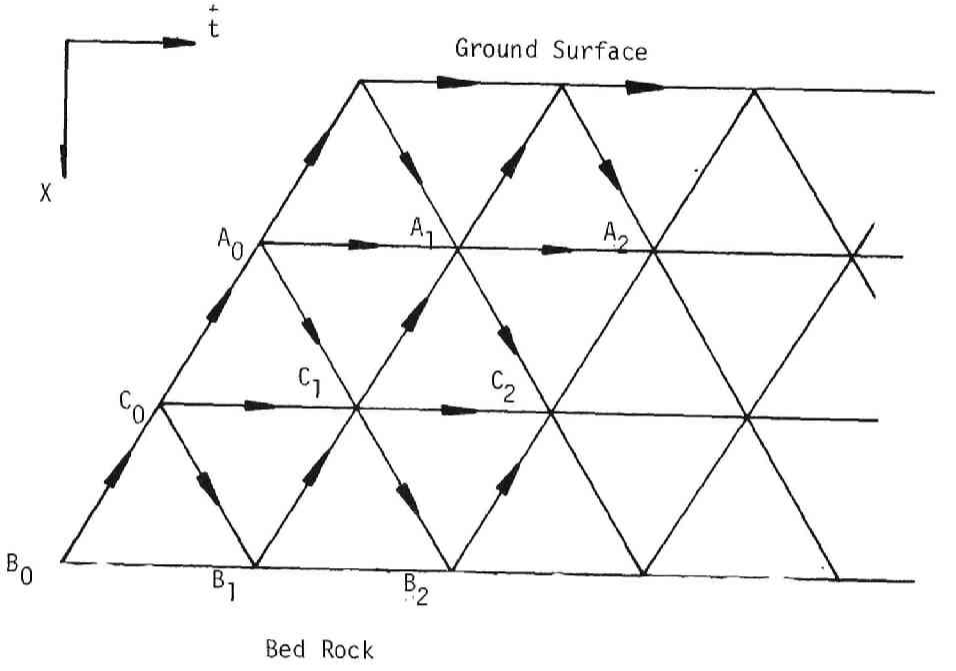

Fig.7.4 Characteristic net

7.4 Numerical Examples and Discussion

In this section, we will examine the underground motion using the Eqs.(7.32) and (7.33) from the surface record. At the boundary of the layers, the mean value of parameters in two layers was used for finite difference method.

Example A

Table 7.1 shows the parameters of the ground employed in the example A. An elastic layer of dry sand 9.3 m thick lies on the horizontal saturated clay layer. The clay layer is 42.3 m thick. The parameter m in Eq.(7.29) can be assumed to take as follows from the constant strain-rate triaxial compression test,

$$\begin{aligned} m &= 49 && (|\varepsilon_{12}| \leq 10^{-3}) \\ m &= 49-(|\varepsilon_{12}|-10^{-3}) && (10^{-2} \geq |\varepsilon_{12}| \geq 10^{-3}) \\ m &= 40 && (|\varepsilon_{12}| \geq 10^{-2}) \end{aligned} \qquad (7.37)$$

m depends on the amplitude of strain. The void ratio is calculated from the variation of the density with depth. The other parameters; K_0, M^*, λ and κ are taken as $K_0=0.5$, $M^*=1.4$, $\lambda= 0.127$, $\kappa= 0.021$.

The time trace of velocity on the surface is assumed to be sinusoidal and expressed by

$$V_{2(0)} = A_0 \sin(2\pi ft), \qquad A_0 = 0.15 \text{m/sec}, \quad f \quad 1.0 \qquad (7.38)$$

Fig. 7.5 represents the calculated stress-strain relation at the depth of 33.1 m in the ground. In this figure, the viscoplastic strain is produced and the hysterisis damping loop can be recognized. The velocity record at the depth of 50.4 m is shown in Fig.7.6 by solid line. It is obviously known, as would be anticipated, that the velocity on the surface is considerably amplified.

Layer	H	G	ρ	C_1	
1	3.0	440	196	0	Elastic layer
2	3.1	480	200	0	
3	3.2	520	204	0	
4	3.28	560	208	10^{-6}	Clay Layer
5	3.36	600	212	10^{-5}	
6	36.12	640	216	10^{-4}	

H ; depth (m)

G ; Shear modulus(kg/cm^2)

ρ ; density ($kg\ sec^2/m^4$)

C_1 ; prameter in Eq.(7.29)(1/sec)

Table 7.1 Parameters of example A.

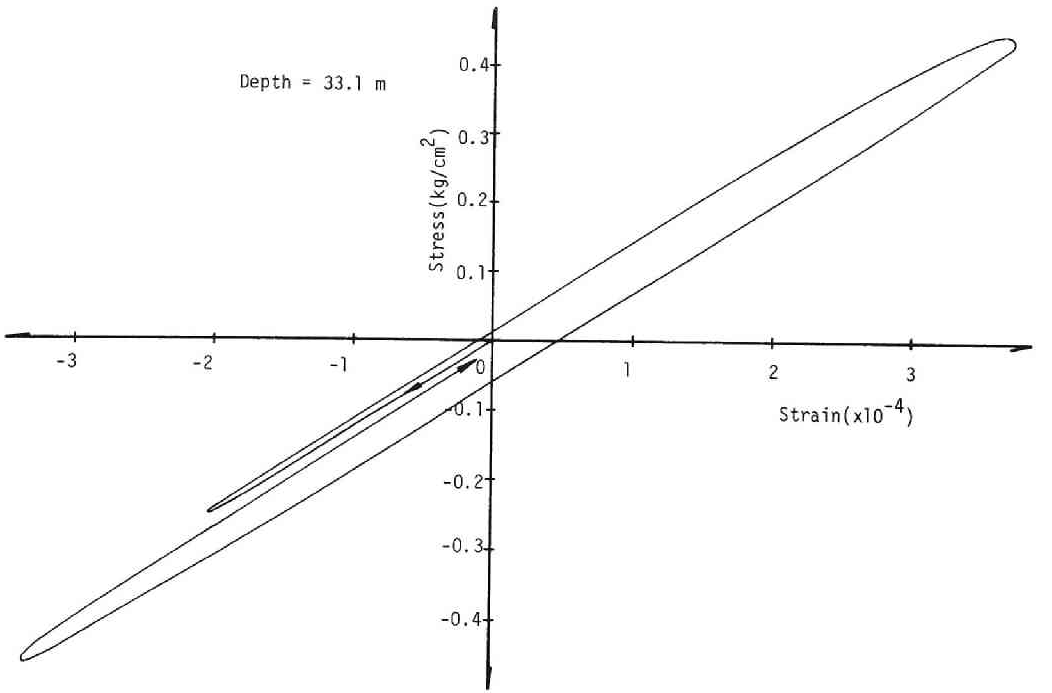

Fig.7.5 Stress-strain relation(calculated result).

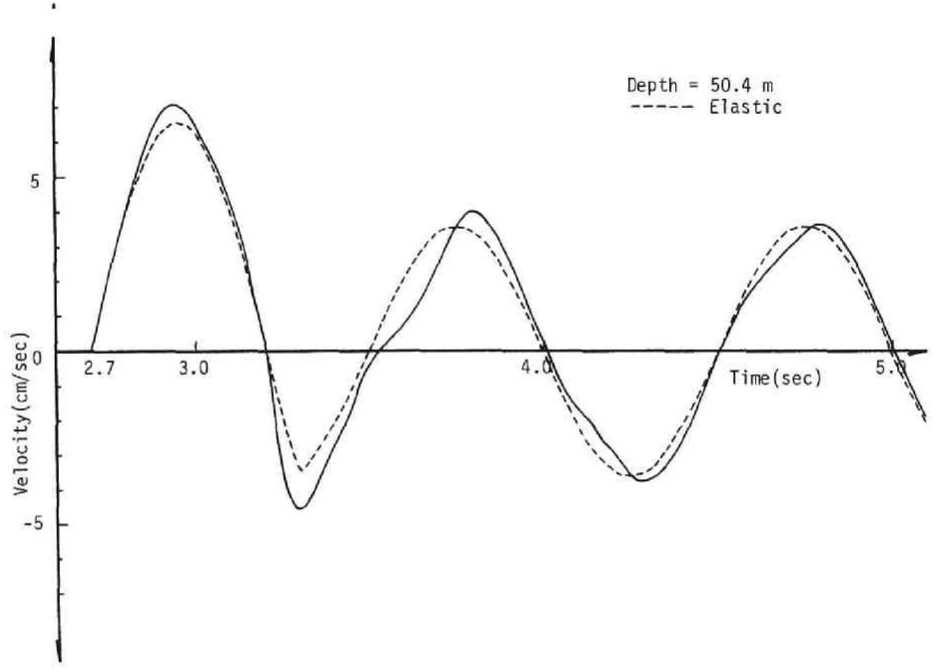

Fig.7.6 Velocity response

The dotted line shows the velocity record, which has been calculated under an assumption that the all layers are linearly elastic. Comparing two calculated results, it may be noted that the absolute value of velocity in clay layer which has been assumed to be elastic-viscoplastic in behavior is greater than the result calculated under the assumption described above. The difference of the amplitude of these two cases becomes gradually minute with time. It may be seen in the wave form of stress shown in Fig.7.7 that the difference of response between the two cases vanishes gradually with time as similar as the tendency of the velocity record. The part marked on the time axis shown in Fig.7.7 indicates the period when the state of stress of clay layer is viscoplastic in behavior. Moreover, it may be noted that the magnitude of stress, at which the viscoplastic behavior initiates, increases with number of cycles repeated, caused by the hardening property of clay. Fig.7.8 shows the typical effective stress path during the shear wave propagation. In this figure, the mean stress decreases and the residual pore pressure increases.

Example B

In example A, the sinusoidal velocity curve was used as a boundary condition, but for practical aim of engineering, the more realistic wave propagation must be considered. Then, in this example, a seismic surface acceleration record was used as a boundary condition by transforming into the velocity record. The frequency component of accelerogram more than 10 Hz was cut off by performing the base line correction. The first 10 sec of the S69E component of accelerogram at Taft during the 1952 Kern Country, California Earthquake was used, shown in Fig.7.9. Table 7.2 shows the parameters of the ground employed in Example B. Fig.7.10 shows the velocity record at the depth of 59.9 m, the dotted line shows the result of the case where all layers comprised are elastic and the other shows the result

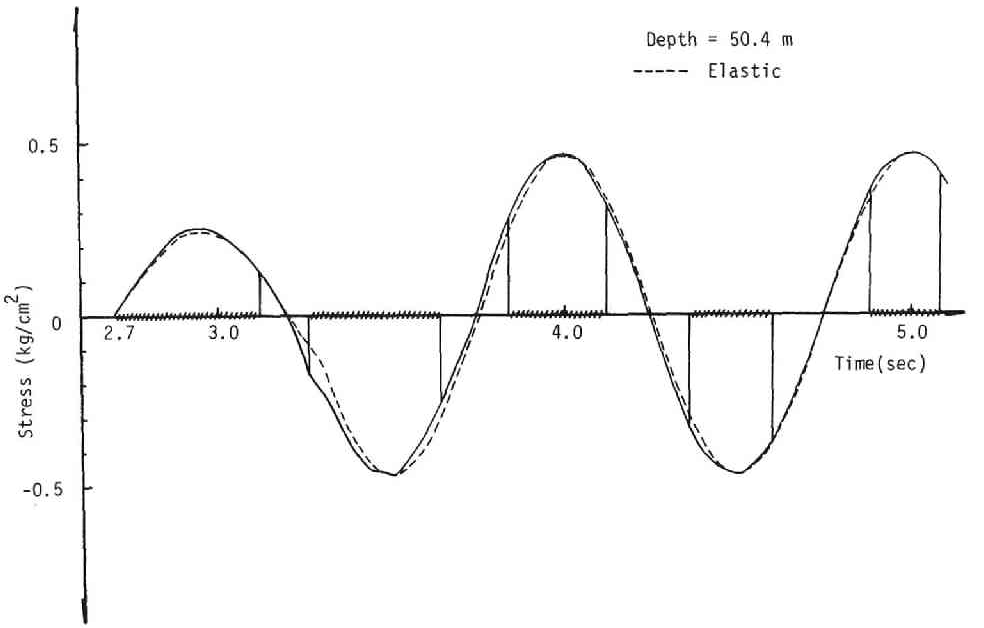

Fig.7.7 Stress response

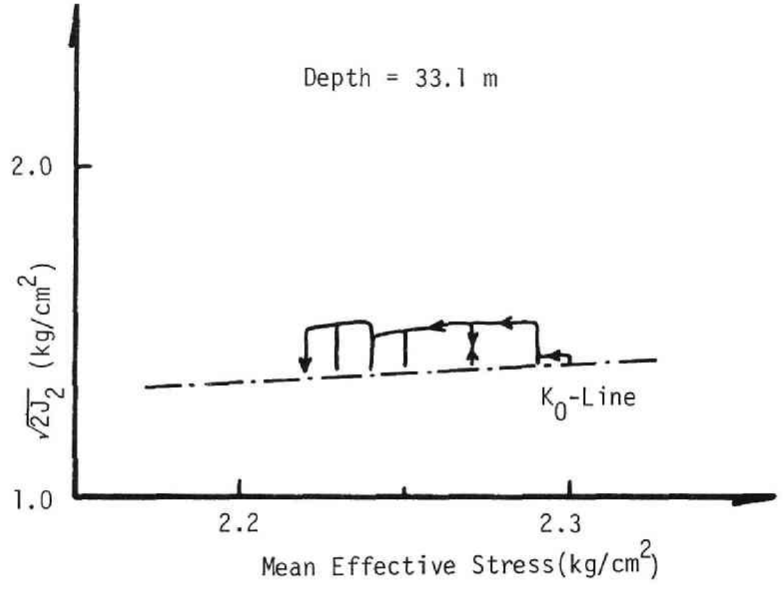

Fig.7.8 Effective stress path(calculated result).

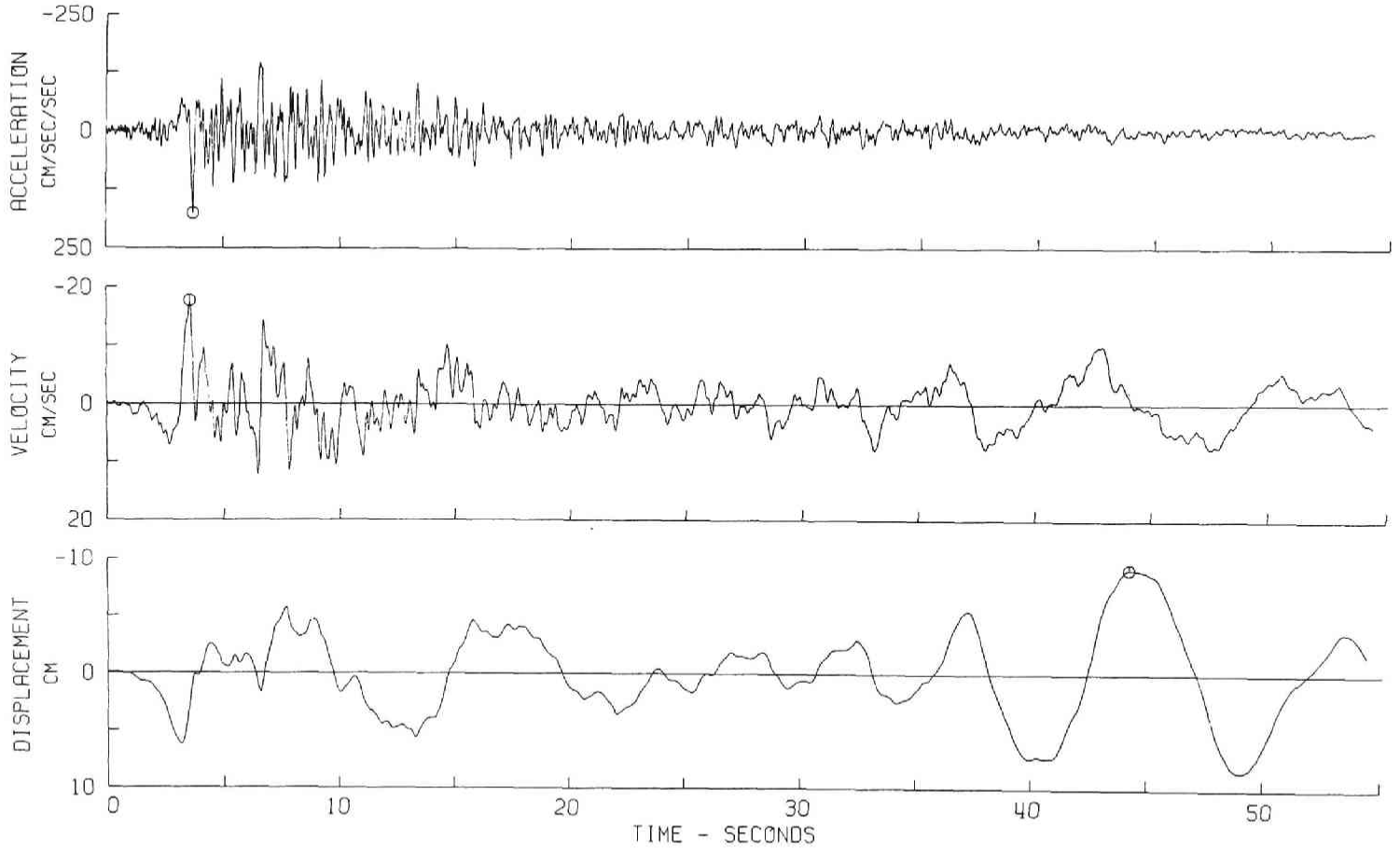

Fig.7.9 S69E component of accelerogram at Taft during the 1952 Kern Country, California Earthquake.

Layer	H	ρ	C	C_1	m
1	4	196	200	0	0
2	4	200	200	0	0
3	4	204	200	0	0
4	6	208	300	10^{-4}	30
5	6	212	300	10^{-4}	30
6	104	216	400	10^{-4}	10

H: depth(m), C: Shear wave velocity(m/sec)

ρ: dencity($kgsec^2/m^4$)

C_1 parameter in Eq.(7.29)(1/sec)

m : parameter in Eq.(7.29)

Table 7.2 Parameters of example B.

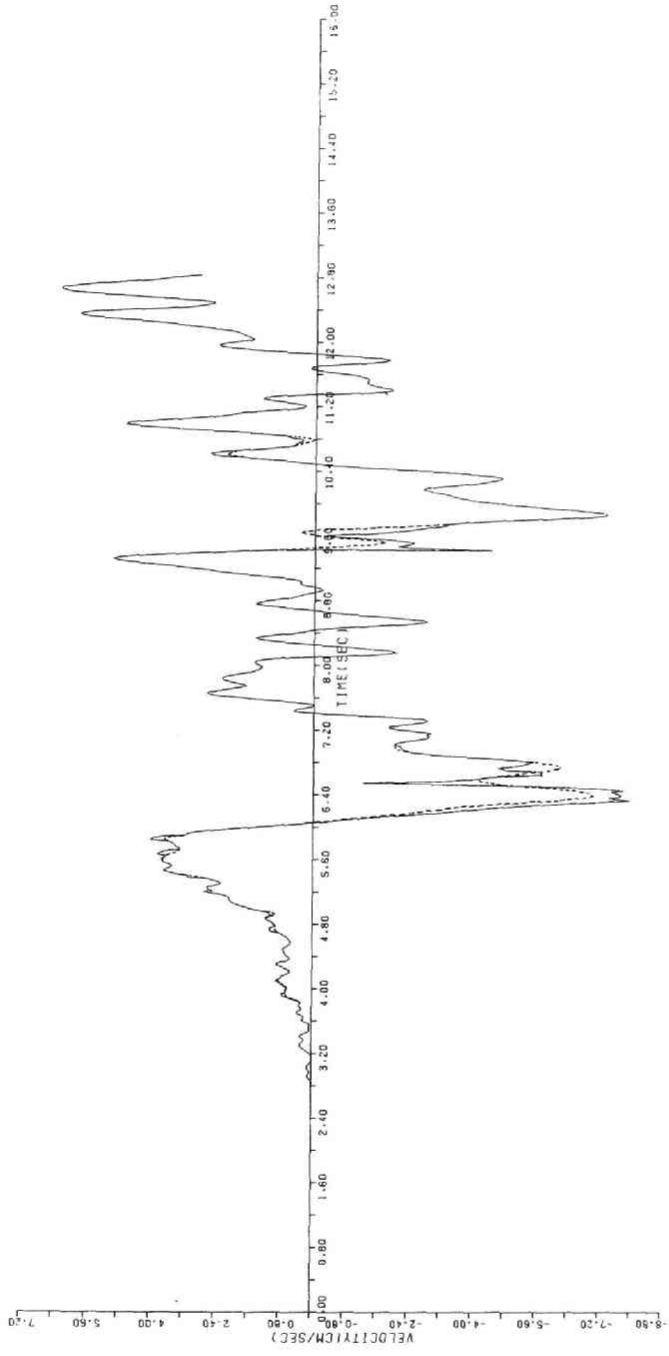

Fig.7.10 Velocity response

of the case of saturated elastic-viscoplastic ground. The velocity response for the elastic-viscoplastic ground is more predominant than that of the elastic ground in general. Fig.7.11 represents the strain response and Fig.7.12 shows the stress response at the depth of 59.5 m. The maximum value of the stress and strain responses for elastic case is slightly smaller than that of the other case depicted by solid line. These phenomena can be interpreted that the wave energy dissipates during the wave propagation through an elastic-viscoplastic soil layer by propducing an inelastic strain. Even if the surface velocity responses are equal, the larger stress, strain, velocity may be induced in the saturated clay layer than in the elastic ground. During 10 sec, the mean effective stress decreases by 0.04 kg/cm^2 in this case at the depth of 59.5 m.

7.5 Conclusion

In Chapter 5, the stress-strain relation of cohesive soil was developed. The main concern of this thesis is to solve various engineering problems as a boundary value problem using a realistic stress-strain relation of soil. In this chapter, the author has presented the calculation of strain, stress and velocity induced in the subground during the shear wave wave propagation through clay layers. The clay layer is regarded as elastic-viscoplastic body. The stress-strain relation under the isotropic consolidation was formally extended to K_0-consolidated state so as to be applied for the anisotropic consolidation. Some reserchers investigated the effect of the non-linearity of soil on the motion of ground, but the effect of the non-linearity in the time range in consideration of visco-plastic nature of soil has seldom been examined. Comparing the motion of the elastic ground with that of the elastic-viscoplastic ground during the seismic wave propagation, the effect of time dependency of stress-strain relation was examined.

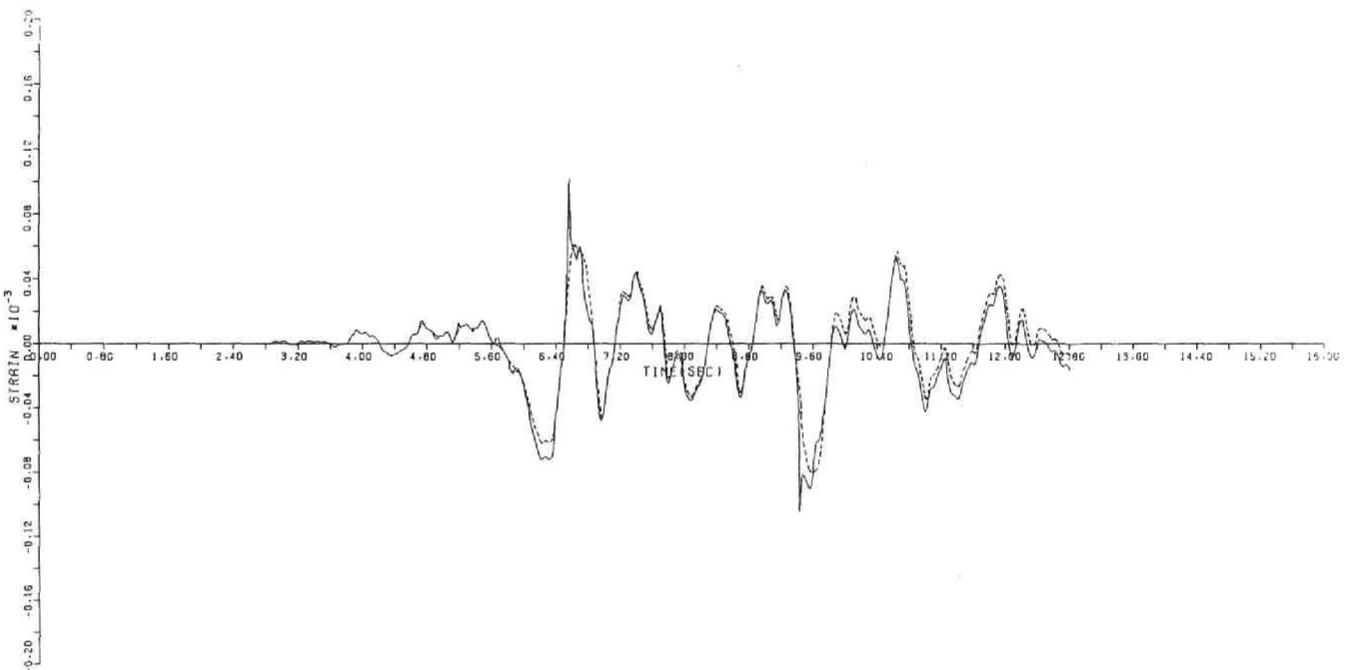

Fig.7.11 Strain response

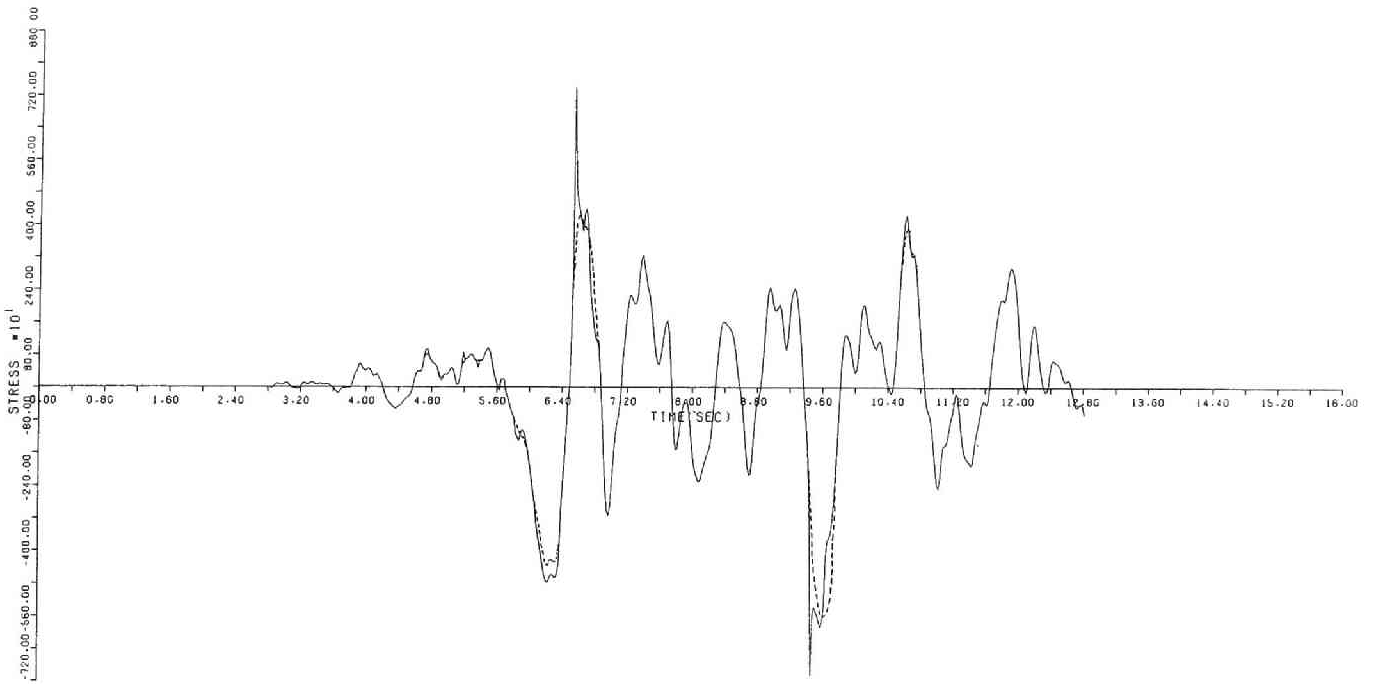

Fig.7.12 Stress response

At the same time, the development of the pore water pressure during earthquake motion was discussed. The method of characteristics was used because of short time of computation and easiness in taking a non-linearity of the material into analysis. The main conclusions obtained in this chapter are as follows.

(1) The motion of the layered cohesive soil during the earthquake can be calculated by using the method of characteristics. In this chapter, from the surface records, the velocity, stress and strain induced under the ground were calculated. The stress-strain relation of cohesive soil was extended to K_0-consolidated state from that developed in Chapter 5 in order to apply it to the layered soil condition.

(2) The difference between the non-linear and the linear elastic analyses was noted for the calculated results. From these results, even if the surface record is same between the elastic ground and the elastic-viscoplastic ground, the stress, strain and velocity responses of the elastic-viscoplastic ground are greater than those of elastic ground. These response characteristics vary with the time, in which the hardening property of clay can be obviously recognized. The characteristics of response become to be elastic in behavior with time.

(3) The pore water pressure developed during loading was estimated. From the examples given, it is noted that the residual pore water pressure may be developed during earthquake, but the absolute value of the pore water pressure is relatively small compared to consolidation pressure.

References for Chapter 7

1) see ref. 5) in Chapter 5

2) see ref. 6) in Chapter 5

3) Finn, W.D.L., K.W.Lee and G.R. Martin: An Effective Stress Model for Liquefaction, J. GED, ASCE, Vol.103, No.GT6, Proc. Paper 13008, June, 1977, pp.517-531.

4) Sato, T.: Study on the Wave Propagation Characteristics Considering a Nonlinear Behavior of Gound, Doctor Thesis, Kyoto Univ., 1975 (in Japanese).

5) Idriss, I.M. and H.B. Seed: Seismic Respose of Horizontal Soil Layers, Proc. ASCE, Vol.94, No.SM4, 1968, pp.1003-1031.

6) Streeter, V.L., E.B. Wylie and F.E. Richart,Jr.: Soil Motion Computation by Characteristics Method, J. GED, ASCE, Vol.100, No.GT3, Proc. Paper 10410, Mar., 1974, pp.247-263.

7) Oka,F.: Dynamic Response of Layered Cohesive Soils, 32th Annual Meeting of JSCE, 1977, pp.291-292.

8) Shima, E.: Seismic Surface Waves Detected by the Strong Motion Acceleration Seismograph, Proc. 8th Japan Earthquake Engng. Symp., 1970, pp.277-284.

9) see ref. 22) in Chapter 5.

Chapter 8 Conclusions

The main concerns of this thesis were as follows.

(1) To propose the constitutive theory of inelastic material from a point of view of mathematical continuum mechanics and to refine it for saturated cohesive soil.

(2) To investigate experimentally and analytically the dynamic behavior of cohesive soil during the wave propagation.

(3) Application of the proposed realistic stress-strain relation of cohesive soil to the engineering boundary value problem.

Besides briefly summarizing the important conclusions obtained in each chapter, the general synopsis of the work presented in the preceding chapters and recommendation for future work are given in the present chapter.

In Chapter 1, the general scope of this thesis and, the remarks and the history of the soil dynamics are noted.

In Chapter 2, the experimental results obtained from the wave propagation test are presented, which was carried out by using the shock-tube together with the special triaxial cell. The bar wave propagation through a normally consolidated cohesive soil was observed at the experiment. From the test results, it is noted that the attenuation and the change of wave shape depend on the stress level, in other words, the cohesive soil possesses a non-linear inelasticity. The wave velocity is determined mainly by the pre-consolidation pressure. The pore-pressure has also been observed at the wave propagation test, of which wave form was similar to that of the stress. The stress wave was analyzed by the Fourier transformation. As a result, it is concluded that the viscoelastic property of cohesive soil can be described by a linear spring-Voigt model, taking into account

the characteristics of the phase velocity and the attenuation of stress. The author has mainly treated the normally consolidated clay but the dynamic characteristics of anisotropically or over-consolidated clay should also be clarified in the future study.

In Chapter 3, the general constitutive theory of inelastic material was discussed from a view point of rational continuum mechanics and thermodynamics. The proposed constitutive relation of inelastic material is more general than the Perzyna's elastic-viscoplastic body. The physical relation between a plastic potential and the energy function was clarified. Since there remain some uncertainties in the continuum thermodynamics on which the deduction of the constitutive theory has been essentially based in the thesis,the theory of the continuum thermodynamics itself should be improved more rationally in the future study.

In Chapter 4,in order to examine the characteristics of the multi-phase mixture which is an essential nature of saturated soil, the solid-fluid mixture theory was deduced, based on the Green & Naghdi's theory. By applying this theory to the saturated soil, the Terzaghi's effective stress concept was reexamined and the general equation governing the consolidation phenomenon was deduced. Finally, the constitutive theory of a mixture composed of a viscoelastic-viscoplastic material and an elastic fluid was developed on the basis of an internal variable theory and the rational thermodynamics. In the future study, the unsaturated soil must be investigated from a view point of the theory of three-phase mixture.

In Chapter 5, the constitutive equation of normally consolidated clay was proposed for interpreting the dynamic behavior of soil in a wide range of frequency. The phenomenological nature of parameters involved in the stress-strain relation was investigated in detail by using the triaxial

test results. The proposed theory can explain the dynamic stress path and stress-strain relation in various test results; for instances, undrained creep test, undrained strain-rate controlled triaxial test, undrained stress relaxation test. The viscoelastic parameters were adequately assessed by analyzing the one-dimensional stress wave propagation problem in Chapter 6, because viscoelastic-viscoplastic behavior is predominantly observed in the test performed with a higher rate of loading.

In Chapter 6, the one-dimensional bar wave propagation through clay was analyzed by using the characteristic method. The mechanical model used for calculation was viscoelastic-viscoplastic body obtained in Chapter 5. One of the main conclusion in Chapter 6 is that the energy dissipation due to an interaction between solid and fluid is less than that due to the viscoplasticity of solid phase. Therefore, we may be able to assume that v_i^f is equal to v_i^s, and the equation of motion becomes simpler. As a result, the wave propagation characteristics through cohesive soil can be adequately described by the viscoelastic-viscoplastic model. In the calculation, the developement of the pore water pressure was predicted by assuming that $\varepsilon_{kk}=0$ at any point of material, but this assumption may not be realistic, considered from the test condition. Accordingly, the pore-pressure predicted was slightly higher than that observed in the experiment.

In Chapter 7, the elastic-viscoplastic stress-strain relation is applied to the dynamic response of layered cohesive soil system. The stress, strain and velocity under the ground can be determined from the surface record of earthquake. In this chapter, the only cohesive soil layered system is treated, but real gound is composed of cohesive and cohesionless soil. Then, future studies should be devoted to the dynamic

analysis for composite layered soil system.